

OLYMPIC DAM EXPANSION

DRAFT ENVIRONMENTAL IMPACT STATEMENT 2009

APPENDIX J

SURFACE WATER



bhpbilliton

resourcing the future

ISBN 978-0-9806218-0-8 (set)
ISBN 978-0-9806218-4-6 (appendices)

SURFACE WATER

CONTENTS

J1	Regional surface water assessment	3
	J1.1 Methodology	5
	J1.1.1 Desktop investigation	5
	J1.1.2 Field survey	5
	J1.2 Results	6
	J1.3 References	12
J2	Pit lake assessment	13



APPENDIX J1

Regional surface water assessment

J1 REGIONAL SURFACE WATER SUPPLEMENTARY INFORMATION

Chapter 11 of the Draft EIS presents the findings of the surface water assessments undertaken for the proposed Olympic Dam expansion. The assessment was undertaken by ENSR Australia Pty Ltd (ENSR) (southern infrastructure corridor) and RPS Ecos Pty Ltd (gas pipeline corridor options). This appendix provides supplementary information in relation to the methodology undertaken and detailed findings.

J1.1 METHODOLOGY

J1.1.1 Desktop investigation

Extensive work has been undertaken previously to identify and describe the physiographic features throughout the project area (i.e. the surface features of the earth, with an emphasis on the origin of landforms). The broader physiographic features of the Andamooka-Torrens region in the northern part of the project area were documented by Johns in 1968 (Johns, 1968). Detailed terrain mapping undertaken in the vicinity of Roxby Downs and the mine site was completed as part of the 1982 EIS (Kinhill Stearns Roger 1982). Finer-scaled land system mapping undertaken by PIRSA is also available for the study area. These land systems are based on recurring patterns of topography, soil, geology and vegetation, as identified through aerial photography coupled with elevation models and ground truthing.

In addition to reviewing these publications, the desktop investigation involved:

- reviewing the surface water chapters and appendices from the 1982 and 1997 Olympic Dam EISs (Kinhill Stearns Roger 1982, Kinhill 1997)
- reviewing BHP Billiton's annual environmental reports to obtain relevant information
- discussions with Olympic Dam site personnel to gain a first hand understanding of rainfall intensities and durations, and the existing water catchments and flow paths on the site and at Roxby Downs
- identifying legislation, policies and guidelines including water resource plans, and/or land management plans of relevance to the study area. The primary sources of relevance are the South Australian Government Environmental Protection (Water Quality) Policy 2003, and the Natural Resource Management Plan 2006
- reviewing the maps of drainage basins developed by the Department of Water, Land and Biodiversity Conservation
- reviewing the 1:250,000 topographic maps for the study area (see references) to identify major water features and surface drainage patterns within each drainage basin, and to assess channel slope
- reviewing aerial photography, both current and historic, to identify the location and extent of inundation where aerial photography coincides with wet periods
- searching the Bureau of Meteorology data to gain an appreciation of flooding history and flood levels across the study area
- searching stream gauging stations and previous water quality monitoring data where available (eg. AUSRIVAS program)
- identifying sensitive downstream environments based on information obtained during the ecological assessments for the Olympic Dam EIS in addition to published information including the Commonwealth Department of Environment and Water Resources databases, Ramsar listings and the Directory of Important Wetlands in Australia (Environment Australia 2001)
- identifying present surface water users within the corridor and downstream users.

J1.1.2 Field survey

The field survey for the southern infrastructure corridor was undertaken over eight days from 10–17 July 2006. Heavy rainfall occurred during the survey, with 19.6 mm recorded at Andamooka on 14 July, 24 mm at Woomera on 14 and 15 July, and 17.8 mm at Port Augusta from 14–16 July. This rain event enabled a good understanding of surface water flows in the areas of assessment. The survey area included the Special Mining Lease, the Roxby Downs Municipality and the infrastructure corridors.

Water quality parameters in terminal salt lakes were measured using a TPS 81 meter that was calibrated before field work commenced. The probes were placed into the water at a depth of >0.20 m (where possible) and cleaned between sampling sites using deionised water. The parameters measured were:

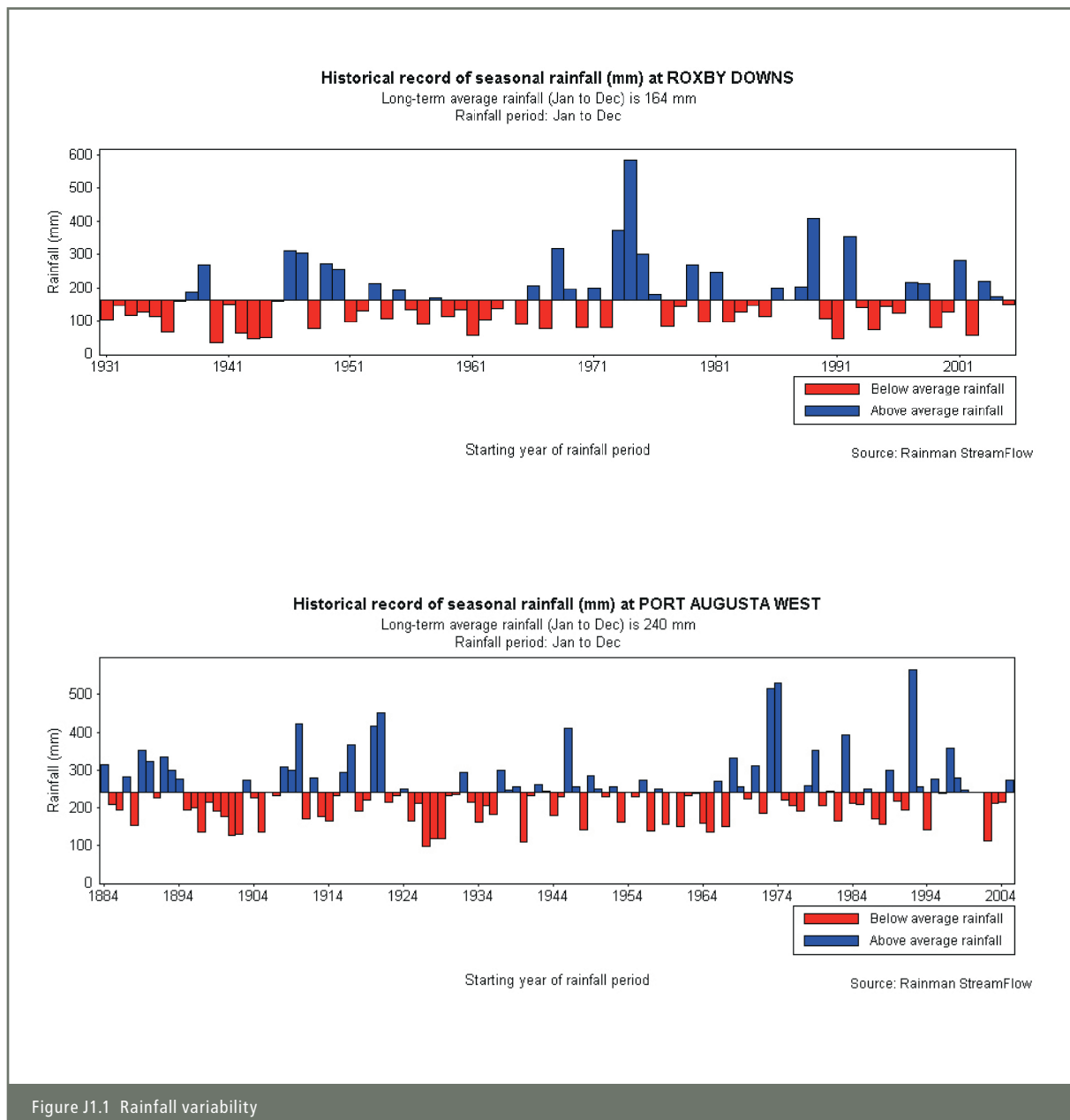
- dissolved oxygen (DO) – this measures the amount of oxygen available in the water and is an indicator of the water body's ability to support life. Dissolved oxygen is recorded in parts per million (ppm)
- electrical conductivity (EC) – this measures the salinity of the water body in microsiemen per centimetre ($\mu\text{s}/\text{cm}$) or deci-siemen per metre (ds/ms)
- pH (negative log of hydrogen ion activity) – this indicates the alkalinity or acidity of the water on a scale of 1 to 14
- temperature – this affects the solubility of oxygen in water (the higher the temperature, the less oxygen can be dissolved in the water body). Temperature is measured in degrees Celsius
- turbidity – this is used to assess the clarity of water (using the nephelometric turbidity unit (NTU)) and is the result of suspended solids in the water.

The receiving environments of catchments, including significant creeks were examined and photographed, and water samples were collected where surface water was available. Auger holes were also dug in receiving environments to a maximum depth of three metres to identify the presence of shallow groundwater and assess water quality. Paste pH and EC of bed sediments were determined to assess the salinity of the receiving environments and enable commentary on likely groundwater/surface water interaction.

Catchments and watercourses on the gas pipeline corridor options were examined and photographed during ecological surveys undertaken in October 2006 and January 2008. Conditions were dry during these surveys, so sampling was restricted to the collection of surface water samples at four locations where it was present in waterholes or springs in the corridor.

J1.2 RESULTS

The following tables and figures provide data to supplement the information summarised within the Surface Water chapter of the Draft EIS (Chapter 11).



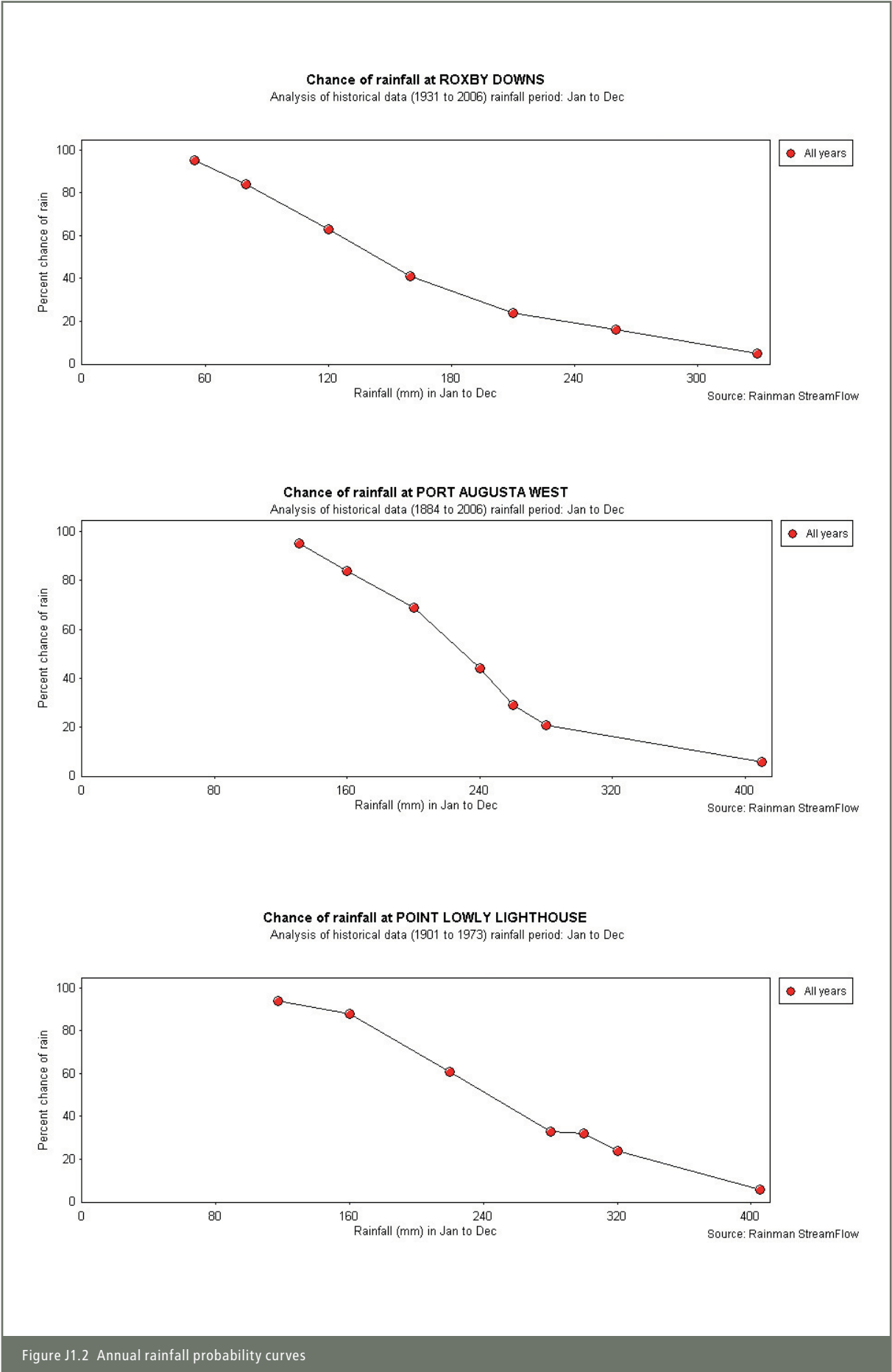


Figure J1.2 Annual rainfall probability curves

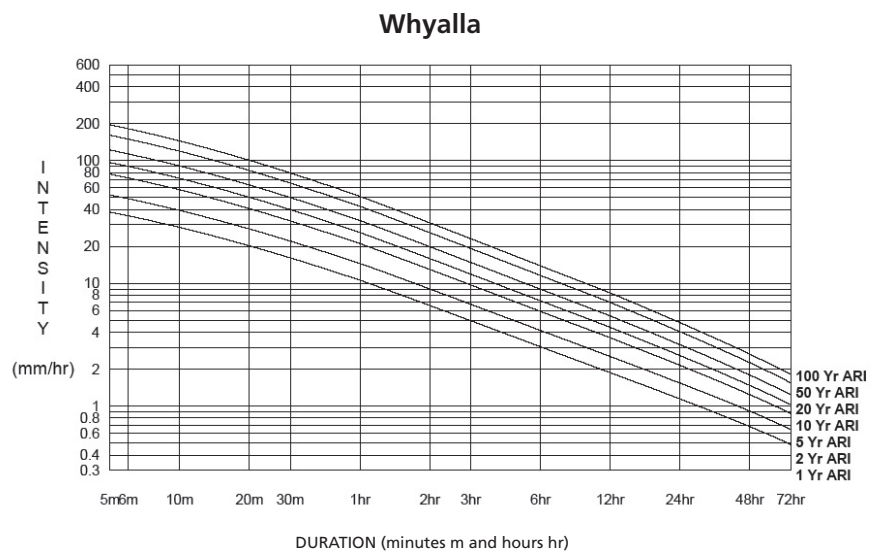
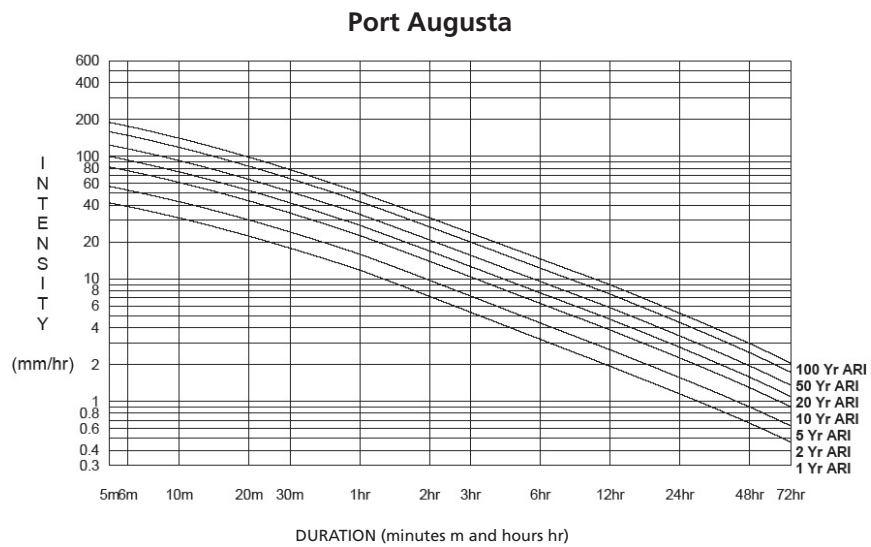
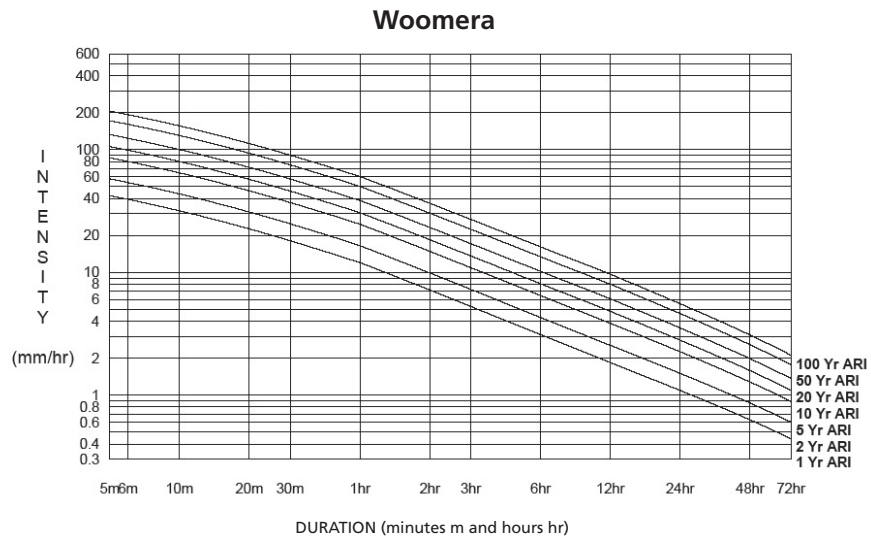


Figure J1.3 Rainfall intensity, frequency and distribution curves

Sample ID	Location (see Figure 11.1 for locations)	Rain prior	Date	Conductivity (mS/cm)	pH	DO (%sat)	DO (ppm)	Temp (°C)	Turbidity
–	Lake Richardson and Red Lake	No	12/07/06	140	8.7	–	–	–	–
–	Lake Windabout – at highway crossing (stagnant pond)	No	13/07/06	128	6.5	–	–	–	–
–	Ironstone lagoon – groundwater	No	13/07/06	166	6.1	–	0.5	–	–
–	Pernatty below transmission line – green stagnant pond	No	13/07/06	157	6.7	–	–	–	–
–	Pernatty below transmission line – Red stained pond	No	13/07/06	193	7.5	–	–	–	–
SW1	Tributary of Mason Creek at highway crossing	Yes	14/07/06	0.29	8.5	–	10.6	13.2	400
–	Tributary of Brackish Swamp	Yes	14/07/06	0.24	9.0	100	–	–	–
SW2	Ironstone lagoon – at highway crossing	Yes	16/07/06	144	7.6	85	8.9	13.3	10
SW3	Wocalla Creek – at highway crossing	Yes	16/07/06	1.3	8.9	73	7.9	13.2	80
SW4	Lake Windabout – at highway crossing	Yes	16/07/06	39.4	7.3	106	10.8	13.6	<10

Table J1.1. Field water quality results

Table J1.2 Laboratory water quality results – southern infrastructure corridor

Parameter	Units	LOR ¹	SW1 Mason Creek	SW2 Ironstone Lagoon	SW3 Woocala Creek	SW4 Lake Windabout
pH Value	pH Unit	0.01	7.1	6.76	7.52	6.84
Electrical Conductivity	µS/cm	1	81	–	231	41,100
Total Dissolved Solids	mg/L	1	85	140,000	468	22,300
Total Anions	meq/L	0.01	1.1	2,510	1.32	457
Total Cations	meq/L	0.01	0.96	2,300	1.37	464
Ionic Balance	%	0.01	–	4.38	–	0.81
Hydroxide Alkalinity as CaCO ₃	mg/L	1	<1	<1	<1	<1
Carbonate Alkalinity as CaCO ₃	mg/L	1	<1	<1	<1	<1
Bicarbonate Alkalinity as CaCO ₃	mg/L	1	29	33	34	12
Total Alkalinity as CaCO ₃	mg/L	1	29	33	34	12
Acidity as CaCO ₃	mg/L	1	6	29	6	12
Sulphate as SO ₄ ²⁻	mg/L	1	2	2,550	12	572
Chloride	mg/L	1	17	87,000	14	15,800
Calcium	mg/L	1	1	304	1	99
Magnesium	mg/L	1	<1	2,100	1	539
Sodium	mg/L	1	20	48,300	26	9,510
Potassium	mg/L	1	1	256	4	64
Arsenic	mg/L	0.001	<0.001	<0.050	<0.001	<0.001
Cadmium	mg/L	0.0001	0.0002	0.0006	0.0004	0.0003
Chromium	mg/L	0.001	<0.001	<0.005	<0.001	0.001
Copper	mg/L	0.001	0.004	<0.050	0.006	0.002
Lead	mg/L	0.001	0.002	<0.005	0.001	<0.001
Nickel	mg/L	0.001	0.002	<0.050	0.002	0.002
Zinc	mg/L	0.005	0.018	<0.050	0.045	0.006
Mercury	mg/L	0.0001	<0.0001	<0.0001	<0.0001	<0.0001

¹ Limits of reporting.

Table J1.2 Laboratory water quality results – gas pipeline corridor

Parameter	Units	PQL ¹	GC1 Frome River	GC2 Cooryanna Ck Tributary	GC128 Reedy Springs	GC134 St Mary Pool
pH value	pH unit	0.1	9.3	8.1	8.1	7.9
Electrical conductivity	µS/cm	20	2450	355	2420	324
Total dissolved solids	mg/L	5	1400	1100	1400	210
Total anions	meq/L	0.2	22	4.8	11	5.1
Total cations	meq/L	0.2	26	3.9	28	3.4
Ionic Balance	%	1	8.3	10	44	21
Hydroxide alkalinity as CaCO ₃	mg/L	10	<10	<10	<10	<10
Carbonate alkalinity as CaCO ₃	mg/L	10	214	<10	<10	<10
Bicarbonate alkalinity as CaCO ₃	mg/L	10	631	152	225	186
Total alkalinity as CaCO ₃	mg/L	20	844	152	225	186
Acidity as CaCO ₃	mg/L	20	<20	<20	25	<20
Sulphate as SO ₄ ²⁻	mg/L	0.5	8.1	39	38	17
Chloride	mg/L	0.5	210	16	180	18
Calcium	mg/L	0.1	4.7	15.7	10.5	32.9
Magnesium	mg/L	0.1	1.2	4.33	1.26	4.92
Sodium	mg/L	0.1	581	56.4	621	26.7
Potassium	mg/L	1	13	11	8.19	5.92
Arsenic	mg/L	0.005	<0.005	6	<0.005	<0.005
Cadmium	mg/L	0.005	<0.005	<0.005	<0.005	<0.005
Chromium	mg/L	0.005	<0.005	<0.005	<0.005	<0.005
Copper	mg/L	0.005	<0.005	0.005	<0.005	<0.005
Lead	mg/L	0.005	<0.005	<0.005	<0.005	<0.005
Nickel	mg/L	0.005	<0.005	<0.005	<0.005	<0.005
Zinc	mg/L	0.005	0.09	<0.005	<0.005	<0.005
Mercury	mg/L	0.001	<0.001	<0.001	<0.001	<0.001

¹ Practical quantitation limit.

J1.3 REFERENCES

ANZECC & ARMCANZ (2000), Australian and New Zealand Guidelines for Fresh and Marine Water Quality. National Water Quality Management Strategy Paper no. 4. Australian and New Zealand Environment and Conservation Council / Agriculture and Resource Management Council of Australia and New Zealand.

Badman F J (2001) A review of the Kingoonya Soil Conservation District. Report prepared for the Kingoonya Soil Conservation Board. PIRSA Port Augusta 37 pp, in PIRSA (2002) Kingoonya Soil Conservation Board District Plan. Kingoonya Soil Conservation Board.

Environment Australia (2001) A Directory of Important Wetlands in Australia, Third Edition. Environment Australia, Canberra.
Institution of Engineers Australia (2001), Australian Rainfall & Runoff.

Johns RK (1968) Geology and Mineral Resources of the Andamooka-Torrens Area. Geological Survey of South Australia, Bulletin No. 41.

Kinhill Engineers Pty Ltd (1997) 'Olympic Dam Expansion Project: Environmental Impact Statement', May 1997, prepared for WMC Olympic Dam Corporation Pty Ltd.

Kinhill-Stearns Roger Joint Venture (1982) 'Olympic Dam Project: Draft Environmental Impact Statement.' Prepared for Roxby Management Services Pty Ltd, Adelaide.

Planning SA (2003), Development Plan: Port Augusta (City), Consolidated 28 August 2003.

SA EPA (2003), Environment Protection (Water Quality) Policy and Explanatory Report 2003, May 2003, Adelaide.



APPENDIX J2

Pit lake assessment

30 July 2008

Reference No. 06641442-L19

Dr Kelly Usher
Olympic Dam EIS Project
GPO Box 11052
ADELAIDE SA 5001

REVIEW OF ENSR REPORT PREPARED FOR BHP BILLITON ENTITLED “OLYMPIC DAM EXPANSION – PIT LAKE LIMNOLOGICAL AND GEOCHEMICAL ASSESSMENT”

Dear Dr Usher

As requested by you (e-mail dated 20 May 2008), Golder Associates Pty Ltd (Golder) reviewed the draft report prepared by ENSR Australia Pty Ltd (ENSR) entitled “Olympic Dam Expansion – Pit Lake Limnological and Geochemical Assessment” (Document No B43329_RPTDraft_24Apr08).

We have also reviewed the earlier draft report and discussed some aspects of the study directly with Mr Chris Gimber of ENSR (19 February 2008).

It is my opinion that the work has been carried out thoroughly and to an appropriate technical standard for the Olympic Dam EIS. The scope of work and the outcomes are in line with normal industry practice and seem acceptable for the intended purpose.

The long-term (3000 year) forecasts of pit lake levels and water quality exceed normal industry practice and projections over this time frame should be viewed with caution. However, we agree with the author’s approach of considering both 100 year climate projections based on model simulations by the CSIRO and climate conditions over the last 10,000 years as a basis of understanding the range of variability that has previously occurred.

GOLDER ASSOCIATES PTY LTD



Dr Jan Vermaak
Associate

JJV/JDW/sp

m:\jobs406\mining\06641442_bhpb_olympic dam\correspondence\06641442-119.doc

Prepared for:
BHP Billiton

Olympic Dam Expansion - Pit Lake Limnological and Geochemical Assessment

Final

Contents

1.0	INTRODUCTION.....	1
2.0	METHODOLOGY.....	2
2.1	Final Void Profile.....	2
2.2	Climatic Data.....	2
2.3	Water Balance.....	3
2.3.1	Model Timestep.....	4
2.3.2	Representing Uncertainty.....	4
2.3.3	Model Inputs.....	4
2.3.3.1	Incident Rainfall.....	4
2.3.3.2	External Catchment Runoff.....	5
2.3.3.3	Pit Wall Runoff.....	5
2.3.3.4	Evaporation.....	5
2.3.3.5	Groundwater.....	6
2.3.4	Sensitivity Analysis.....	6
2.3.5	Alternative Scenarios.....	6
2.4	Water Chemistry.....	6
2.4.1	Chemistry of Input Waters.....	6
2.4.2	Geochemical Model.....	8
2.4.3	Sensitivity Analysis.....	14
2.5	Limnology.....	15
2.5.1	Limnological Model.....	15
2.5.2	Sensitivity Analysis.....	15
3.0	FINAL VOID PROFILE.....	17
4.0	CLIMATE.....	19
4.1	Overview.....	19
4.2	Climate Data.....	19
4.2.1	Rainfall.....	19
4.2.1.1	Observed Data.....	19
4.2.1.2	Patched-Point Data.....	20
4.2.1.3	Stochastic Data.....	21
4.2.2	Pan Evaporation.....	23
4.2.3	Air Temperature.....	23
4.2.4	Shortwave Solar Radiation.....	24
4.2.5	Water Vapour Pressure.....	25
4.2.6	Wind Speed.....	26
4.3	Climate change.....	27
4.3.1	Rainfall.....	27
4.3.2	Evaporation.....	28
5.0	WATER BALANCE.....	30
5.1	Model Components.....	30
5.1.1	External Catchment Runoff.....	30
5.1.1.1	Catchment Area.....	30

	5.1.1.2	Hydrology	30
	5.1.2	Pit Wall Runoff.....	33
		5.1.2.1 Catchment Area.....	33
		5.1.2.2 Hydrology	33
	5.1.3	Evaporation	34
		5.1.3.1 Pan factor	34
		5.1.3.2 Salinity effects	34
	5.1.4	Groundwater.....	35
	5.1.5	Summary of Distributions.....	38
5.2		Model Results	39
	5.2.1	Pit Lake Water Level.....	39
		5.2.1.1 Hydrogeological Implications.....	41
		5.2.1.2 Water Fluxes	41
	5.2.2	Sensitivity Analysis	41
		5.2.2.1 Input Variables.....	41
		5.2.2.2 Seepage	42
		5.2.2.3 Timestep.....	42
	5.2.3	Alternative Scenarios.....	44
		5.2.3.1 Climate Change.....	44
		5.2.3.2 Extreme Rainfall Event.....	46
6.0		WATER CHEMISTRY	47
	6.1	Chemistry of Input Waters	47
		6.1.1 Incident Rainfall.....	47
		6.1.2 External Catchment Runoff.....	47
		6.1.3 Pit Wall Runoff.....	50
		6.1.4 Andamooka Limestone Aquifer	52
		6.1.5 Corraberra Sandstone Aquifer	53
		6.1.6 Basement Aquifer	54
	6.2	Saturation State of Mineral Phases for Input Waters	57
	6.3	Transient Model Evolution	58
		6.3.1 Mineral Precipitation	58
		6.3.2 Water Chemistry.....	62
		6.3.3 Crust Development.....	64
7.0		LIMNOLOGY	65
	7.1	Limnological Processes.....	65
	7.2	Factors Influencing Mixing.....	68
		7.2.1 Meteorological Drivers	68
		7.2.2 Salinity	68
	7.3	Model Scenarios.....	69
	7.4	Model Results	70
		7.4.1 Case L1a (salinity 10,000 mg/L).....	70
		7.4.2 Case L1b (salinity 20,000 mg/L).....	70
		7.4.3 Case L1c (salinity 30,000 mg/L).....	70
		7.4.4 Case L1d (salinity 40,000 mg/L).....	71

7.4.5	Cases L2a,b,c	71
7.5	Predicted Stratification and Mixing Cycles.....	79
8.0	DISCUSSION.....	80
8.1	Proposed Lake Uses	80
8.2	Lake Development Stages.....	80
8.3	Ongoing Review of Model Predictions	81
9.0	CONCLUSION.....	82
10.0	BIBLIOGRAPHY.....	83

List of Tables

Table 1:	Summary of Climatic Data Inputs Used.....	2
Table 2:	Potential Secondary Mineral Phases	10
Table 3:	Geochemical Model Sensitivity Analysis Scenarios.....	14
Table 4:	Limnological Sensitivity Analysis Scenarios	16
Table 5:	Final Void Profile	17
Table 6:	Statistical summary of historical monthly rainfall (mm) recorded at Roxby Downs.....	19
Table 7:	Probability of monthly rainfall recorded at Roxby Downs; amounts of rain (mm) received or exceeded in 100% - 0% of years.....	20
Table 8:	Gauging stations in the vicinity of Olympic Dam.....	20
Table 9:	Comparison between the stochastic rainfall data and source data.....	21
Table 10:	Summary statistics of daily patched point pan evaporation (mm/day) data for the period 1889 - 2006	23
Table 11:	Summary statistics of daily air temperature (°C) modelled for the period 1970 -1997.....	24
Table 12:	Shortwave solar radiation summary statistics.....	25
Table 13:	Rainfall change prediction for 2070 at Olympic Dam	27
Table 14:	Potential evapotranspiration change prediction for 2070 at Olympic Dam.....	29
Table 15:	VRC Based on Stream Gauging Data	32
Table 16:	AWBM Parameters for Drainage Division V for use on Ungauged Catchments (Boughton et al, 2007)	32
Table 17:	Relationship Between Surface Storage Capacity and VRC	33
Table 18:	Relationship between salinity and evaporation rate.....	35
Table 19:	Adopted probability distributions for model input parameters.....	38
Table 20:	Water Level Predictions (mAHD)	39
Table 21:	Steady State Inflows (ML/a).....	41
Table 22:	Probability of Groundwater Gradient Reversal	42
Table 23:	Water Level Predictions – 50% Increase in Mean Annual Rainfall (mAHD).....	44
Table 24:	Water Level Predictions – 30% Decrease in Mean Annual Rainfall (mAHD)	45
Table 25:	Chemistry of incident rainfall (mg/L, unless noted otherwise)	47
Table 26:	Chemistry of the External Catchment Surface Runoff aquifer (mg/l, unless noted otherwise)	48
Table 27:	Surface Area of Rock Types Exposed in the Pit Wall	50
Table 28:	Chemistry of the Pit Wall Runoff	51
Table 29:	Chemistry of the Andamooka Limestone Aquifer (mg/L, unless noted otherwise)	52
Table 30:	Chemistry of the Corraberra Sandstone/Arcoona Quartzite Aquifer (mg/L, Unless Noted Otherwise)	53
Table 31:	Chemistry of the Basement Aquifer (mg/L, unless noted otherwise)	55
Table 32:	Saturation state of mineral phases for input waters	57
Table 33:	Predicted Mineral Precipitation for 'Base Case' scenario (Case G1)	58
Table 34:	Sensitivity to Mineral Precipitation – Expressed as Timing (post closure)	59
Table 35:	Summary of probable geochemical controls for specific solutes in pit lakes (Eary, 1999).....	60

Table 36: Predicted Pit Lake Water Quality Based on 'Base Case' Scenario (Case G1) (mg/L, unless noted otherwise)	62
Table 37: Ranges of Pit Lake Water Quality for all Sensitivity Scenarios Investigated (mg/L, unless noted otherwise)	63
Table 38: Establishment time for salinity scenarios	70

List of Figures

Figure 1: Geochemical Model Setup
Figure 2: Range of Eh-pH conditions in natural environments based on data of Baas-Becking et al. (1960)
Figure 3: Saturation indices in hard rock pit lakes for equilibrium partial pressures of CO ₂ (gas) (Eary, 1999)
Figure 4: Pit Contours
Figure 5: Comparison between observed, patched point and stochastic rainfall datasets
Figure 6: Stochastic annual rainfall for "centre of mine void"
Figure 7: Monthly air temperature (°C) modelled for the period 1970 - 1997
Figure 8: Monthly air temperature variation (°C)
Figure 9: Monthly shortwave solar radiation (W/m ²) for the period 1970 to 1997
Figure 10: Variation in water vapour pressure (hPa) from 1970 to 1997
Figure 11: Frequency Histogram
Figure 12: Pit Catchment Plan
Figure 13: Major geological units
Figure 14: Predicted pit lake water levels
Figure 15: Perspective View
Figure 16: Tornado Chart Showing Parameter Sensitivity
Figure 17: Timestep comparison during initial lake formations
Figure 18: Timestep comparison during quasi-steady state water level condition
Figure 19: Water Level Predictions with 50% Increase in Mean Annual Rainfall
Figure 20: Water Level Predictions with 30% Decrease in Mean Annual Rainfall
Figure 21: Effect of PMP on 50 th percentile pit lake water levels
Figure 22: Major Factors in Stratification (redrawn after Boland and Lawton, 1996)
Figure 23: Major Factors in Mixing (redrawn after Boland and Lawton, 1996)
Figure 24: Salinity of Inflow Surface Water
Figure 25: Case L1a (salinity 10,000 mg/L)
Figure 26: Case L1b (salinity 20,000 mg/L)
Figure 27: Case L1c (salinity 30,000 mg/L)
Figure 28: Case L1d (salinity 40,000 mg/L)
Figure 29: Case L2a (salinity 30,000 mg/L, K _d 0.1)
Figure 30: Case L2b (salinity 30,000 mg/L, K _d 0.5)
Figure 31: Case L2c (salinity 30,000 mg/L, K _d 2.0)

List of Attachments

Attachment 1: Water Quality Sensitivity Analyses
Attachment 2: Uranium species included in the geochemical model

Executive Summary

The proposed Olympic Dam open cut mine would result in a final void with a footprint of 1,119 ha, being approximately 3.5 km wide by 4.1 km long. The depth of the final void would be approximately 1 km. At completion of mining pit dewatering would cease and direct rainfall, surface runoff and groundwater seepage would enter the void. The purpose of this study was to establish whether a permanent pit lake would form, assess the risk of overflow of pit lake water from the void into the surrounding environment, predict the pit lake water quality and identify the limnological processes operating within the pit lake.

The study utilised three conceptual/numerical models as described below:

- Water Balance Model – developed using GoldSim, the water balance model incorporates uncertainty analysis utilising Monte Carlo techniques, modification of evaporation rates due to salinity changes and transient groundwater inflow predictions. Sensitivity analysis was performed on input parameters and the model timestep, and included consideration of climate change and extreme storm events;
- Water Quality Model – developed using PHREEQC, the water quality model was automated to simulate the evolution of the pit lake over time. The model included mixing of input waters, precipitation of minerals and evapoconcentration effects. Sensitivity analysis was performed on key model variables including carbon dioxide partial pressure, pit wall oxidation rate, groundwater chemistry and lake water level; and
- Limnology Model – developed using DYRESM, the one-dimensional model predicts the vertical variation in temperature, salinity and density. Sensitivity analysis was performed on lake turbidity and salinity.

The evolution of the pit lake was found to be a slow process within the semi-arid setting of Olympic Dam. Hydrologic and geochemical steady state conditions are not likely to be realised for at least 3,000 years.

The water balance predicts that a permanent lake would form within the open cut mine void. The primary source of water to the open pit is expected to be groundwater seepage, followed by pit wall runoff and incident rainfall. Runoff from external catchments intersected by the pit is expected to be a relatively small source.

The water balance indicates that overflows from the pit are not expected to occur at any time. Scenarios considering the effect of climate change, extreme rainfall events and enhanced groundwater inflow also indicate that overflows would not occur.

The pit lake is expected to equilibrate at a quasi steady state elevation of between -310 mAHD (97.5 percentile) and -690 mAHD (2.5 percentile). The 50th percentile water level is -530 mAHD, which equates to a water depth of approximately 340 m and would sit some 630 m below natural ground level.

The elevation of the pit lake water surface would sit below the elevation of the major aquifers intersected by the pit. The pit lake would act as a permanent groundwater sink and would drain the regional groundwater system indefinitely. The effect of this on the regional groundwater system and groundwater users is discussed in the EIS.

Evapo-concentration is the dominant process affecting the water chemistry of the pit lake. It is predicted that in the early stages of formation the pit lake would have a salinity approximately half that of seawater. Within approximately 250 years the salinity is predicted to be equivalent to seawater, and over time, would become progressively hypersaline. As the salinity increases it is expected that a range of secondary minerals would form within the lake, predominantly at the lake surface where evapo-concentration effects are highest.

Limnological assessment and modelling suggests that as the salinity increases (and hence also the density), near mixed conditions would occur throughout the year. Heating and cooling would continue to occur at the surface, however the density changes associated with this would be small and mixed conditions are expected to prevail.

Four major stages in the evolution of the pit lake have been identified as described below:

- Lake formation (0-100 years post closure).
 - water levels would rise rapidly;
 - metal concentrations would be relatively low, but increase over time since the pit would act as a sink for groundwater and surface water inflows;
 - ferrihydrite is predicted to readily precipitate and form a coating over the bed of the pit lake, and would also influence (reduce) the concentration of a range of metals through adsorption;
 - barium and arsenic concentrations would be maintained very low due to precipitation of barite; and
 - the lake may periodically stratify during summer, causing anoxic zones to form at depth, however the surface water inflows and increasing water levels may cause periodic mixing.
- Stratified lake (100-250 years post closure).
 - water level increases would begin to slow;
 - localised calcite crusting may form at the edges of the lake due to evapoconcentration. Co-precipitation of metals (e.g. manganese, zinc and nickel) may occur; and
 - stratification is likely to be pronounced during summer, with mixed conditions during winter.
- Periodic surface crust (250-3,000 years post closure).
 - salinity is expected to approach that of sea water by about 250 years post closure;
 - the salinity would become the dominant factor affecting water density and stratification during summer is expected to decline. Near mixed conditions would occur throughout the year (i.e. water parameters would be the same throughout the entire water column);
 - gypsum surface crusting is expected to form, possibly displacing or coexisting with calcite;
 - it is expected that the crust would be relatively insoluble, but may be periodically redissolved during large storm events; and
 - uranium concentrations may begin to decline in the latter part of this stage due to precipitation of sodium autinite.

- Extensive salt crusting (> 3,000 years post closure).
 - an extensive halite salt crust is predicted to form at the surface; and
 - the salt crust is likely to be permanent, but could possibly dissolve during large storm events.

1.0 Introduction

This report describes the potential for development of a lake within the final void of the proposed open cut mine at Olympic Dam. Lake limnological and geochemical processes are discussed to provide an insight into the likely water quality of the pit lake that may develop within the final void.

The study objectives are to:

- predict whether a of pit lake would form within the final void;
- quantify the risk of overflow of pit lake water to the surface environment;
- assess whether the final void would be a permanent sink for groundwater from the two major aquifer systems (i.e. Corraberra Sandstone aquifer, Andamooka Limestone aquifer);
- predict pit lake water quality including pH, salinity and metals;
- predict mineral precipitation sequences and timing;
- assess whether the pit lake would be subject to seasonal stratification; and
- identify the major stages of pit lake evolution.

The evolution of the pit lake is likely to be a slow process within the semi-arid environment setting. A very long timeframe (3,000 years) is considered in this study in order to identify the hydrologic and geochemical steady state conditions that would eventually be achieved.

There is uncertainty in the processes and variables controlling the formation of the lake and the physical and chemical processes within the pit lake. A combination of uncertainty analysis using Monte Carlo techniques and sensitivity analysis is adopted to address the uncertainty.

This report comprises a technical paper forming part of the Olympic Dam Expansion EIS. Refer to the EIS for details of the proposal, setting and context of the supporting technical studies.

This report is a technical study of the pit lake formation, chemistry and limnology. Environmental implications associated with the presence of a lake are not addressed in this study. The EIS discusses the potential environmental impacts on flora, fauna, humans and natural systems (e.g. groundwater, surface water hydrology).

2.0 Methodology

2.1 Final Void Profile

The final void geometry is based on the mine plan optimisation model generated by BHP Billiton Resource Development Group in February 2008. The final void is based on the 2050 mined profile. The geometry is indicative only, and the final levels will depend on future mine planning, resource and economic factors. For the purposes of this study, minor variations in internal geometry are unlikely to result in significant changes to the pit lake formation and behaviour because of the large pit footprint and large pit storage capacity.

2.2 Climatic Data

Three types of conceptual / numerical models were used in the pit lake assessment: water balance model; water quality model; and limnological model. **Table 1** presents a summary of the climate data used for each of these models.

Table 1: Summary of Climatic Data Inputs Used

Climate data	Model type		
	Water balance	Water quality	Limnology
Rainfall	3000 years (annual) stochastic ^(a) 117 years (daily) patched point ^(b)	3000 years (annual) stochastic	15 years patched point (1970 – 1985)
Pan evaporation	117 years patched-point (repeated)	117 years patched-point (repeated)	Not used
Air temperature	Not used	Not used	15 patched point (1970 – 1985)
Shortwave solar radiation	Not used	Not used	15 years patched-point* (1970 – 1985)
Longwave solar radiation	Not used	Not used	15 years observed (Andamooka 1970 – 1985)
Water vapour pressure	Not used	Not used	15 years patched-point* (1970 – 1985)
Wind speed	Not used	Not used	4 years observed data (mine site data 1993 – 1996), condensed and repeated

Notes: * Observed data not available

(a) stochastic data used for annual model timestep

(b) patched point data used for daily model timestep

15 years data adopted in limnology study covers period 1992 – 2003 which is the only time period when all data inputs are collected concurrently

Patched-point data covering a period of 117 years (1889-2006) was sourced from the DataDrill database, developed by the Queensland Department of Natural Resources and Mines (QNR&M) and covering the whole of Australia. DataDrill accesses grids of data interpolated (using splining and kriging techniques) from point observations by the Bureau of Meteorology (BOM). The patched-point data is considered superior to site observations for modelling purposes because it draws on a greater dataset, both spatially and in time. Comparison was made between the patched-point data and the observed data.

Using historical climate data (or patched-point data) as inputs into hydrological models provides results that are based on only one realisation of the past climate. Stochastic climate data provide alternative realisations that are equally likely to occur, and can therefore be used as inputs into hydrological and ecological models to quantify uncertainty in environmental systems associated with climate variability (as opposed to climate change). Stochastic rainfall data was generated using the Stochastic Climate Library (SCL) developed by the Cooperative Research Centre (CRC) for Catchment Hydrology. Three thousand years of stochastic rainfall data was developed based on 200 replicates of the 117 year patched-point data. Statistical comparison was made between the observed, patched-point and stochastic rainfall datasets.

Various meteorological data is required as input to the limnological model. It was therefore necessary to operate the model over the period in which all data inputs were collected concurrently (i.e. 1970-1987). Patched-point data over this period was used for shortwave radiation and water vapour pressure because site collected data was not available.

The predictions made in this report span 3,000 years, and therefore it is likely that the observed climatic data collected over the last century (on which the model input data is based) will differ from that occurring in the future. Both natural and anthropogenic causes of climate change are likely to occur. The potential effects of climate change on the pit lake water balance were considered in this study. Climate change scenarios were considered in the water balance model. Anthropogenic climate change predictions were sourced from the CSIRO (2007) and IPCC (2007) studies. The potential for natural climate change was assessed by consideration of paleoclimatology to identify the range of climates experienced in the Holocene Epoch (i.e. last 10,000 years).

2.3 Water Balance

The development of a pit lake within the final mine void is dependent on the relationship between the following dominant factors:

- Incident rainfall (R);
- Surface water runoff (S);
 - External catchment; and
 - Pit wall.
- Groundwater seepage (G);
 - Andamooka limestone aquifer;
 - Corraberra sandstone / Arcoona quartzite aquifer; and
 - Basement (ODBC) aquifer;
- Evaporation (E).

Where, $\Delta storage = R + S + G - E$

A water balance model of the pit lake was developed in GoldSim, a widely adopted platform for mine site water balance studies. Key features of the Olympic Dam pit lake model include:

- Uncertainty analysis utilising Monte Carlo techniques;
- Modification of evaporation rate due to salinity increases arising from evapo-concentration;
- Modification of pit wall catchment areas based on the pit lake area;
- Incorporation of transient groundwater inflow predictions due to Rock Storage Facility (RSF) and Tailings Storage Facility (TSF) influences;
- Sensitivity analysis of input parameters and the model timestep;
- Consideration of climate change;
- Consideration of extreme storm events.

The model was routed for 3,000 years, which was found to be of a sufficiently long duration to reach steady-state conditions. The water balance model was used to predict the likely pit lake filling rate, and identify the range of water levels that may develop.

2.3.1 Model Timestep

The model was based on an annual timestep on the basis that the storage capacity of the final void is three orders of magnitude greater than the average combined annual inflows, and two orders of magnitude greater than the peak combined annual inflows. This suggests that the pit lake water level will not be sensitive to individual storm events or short-term (i.e. sub-annual) wet periods.

A sensitivity model run was completed using 117 years of daily data to demonstrate the adequacy of an annual timestep.

2.3.2 Model Uncertainty

Many of the water balance model variables are not measured values and the selection of appropriate values introduces some inherent uncertainty. The water balance was constructed using probabilistic simulation, which involves explicitly representing this uncertainty by specifying inputs as probability distributions and specifying any random events that could affect the system. The probability distributions are assumed based on the range of expected values.

GoldSim uses advanced Monte Carlo simulation techniques to propagate the uncertainty in model inputs to model outputs.

Since the inputs describing the water balance are uncertain, the pit lake level predictions are also uncertain. That is, the result of any analysis based on inputs represented by probability distributions is itself a probability distribution. This type of result is typically more useful for understanding risks than a traditional deterministic simulation which provides a single result based on "the best guess" or "worst case" values, without providing context of the likelihood of this scenario actually occurring.

2.3.3 Model Inputs

2.3.3.1 Incident Rainfall

Incident rainfall onto the pit lake surface was assumed to directly contribute to pit water levels, that is, there are no losses. The water balance model considers the surface area of the lake when estimating the volume of incident rainfall.

2.3.3.2 External Catchment Runoff

The most suitable hydrological modelling technique based on the annual timestep is a lumped parameter called the Volumetric Runoff Coefficient (VRC). The VRC is a catchment-specific parameter that is derived using rainfall and stream gauging data. The VRC represents the proportion of rainfall that becomes runoff over an extended period. This technique is not suited to short duration or event-specific assessment, because antecedent conditions play a critical role, however for long term water balances with a coarse resolution, this provides a reliable technique and is adopted in this assessment.

There is no runoff gauging data in the vicinity of Olympic Dam so a VRC could not be derived explicitly. The following methodology was adopted for estimation of an appropriate VRC:

- Literature review to identify VRC in similar semi-arid Australian climates and landscapes;
- Review of stream gauging data in other regions of South Australia and Northern Territory to derive VRC from first principles;
- Establishment of a hydrological model suitable for estimating flows from ungauged catchments. The Australian Water Balance Model (AWBM) (Boughton 1993) is well-suited and widely applied for estimating flows from ungauged catchments, and was adopted in this assessment.

AWBM is a partial area saturation overland flow model. The use of partial areas divides the catchment into regions that produce runoff (contributing areas) during a rainfall-runoff event and those that do not. These contributing areas vary within a catchment according to antecedent catchment conditions, allowing for the spatial variability of surface storage in a catchment. The use of the partial area saturation overland flow approach is simple, and provides a good representation of the physical processes occurring in most Australian catchments (Boughton, 1993). This is because daily infiltration capacity is rarely exceeded, and the major source of runoff is from saturated areas.

The AWBM was used to investigate likely ranges of VRC for the water balance model, in addition to generating daily runoff data for the timestep sensitivity analysis.

2.3.3.3 Pit Wall Runoff

A similar approach to that described above was adopted to estimate the hydrological response of the pit walls. The literature review focussed on observations made in other mine voids from around the world. The AWBM was also modified to represent the pit walls to inform the selection of an appropriate VRC and develop daily runoff data for the timestep sensitivity analysis.

2.3.3.4 Evaporation

Evaporation from the pit lake was based on patched-point evaporation data, with the following correction factors:

- Pan factor – The pan factor accounts for the difference between measured “pan evaporation” and evaporation that occurs from an open water body. Pan evaporation is measured in a small dish that takes extra heat in through the sides of the pan and tends to overestimate lake evaporation. Evaporation rates from large water bodies are also diminished by the accumulation of humidity above the water surface (amongst other factors); and
- Salinity factor – The salinity factor accounts for the reduction in evaporation rate at increasing salinity. This reduction occurs due to the difference in vapour pressure over a saline solution compared to that over freshwater.

2.3.3.5 Groundwater

Groundwater inflow to the pit was predicted using the regional groundwater flow model. A groundwater inflow time series was extracted from the "Base Case" hydrogeological model which considers the permanent groundwater sink created by the pit, and seepage from the TSF and RSF. Details of the model are provided in the EIS.

2.3.4 Sensitivity Analysis

Sensitivity analysis was undertaken on the water balance model by running the model multiple times, systematically sampling each variable over a specified range, while holding all other variables constant. Sensitivity plots were produced (e.g. tornado chart) in order to compare variables to which the model is most sensitive.

2.3.5 Alternative Scenarios

The effect of climate change and an extreme rainfall event on the water level predictions was assessed through additional model runs. The extreme rainfall event considered the effect of a Probable Maximum Precipitation (PMP) event on the pit water levels.

2.4 Water Chemistry

2.4.1 Chemistry of Input Waters

External Catchment Runoff

There has been no detailed water quality data collected for surface waters in the vicinity of the proposed mine void. Opportunistic grab samples were collected during EIS fieldwork programs by ENSR in July 2006, and by REM in January 2007. Physico-chemical parameters (turbidity, pH, EC, temperature) were measured in the field on all samples, and two samples were analysed by ALS Environmental for a limited suite of analytes (HCO_3 , Cl, SO_4 , As, Ca, Cu, K, Mg, Na, Ni, Zn). The two samples subject to laboratory analysis were collected from land systems different to that in the vicinity of the proposed mine void, however the total dissolved solids (TDS) and electrical conductivity (EC25) of these samples compare well with those collected near to the final void, and therefore in the absence of site-specific data have been adopted to represent external catchment runoff.

The water quality of the pit lake is expected to be relatively insensitive to the composition of the external catchment runoff, since it has relatively low salinity when compared to other inputs such as groundwater inflow and pit wall runoff.

Runoff from the majority of the RSF would be drained away from the final void due to the geometry of the RSF design. A small portion of the outer batters may potentially drain towards the final void, however it is proposed that these outer batters are constructed of benign mine rock for their entire depth, and are therefore unlikely to produce runoff that has major differences to the produced from the surrounding landscape.

Pit Wall Runoff

The composition of pit wall runoff was estimated based on kinetic testing data completed as part of mine rock characterisation and RSF impact assessment. Full details of the kinetic testing program are provided in ENSR (2008).

ENSR (2008) provides salt and metal production rates for the various rock types likely to be exposed in the pit wall. The production rates are expressed in terms of mass of solute produced (i.e. available to flushing in stormwater runoff) per mass of rock.

The water chemistry of pit wall runoff was estimated using the following approach:

- estimation of surface area exposure of each rock type in the pit wall. This is based on vertical thickness of each rock unit and the circumference of the pit at the elevation of the rock unit;
- estimation of the mass of rock exposed in the pit wall assuming an oxidation depth of 5 mm. Consideration was also given to greater and lesser oxidation depths in the sensitivity analysis;
- estimation of the mass of salt and metals produced during weathering, based on the production rates calculated from kinetic testing; and
- estimation of the annual average runoff concentration using the runoff volume from the water balance model output.

This approach assumes that all oxidation products generated at the pit wall are transported by surface runoff into the pit lake.

It is noted that the elemental production rates determined in laboratory kinetic testing were applied directly for this study. The particle size of rock used in kinetic tests was crushed to -25 mm, which is typically representative of the most reactive particles in the pit wall.

Given the large area of pit wall exposure, the chemistry of the pit wall is expected to be an important control of pit lake chemistry. Sensitivity of the model to solute generation rates was assessed by adjusting the solute generation +/- 50 %. This is equivalent to considering oxidation depths of 2.5 mm and 7.5 mm, or differences between the particle sizes in the pit walls compared with the kinetic tests.

Andamooka Limestone Aquifer

Regular groundwater monitoring is undertaken in the vicinity of the proposed pit as part of the environmental monitoring program for the existing operations. Monitoring is undertaken near the existing TSF and away from the TSF in order to establish background conditions against which impact can be measured.

The dataset of background observations in the Andamooka Limestone aquifer consists of eight locations containing several observations over the period 1997-2007. This same data is used by BHP Billiton for comparison between monitoring results collected near to the TSF and background conditions in annual environmental reporting. A detailed suite of analytes is included in the chemical analysis (refer to **Section 6.1** for details).

While the chemical dataset appears complete and the charge balance is reasonable, analysis of the stoichiometry of major anions and cations indicates some potential inconsistency in the calcium, magnesium, bicarbonate and sulfate ratios expected from the mineralogy of the Andamooka Limestone formation. Manual adjustments were made to several anion and cation ratios in two sensitivity runs, to reflect those that would be expected from a groundwater sourced from this formation. One sensitivity run assesses a Ca:Mg:HCO₃ type groundwater, and the other assesses a Ca:SO₄ groundwater.

Corraberra Sandstone Aquifer

Groundwater monitoring data for the Corraberra Sandstone aquifer is available for the period 1994-2003. Monitoring was undertaken near the TSF and regionally (i.e. background) for the purpose of gauging impact of the TSF as described above. The dataset of background observations consists of three locations containing several observations. A detailed suite of analytes is included in the chemical analysis (refer **Section 6.1** for details).

Similar observations made above for the Andamooka Limestone regarding the stoichiometry of major anions and cations applies to the Corraberra aquifer. Two sensitivity runs were performed using modified ion ratios as described above.

Basement Aquifer

The basement is very low yielding and water quality data is rare. The most complete dataset was developed during early exploration and is compiled in AGC (1982). This consisted of seven boreholes penetrating into the basement, with water samples collected and analysed for major anions, cations and metals.

Sampling was also undertaken during construction of a new decline as part of the existing underground operations. The sample was collected by BHP Billiton environmental staff in November 2006 and analysed for a range of analytes at ALS Environmental.

Samples of water were sourced from the existing underground mine workings and collected from A block and F block dam by BHPB in October 2006. The water produced from the existing underground operation represents a mix of the major aquifer units described above. While the water quality is compromised by the influence of CAF (cement aggregate fill), the data on trace metals is likely to be less affected and was used to fill gaps in the basement aquifer data.

Similar observations made above for the Andamooka Limestone regarding the stoichiometry of major anions and cations applies to the Basement aquifer. Two sensitivity runs were performed using modified ion ratios as described above.

2.4.2 Geochemical Model

Model Code

Geochemical modelling is used as a tool to perform a wide variety of low temperature aqueous geochemical calculations. The geochemical model used for this study was the PHREEQC model, which was developed by Parkhurst (1995) for speciation, batch reaction, one dimensional transport and inverse geochemical calculations. The model can be used for simulating chemical reactions and transport processes in natural or polluted water and is widely used for this purpose. It is based on equilibrium chemistry of aqueous solutions interacting with minerals, gases, solid solution, exchange phase and sorption surfaces. An extensive chemical data base allows application of the reaction, transport, and inverse-modelling capabilities to almost any chemical reaction that is recognised to influence rain, soil, ground and surface water quality.

For the purposes of this study equilibrium is assumed. Care is therefore required during interpretation of results because some solids may react slowly (kinetically controlled) or require relatively high degrees of saturation to precipitate, remaining in solution in metastable states. If degrees of supersaturation are high, then sudden events (e.g. inputs of cold water and consequent mixing of fresh and saline waters with dilution) may induce nucleation and growth as long as the resulting solution still remains supersaturated. The geochemical modelling is therefore only a tool to assist in the understanding of the complex system.

PHREEQC modelling uses the extended versions of the Debye-Hückel expression to take account of increasing degrees of ion association, beyond simple ion pairing, present in solutions at ionic strengths above 0.1 mu. Beyond an ionic strength of 3 mu Debye-Hückel approaches become increasingly unreliable and results at ionic strengths greater than 3 mu should be interpreted with caution.

The elements / compounds included in the pit water quality study include: carbonate, bicarbonate, chloride, sulfate, aluminium, arsenic, barium, calcium, copper, iron, potassium, magnesium, manganese, sodium, nickel, lead, selenium, uranium, zinc, fluoride, silica and phosphorus.

The WATEQV4 thermodynamic database was adopted for this assessment, with some modifications to include a comprehensive range of uranium species. The full list of uranium species included in the model and data source (where “M” indicates *Minteq database* and “W” indicates *Wateq database*) is provided in **Attachment 2**.

Charge balancing is required to achieve stable model results and was completed using chloride, an abundant and conservative species, unless noted otherwise.

Model Development

The geochemical model was used initially to predict speciation and assess the saturation state of mineral phases within input waters. The model was then automated to simulate the evolution of the lake over time including mixing of input waters, precipitation of minerals and evapo-concentration effects.

The pit lake evolution model was constructed using the structure shown in **Figure 1**.

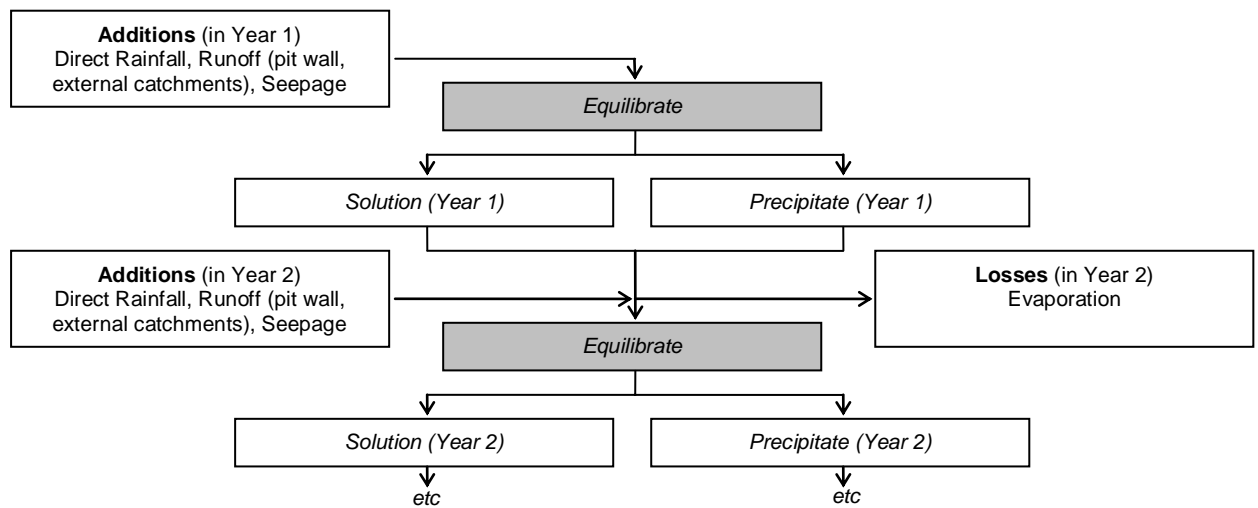


Figure 1: Geochemical Model Setup

The 'additions' to the system comprise input waters described previously and the 'losses' relate to evaporation. Both the additions and losses vary each timestep because they are based on stochastic data as well as a transient water balance. The adopted timestep for the geochemical model was 10 years.

Geochemical Controls

The geochemical model includes the following geochemical processes:

- aqueous speciation;
- precipitation of secondary minerals; and
- adsorption of metals onto iron oxy-hydroxides (surface complexation).

Secondary minerals may form when a solution becomes supersaturated with respect to the mineral phase being considered; although precipitation may not actually occur until moderate degrees of supersaturation are achieved. The factors that affect the saturation state include pH, redox, ion activity and the assemblage of other species.

The geochemical model was set up to permit secondary minerals to form when the saturation index (SI) is positive. In addition mineral phases are permitted to re-dissolve (if present) to the extent necessary to obtain equilibrium (SI=0). A list of possible secondary mineral phases has been developed based principally on reaction kinetics and is presented in **Table 2**. Nordstrom and Alpers (1999) identify common minerals that can be used for geochemical modelling. The selection of secondary mineral phases was compared with their study.

Table 2: Potential Secondary Mineral Phases

Mineral	Reaction	Log K	Major ions and metals in mineral matrix
Plumbogummite	$\text{PbAl}_3(\text{PO}_4)_2(\text{OH})_5 \cdot \text{H}_2\text{O} + 5\text{H}^+ \leftrightarrow \text{Pb}^{+2} + 3\text{Al}^{+3} + 2\text{PO}_4^{-3} + 6\text{H}_2\text{O}$	-32.790	Pb, Al
Amorphous structure of Al silicate* (surrogate: adularia)	$\text{KAlSi}_3\text{O}_8 + 8\text{H}_2\text{O} \leftrightarrow \text{K}^+ + \text{Al}(\text{OH})_4^- + 3\text{H}_4\text{SiO}_4$	-20.573	Al
Alunite-like phase	$\text{KAl}_3(\text{SO}_4)_2(\text{OH})_6 + 6\text{H}^+ \leftrightarrow \text{K}^+ + 3\text{Al}^{+3} + 2\text{SO}_4^{-2} + 6\text{H}_2\text{O}$	-1.4	Al, [at K site: Pb]
Aluminium oxy-hydroxides (surrogate: diaspore)	$\text{AlOOH} + 3\text{H}^+ \leftrightarrow \text{Al}^{+3} + 2\text{H}_2\text{O}$	6.879	Al
Kaolinite	$\text{Al}_2\text{Si}_2\text{O}_5(\text{OH})_4 + 6\text{H}^+ \leftrightarrow 2\text{Al}^{+3} + 2\text{H}_4\text{SiO}_4 + \text{H}_2\text{O}$	7.435	Al
Zeolites (surrogate: leonhardite)	$\text{Ca}_2\text{Al}_4\text{Si}_8\text{O}_{24} \cdot 7\text{H}_2\text{O} + 17\text{H}_2\text{O} \leftrightarrow 2\text{Ca}^{+2} + 4\text{Al}(\text{OH})_4^- + 8\text{H}_4\text{SiO}_4$	-69.756	Al, [at Ca site: Na, K]
Smectite-like phase (surrogate: Montmorillonite-BelleFourche)	$(\text{HNaK})_{0.09}\text{Mg}_{0.29}\text{Fe}_{0.24}\text{Al}_{1.57}\text{Si}_{3.93}\text{O}_{10}(\text{OH})_2 + 10\text{H}_2\text{O} \leftrightarrow 0.09\text{H}^+ + 0.09\text{Na}^+ + 0.09\text{K}^+ + 0.29\text{Mg}^{+2} + 0.24\text{Fe}^{+3} + 1.57\text{Al}(\text{OH})_4^- + 3.93\text{H}_4\text{SiO}_4$	-34.913	Al
Barite	$\text{BaSO}_4 \leftrightarrow \text{Ba}^{+2} + \text{SO}_4^{-2}$	-9.970	Ba, [at Ba site: Pb, Sr]

Mineral	Reaction	Log K	Major ions and metals in mineral matrix
Azurite	$\text{Cu}_3(\text{OH})_2(\text{CO}_3)_2 + 4\text{H}^+ \leftrightarrow 3\text{Cu}^{+2} + 2\text{H}_2\text{O} + 2\text{HCO}_3^-$	3.750	Cu
Malachite	$\text{Cu}_2(\text{OH})_2\text{CO}_3 + 3\text{H}^+ \leftrightarrow 2\text{Cu}^{+2} + 2\text{H}_2\text{O} + \text{HCO}_3^-$	5.150	Cu
Covellite			Cu
Fluorapatite	$\text{Ca}_5(\text{PO}_4)_3\text{F} + 3\text{H}^+ \leftrightarrow 5\text{Ca}^{+2} + 3\text{HPO}_4^{-2} + \text{F}^-$	-17.6	F , [at Ca site: Pb]
FCO ₃ Apatite*	$\text{Ca}_{9.316}\text{Na}_{0.36}\text{Mg}_{0.144}(\text{PO}_4)_{4.8}(\text{CO}_3)_{1.2}\text{F}_{2.48} \leftrightarrow 9.316\text{Ca}^{+2} + 0.36\text{Na}^+ + 0.144\text{Mg}^{+2} + 4.8\text{PO}_4^{-3} + 1.2\text{CO}_3^{-2} + 2.48\text{F}^-$	-114.4	F , [at Ca site: Pb]
Fluorite	$\text{CaF}_2 \leftrightarrow \text{Ca}^{+2} + 2\text{F}^-$	-10.6	F , [at Ca site: Pb , Sr]
Cerussite	$\text{PbCO}_3 \leftrightarrow \text{Pb}^{+2} + \text{CO}_3^{-2}$	-13.13	Pb , [at Pb site: Sr , Ba]
Clpyromorphite	$\text{Pb}_5(\text{PO}_4)_3\text{Cl} \leftrightarrow 5\text{Pb}^{+2} + 3\text{PO}_4^{-3} + \text{Cl}^-$	-84.430	Pb , [at Pb site: Sr , Ba]
Rhodochrosite	$\text{MnCO}_3 \leftrightarrow \text{Mn}^{+2} + \text{CO}_3^{-2}$	-11.13	Mn , [at Mn site: Ni , Co , Zn , Cd , Fe]
Bixbyite	$\text{Mn}_2\text{O}_3 + 6\text{H}^+ \leftrightarrow 2\text{Mn}^{+3} + 3\text{H}_2\text{O}$	-0.611	Mn
Manganite	$\text{MnOOH} + 3\text{H}^+ + \text{e}^- \leftrightarrow \text{Mn}^{+2} + 2\text{H}_2\text{O}$	25.340	Mn
Strontianite	$\text{SrCO}_3 \leftrightarrow \text{Sr}^{+2} + \text{CO}_3^{-2}$	-9.271	Sr , [at Sr site: Pb , Ba]
Celesite	$\text{SrSO}_4 \leftrightarrow \text{Sr}^{+2} + \text{SO}_4^{-2}$	-6.63	Sr , [at Sr site: Pb , Ba]
Na-Autunite	$\text{Na}_2(\text{UO}_2)_2(\text{PO}_4)_2 \leftrightarrow 2\text{Na}^+ + 2\text{UO}_2^{+2} + 2\text{PO}_4^{-3}$	-47.409	U
Rutherfordine	$\text{UO}_2\text{CO}_3 \leftrightarrow \text{UO}_2^{+2} + \text{CO}_3^{-2}$	-14.450	U
Uraninite with non-stoichiometric U-oxide structures (surrogate: U ₄ O ₉)	$\text{U}_4\text{O}_9 + 18\text{H}^+ + 2\text{e}^- \leftrightarrow 4\text{U}^{+4} + 9\text{H}_2\text{O}$	-3.384	U
Uraninite	$\text{UO}_2 + 4\text{H}^+ \leftrightarrow \text{U}^{+4} + 2\text{H}_2\text{O}$	-4.8	U
Schoepite	$\text{UO}_2(\text{OH})_2 \cdot \text{H}_2\text{O} + 2\text{H}^+ = \text{UO}_2^{+2} + 3\text{H}_2\text{O}$	5.404	U
Smithsonite	$\text{ZnCO}_3 \leftrightarrow \text{Zn}^{+2} + \text{CO}_3^{-2}$	-10.0	Zn , [at Zn site: Cd , Mn , Co , Ni]
Scorodite	$\text{FeAsO}_4 \cdot 2\text{H}_2\text{O} \leftrightarrow \text{Fe}^{+3} + \text{AsO}_4^{-3} + 2\text{H}_2\text{O}$	-20.249	As
Huntite	$\text{CaMg}_3(\text{CO}_3)_4 \leftrightarrow 3\text{Mg}^{+2} + \text{Ca}^{+2} + 4\text{CO}_3^{-2}$	-29.968	
Cristobalite	$\text{SiO}_2 + 2\text{H}_2\text{O} \leftrightarrow \text{H}_4\text{SiO}_4$	-3.587	
Magnesite	$\text{MgCO}_3 \leftrightarrow \text{Mg}^{+2} + \text{CO}_3^{-2}$	-8.029	[at Mg site: Mn , Zn , Ni , Co]
Goethite	$\text{FeOOH} + 3\text{H}^+ \leftrightarrow \text{Fe}^{+3} + 2\text{H}_2\text{O}$	-1.0	[at Fe site: Mn , Ni , Co]

Mineral	Reaction	Log K	Major ions and metals in mineral matrix
Calcite	$\text{CaCO}_3^{2-} \leftrightarrow \text{Ca}^{2+} + \text{CO}_3^{2-}$	8.480	[at Ca site: Mn, Sr, Zn, Ni, Co, Mg]
Gypsum	$\text{CaSO}_4 \cdot 2\text{H}_2\text{O} \leftrightarrow \text{Ca}^{+2} + \text{SO}_4^{-2} + 2\text{H}_2\text{O}$	-4.58	[at Ca site: Sr, Ba]
Jarosite-Na*	$\text{NaFe}_3(\text{SO}_4)_2(\text{OH})_6 + 6\text{H}^+ \leftrightarrow \text{Na}^+ + 3\text{Fe}^{+3} + 2\text{SO}_4^{-2} + 6\text{H}_2\text{O}$	-5.280	
Halite	$\text{NaCl} \leftrightarrow \text{Na}^+ + \text{Cl}^-$	1.582	[at 2xNa sites: Sr, Pb]
Ferrihydrite	Based on Dzombak and Morel (1990)		Various metals

Notes: Metals in parenthesis may be co-precipitated at the site nominated

The thermodynamic database that underlies the geochemical model does not include all likely mineral phases and structures. There are often many crystalline forms of minerals that are not included in the thermodynamic database. The approach for this study has been to adopt mineral phases included in the database that most closely represent mineral phases expected to occur. Hence, some of the minerals have been used as “surrogates” for similar (amorphous) mineral phases that are expected to form. Discussion is provided in the results regarding the likelihood and form of the mineral phases exhibiting control.

Co-precipitation mechanisms are also likely to be a control on metal solubility; however, given the lack of information regarding necessary input parameters, qualitative commentary is only possible at this stage. Metals that may be co-precipitated within mineral phases are included in **Table 2**.

Adsorption of ions onto iron oxy-hydroxides was included in the geochemical model as a surface complexation reaction. The properties of the iron oxy-hydroxides are based on Dzombak and Morel (1990) hydrous ferric oxide experimentation (i.e. 0.2 mol weak sites per mol Fe, 0.005 mol strong sites per mol Fe, surface area of $5.33 \times 10^4 \text{ m}^2/\text{mol}$).

pH

pH of the pit lake was estimated from the mixing ratios of inputs waters. The pH is principally a function of the input water pH, but also affected by redox potential and carbon dioxide partial pressure assumptions.

Redox Potential

A range of redox conditions are anticipated within the pit lake. It is expected that near-surface layers in contact with atmosphere would be relatively well mixed and remain oxygenated, primarily as a result of wind induced turbulence. The extent to which the oxygen is distributed vertically within the water column is dependent on whether stratification occurs, and the strength and duration of the stratification. Deeper layers are more likely to be oxygen depleted, especially during stratification events. **Figure 2** shows the relationship between pH and Eh for various environments.

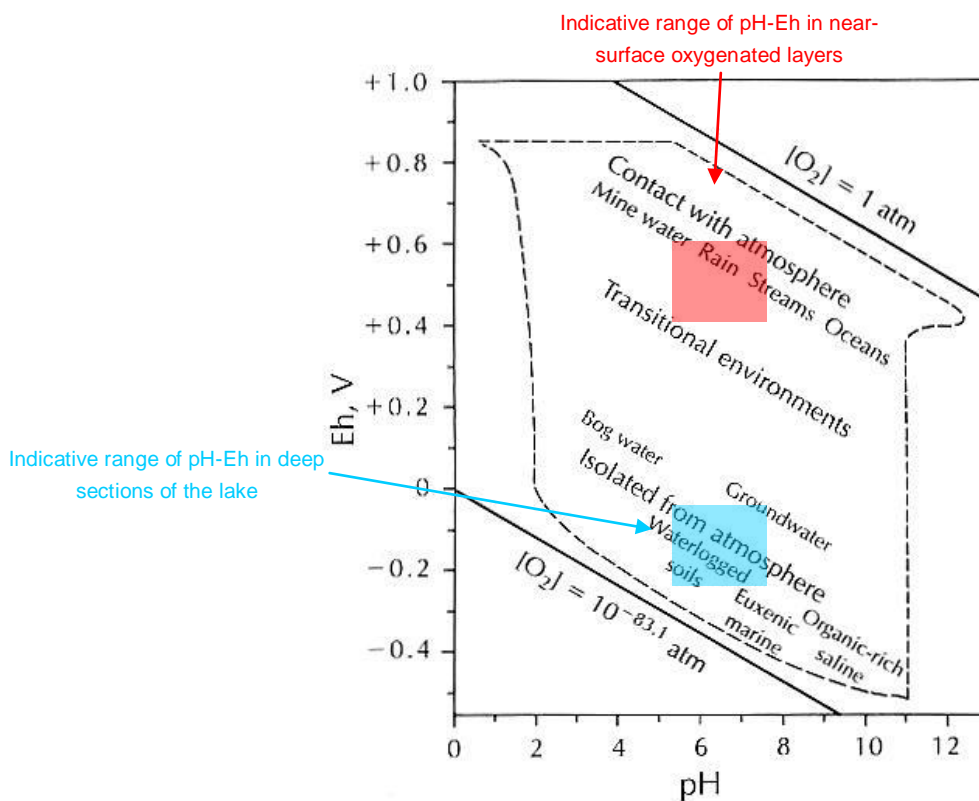


Figure 2: Range of Eh-pH conditions in natural environments based on data of Baas-Becking et al. (1960)

Based on **Figure 2**, Eh is expected to lie in the range +400 to +600 mV within the near-surface horizons of the pit lake. Based on Manahan (2005) $Eh (mV) = 59.2pe$ (at 25°C), a pe range of +6.8 to +10.1 is expected.

Less oxidised conditions would be anticipated at depth within the pit lake. A range of precipitation and dissolution reactions would occur at various levels within the water column due to the variation of redox potential with depth. The processes are not considered in this study because this study is concerned with near-surface water chemistry. The near-surface waters would be accessible to humans and terrestrial fauna and salt precipitation (due to evapo-concentration) would also occur in this region.

Carbon Dioxide

Carbon dioxide is an important gas in lakes. As carbon dioxide dissolves in water, it forms a series of compounds, including carbonic acid, bicarbonate, and carbonate that effect pH. The equilibrium condition that is established with CO₂ (gas) varies with temperature, biological activity and mixing processes. A review of various mine voids around the world was completed by Eary (1999) and the relationship between pH and carbon dioxide shown in **Figure 3** was derived. This indicates that the likely range of CO₂ (g) partial pressures varies from 10⁻² atm to 10^{-3.5} atm (atmospheric carbon dioxide partial pressure). A sensitivity analysis was conducted over this range to assess the effect of this variable.

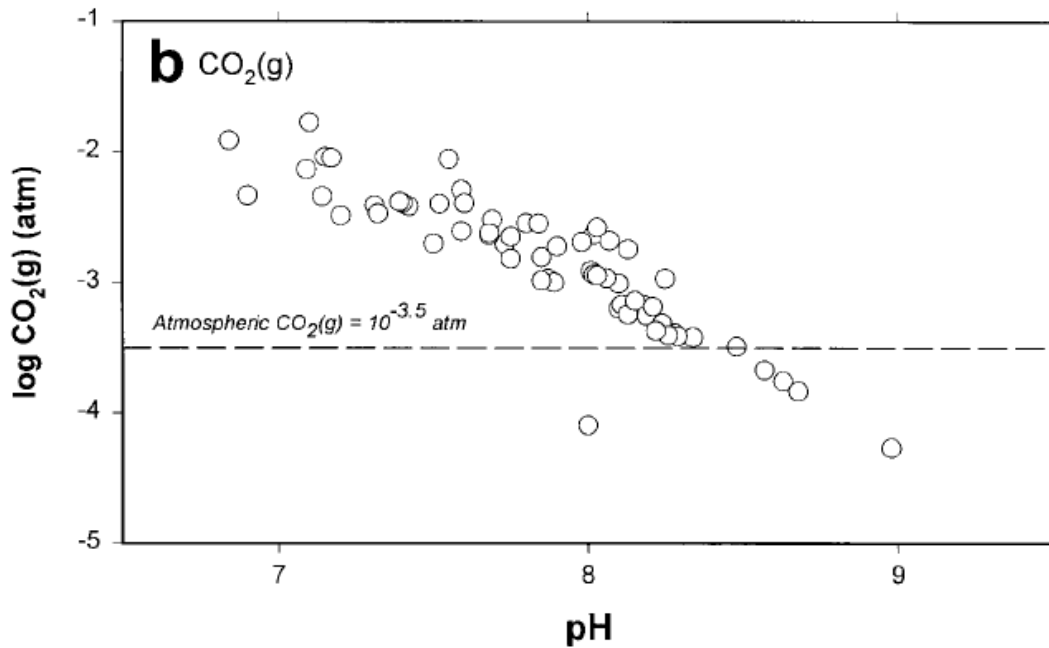


Figure 3: Saturation indices in hard rock pit lakes for equilibrium partial pressures of CO₂ (gas) (Eary, 1999)

2.4.3 Sensitivity Analysis

The range of input parameters assessed through sensitivity analysis is described in **Section 2.4.2** and is summarised in **Table 3**.

Table 3: Geochemical Model Sensitivity Analysis Scenarios

Case	Description	Water balance case	Pit wall generation multiple*	Partial pressure CO ₂ (atm)
G1	Base Case	50 percentile	1.0	10 ^{-3.5}
G2a	Low water level	2.5 percentile	1.0	10 ^{-3.5}
G2b	High water level	97.5 percentile	1.0	10 ^{-3.5}
G3a	Low pit wall solute generation	50 percentile	0.0	10 ^{-3.5}
G3b	High pit wall solute generation	50 percentile	2.0	10 ^{-3.5}
G4	Higher CO ₂ (g) concentration	50 percentile	1.0	10 ^{-2.0}
G5	Ca:Mg:HCO ₃ input groundwaters	50 percentile	1.0	10 ^{-3.5}
G6	Ca:SO ₄ input groundwaters	50 percentile	1.0	10 ^{-3.5}

Notes: * chemistry varied only (i.e. not flow)

^ Where selected ion does not achieve charge balance of the input water, the opposite charge ion (either chloride or potassium) was adopted for that input water. Chloride and potassium were selected since they are conservative and non-reactive

2.5 Limnology

2.5.1 Limnological Model

Model Code

Limnological modelling was undertaken using the one-dimensional hydraulic model DYRESM developed by the Centre for Water Research, University of Western Australia. DYRESM simulates the one-dimensional thermal structure of a lake over time. The model uses a range of environmental variables affecting the stability of the water column and acting to influence seasonal stratification and mixing.

The model was run over a 17 year period (with data sourced from 1970 – 1986), which was the longest duration over which all necessary data inputs were concurrently available. The model period is sufficiently long to allow inter-annual climatic variation to be assessed. The model was operated on a daily timestep.

Model Parameters

Pit lake bathymetry, meteorological data, inflow rates and salinity were used the model as a time series covering the model duration. The inflow rates were developed from the water balance model and the salinities were derived from the geochemical model.

The extinction coefficient is a key model variable describing the attenuation of light in the water column. Under stratified conditions, the depth of the surface layer is largely governed by the rate of attenuation of light energy in the surface layer. It is anticipated that the pit water would be slightly turbid, due to the presence of barite which may inhibit aluminium flocculation, plus the dispersive nature of some rock / soil units. The default value of 0.25 infers that a Secchi disc would not be visible below approximately 15 m, which is considered appropriate for the likely optical characteristics of the water. A sensitivity analysis was conducted using 0.1, 0.5 and 2.0 which equates to visibility ranging from approximately 40 m, 10 m and 2 m respectively.

The water temperature was estimated as the average air temperature over the previous 4 days.

2.5.2 Sensitivity Analysis

The range of input parameters assessed through sensitivity analysis is described in **Section 2.5.2**, and is summarised in **Table 4**.

It was not considered necessary to carry the water balance or geochemical scenarios forward into the limnological sensitivity analysis. The range of possible water level and salinity conditions established in the previous sensitivity analyses can be assessed based on the steady-state model results. That is, the time over which the limnological profiles evolve will vary (as defined previously but the profiles would be similar).

Table 4: Limnological Sensitivity Analysis Scenarios

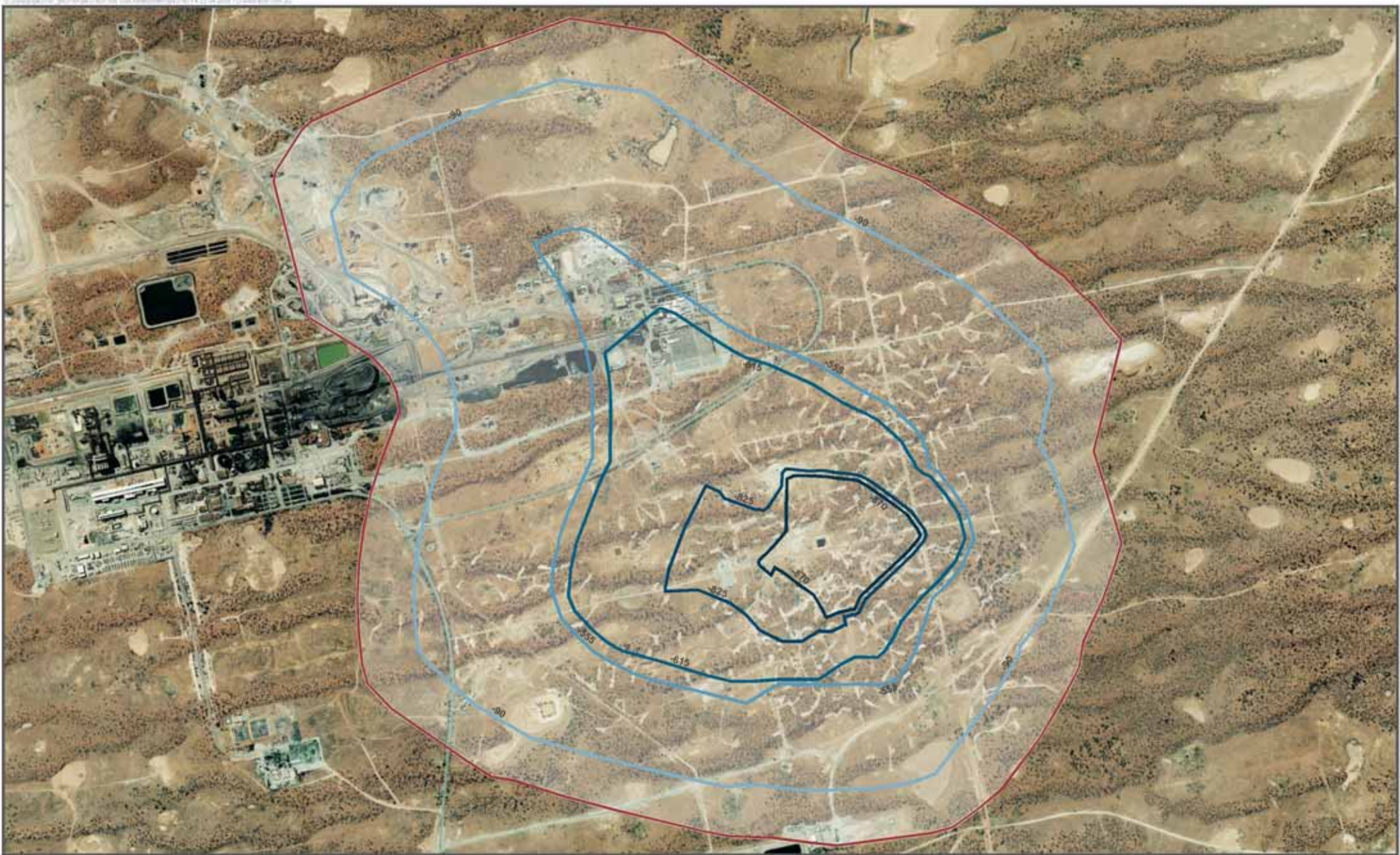
Case	Description	Water balance case	Geochemical model case	Extinction coefficient (K_d)
L1a	Base Case: Salinity ~10,000mg/l	50 th percentile	G1	0.25
L1b	Base Case: Salinity ~20,000mg/l	50 th percentile	G1	0.25
L1c	Base Case: Salinity ~30,000mg/l	50 th percentile	G1	0.25
L1d	Base Case: Salinity ~40,000mg/l	50 th percentile	G1	0.25
L2a	40 m visibility (clear): Salinity ~30,000mg/l	50 th percentile	G1	0.1
L2b	10 m visibility (slightly turbid): Salinity ~30,000mg/l	50 th percentile	G1	0.5
L2c	1 m visibility (turbid): Salinity ~30,000mg/l	50 th percentile	G1	2.0

3.0 Final Void Profile

The final void geometry, provided by BHP Billiton Resource Development Group, is provided in **Table 5** and shown in **Figure 4**. The pit is likely to be constructed using 15 m benches in bedrock (41°) and 18 m benches in sediments (45°), although these details are unlikely to affect the pit lake behaviour.

Table 5: Final Void Profile

Elevation (mAHD)	Area (ha)
-870	29.72
-825	62.61
-615	217.6
-555	280.1
-91	803.3
94.885	1119



- Proposed pit boundary (RL 94.885m AHD)
- RL: -90m AHD
- RL: -55.5m AHD
- RL: -61.5m AHD
- RL: -82.5m AHD
- RL: -87.0m AHD

Figure 4 | Pit Contours
BHPBilliton
Final Void Assessment
 Olympic Dam, South Australia

4.0 Climate

4.1 Overview

Olympic Dam is located in a semi-arid region. Rainfall is low, unpredictable and sporadic, with no seasonal pattern. Average annual rainfall at Roxby Downs is 164 mm and the 10th and 90th percentiles are 71 and 290 mm respectively. On average, rain falls on 49 days per year.

Evaporation rates at Olympic Dam are high throughout the year and the annual average is 3,100 mm. The average evaporation rate far exceeds the average monthly rainfall and as a consequence surface water is rarely present.

4.2 Climate Data

4.2.1 Rainfall

Several rainfall data types were sourced / developed for this study including:

- Observed data – measured data;
- Patched point data – interpolated data from a range of observation points; and
- Stochastic data (based on patched-point data) – generated data with similar characteristics as the data on which it is based.

4.2.1.1 Observed Data

The observed rainfall record for Olympic Dam is insufficient as the available dataset range extends only 11 years from 1993 to 2003. It is only useful for comparison with the continuous observed rainfall dataset recorded at Roxby Downs as this covers a period of 76 years (1931 - 2006). A statistical summary of historical monthly rainfall at Roxby Downs is presented in **Table 6**.

Table 6: Statistical summary of historical monthly rainfall (mm) recorded at Roxby Downs

Statistic	Period												
	Jan	Feb	Mar	Apr	May	Jun	Jul	Aug	Sep	Oct	Nov	Dec	Year
Mean	18	23	14	8	16	13	11	11	10	15	12	13	163
Median	4	8	4	3	9	7	8	7	5	6	9	5	140
Standard deviation	30	34	37	11	22	15	12	12	17	20	15	18	96
Highest on record	154	152	270	48	136	74	50	55	106	104	64	87	582
Lowest on record	0	0	0	0	0	0	0	0	0	0	0	0	33
Mean raindays	2	2	1	2	3	3	2	3	2	2	2	2	26
No. of years	77	77	77	77	77	77	77	77	77	77	76	76	76

Table 7 presents the probability of monthly rainfall at Roxby Downs based on the observed historical rainfall dataset (**Table 6**).

Table 7: Probability of monthly rainfall recorded at Roxby Downs; amounts of rain (mm) received or exceeded in 100% - 0% of years

Statistic	Period												
	Jan	Feb	Mar	Apr	May	Jun	Jul	Aug	Sep	Oct	Nov	Dec	Year
Lowest on record	0	0	0	0	0	0	0	0	0	0	0	0	33
80% yrs at least	0	0	0	0	0	2	0	0	0	0	0	0	88
median, 50% yrs	4	8	4	3	9	7	8	7	5	6	9	5	140
20% yrs at least	31	39	15	13	29	23	17	21	16	27	19	22	216
Highest on record	154	152	270	48	136	74	50	55	106	104	64	87	582
Mean	18	23	14	8	16	13	11	11	10	15	12	13	163
Standard deviation	30	34	37	11	22	15	12	12	17	20	15	18	96

4.2.1.2 Patched-Point Data

Patched-point rainfall data covering a period of 119 years (1889 - 2006) was sourced from the DataDrill database. The gauging stations that were used are shown in **Table 8**. The record period and distance from the Olympic Dam special mining lease (SML) for each gauging station is also displayed. The table shows that prior to 1931 the patched-point dataset is based on interpolation of data from gauging stations that occur a significant distance (> 30 km, based largely on Andamooka and Woomera) from the proposed final void. The dataset is therefore less reliable prior to 1931; however it provides the best available historical information.

Table 8: Gauging stations in the vicinity of Olympic Dam

ID	Station name	Period of record		Distance from SML	Co-ordinates	
		Start	End		Long	Lat
16089	Roxby Downs (Olympic Dam)	1992	1997	1 km	-30.4494	136.8703
16096	Roxby Downs (Olympic Dam)	1997	Current	5 km	-30.4829	136.8772
16065	Andamooka	1965	Current	30 km	-30.4490	137.1692
16040	Roxby Downs Station	1931	Current	32 km	-30.7037	136.7533
16039	Woomera (Purple Downs)	1903	Current	38 km	-30.7888	136.8948
16071	Andamooka Homestead	1880	1907	45 km	-30.7300	137.2000
16035	Roxby Downs (Parakylia Station)	1936	Current	47 km	-30.4027	136.3920
16000	Woomera (Arcoona)	1882	Current	66 km	-31.0229	137.0491
16001	Woomera Aerodrome	1949	Current	78 km	-31.1558	136.8054
17128	Marree (Mulgaria)	1998	Current	79 km	-30.0728	137.5666

ID	Station name	Period of record		Distance from SML	Co-ordinates	
		Start	End		Long	Lat
17061	Stuarts Creek	1877	1930	84 km	-29.7000	137.0400
16004	Burando	1915	1967	87 km	-31.2000	136.6167
16037	Pimba	1915	1990	90 km	-31.2517	136.7983
17025	Finniss Springs	1920	1971	98 km	-29.7450	137.5050

Source: Bureau of Meteorology (2006)

4.2.1.3 Stochastic Data

Stochastic rainfall data was developed based on the patched-point data, with the objective of achieving similar characteristics (e.g. mean, variance and skew) as the source data. **Table 9** presents a comparison of descriptive statistics between the observed data, patched-point data and stochastically generated data.

Table 9: Comparison between the stochastic rainfall data and source data

Location	Roxby Downs (Olympic Dam) ¹	Roxby Downs Station ²	Centre of final void	Centre of final void
Source	Observed	Observed	Patched-point	Stochastic
Period	1993-2003	1931-2006	1889-2006	n/a
Count (years)	11	76	117	3,000
Mean (mm)	144.2	163.1	154.4	156.9
Standard Error	20.8	11.0	7.5	1.5
Median (mm)	124.2	140.0	137.3	143.0
Mode (mm)	ID	103.0	196.5	155.9
Standard Deviation	69.0	96.1	81.5	79.4
Sample Variance	4,759.2	9,242.8	6,637.2	6,308.9
Skewness	-0.03	1.6	1.2	1.2
Range (mm)	212.4	549.0	388.4	610.9
Minimum (mm)	28.0	33.0	24.8	10.2
Maximum (mm)	240.4	582.0	413.2	621.1

- Notes:
1. Combination of BOM station numbers 16089 and 16096
 2. Station number 16040
 3. Stochastic data was generated based on patched-point dataset
 4. ID – insufficient data

Figure 5 compares the rainfall percentiles of the abovementioned datasets. There is close agreement between the stochastic and the patch-point data (upon which the stochastic data is derived). There is some discrepancy towards the upper percentile (extreme) events, where the maximum rainfall prediction is higher in the stochastic dataset. However, the maximum values observed at Roxby Downs station are comparable to that observed in the long term data, and the stochastic data are therefore considered sufficiently representative of the rainfall pattern expected at site.

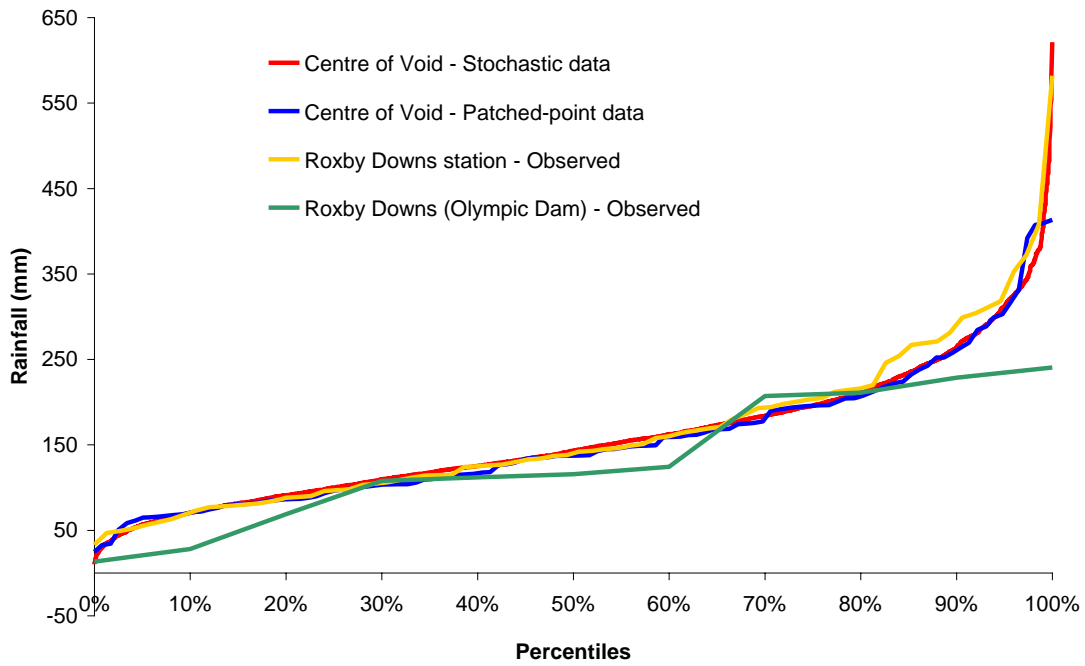


Figure 5: Comparison between observed, patched point and stochastic rainfall datasets

The adopted stochastic annual rainfall (mm) data for this study is shown below in **Figure 6** .

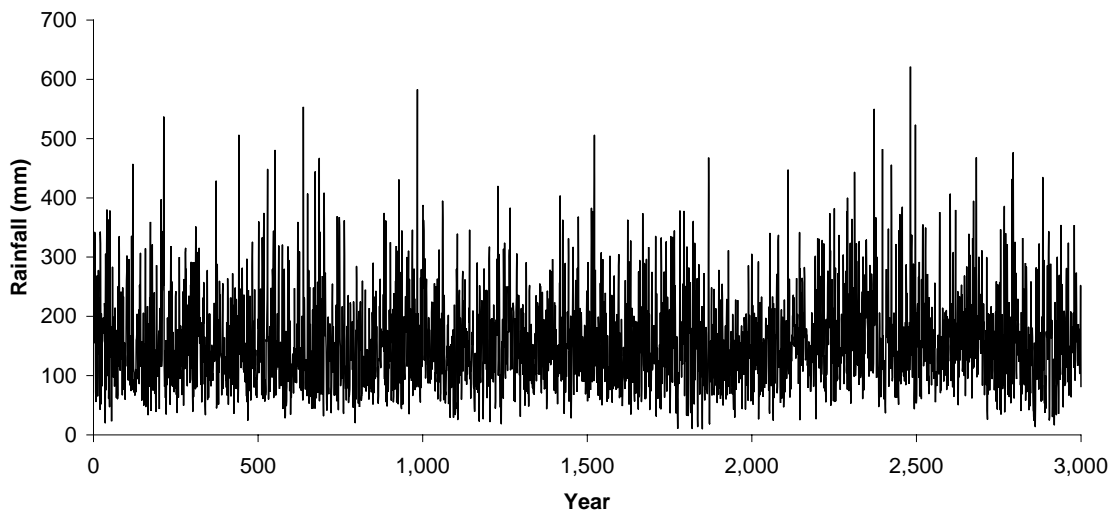


Figure 6: Stochastic annual rainfall for "centre of mine void"

4.2.2 Pan Evaporation

The patched-point data for daily pan evaporation (mm) was sourced from the DataDrill database and a summary of statistics for the period ranging from 1889 to 2006 is presented in **Table 10**.

Table 10: Summary statistics of daily patched point pan evaporation (mm/day) data for the period 1889 – 2006

Statistic	Value	Statistic	Value	Statistic	Value
Mean	8.3	Standard Deviation	4.075	Range	24.6
Standard Error	0.020	Sample Variance	16.61	Minimum	0.2
Median	8	Kurtosis	-1.176	Maximum	24.8
Mode	3.2	Skewness	0.191	Count	42,780

4.2.3 Air Temperature

Figure 7 below illustrates the seasonal variations in air temperature over the period 1970-1997, and includes the 17 year period modelled.

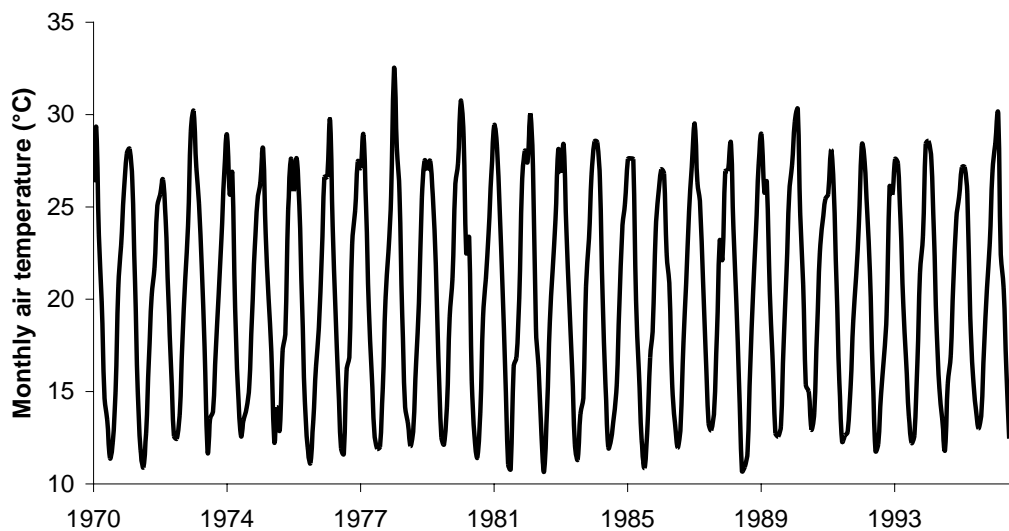


Figure 7: Monthly air temperature (°C) modelled for the period 1970 - 1997

Monthly air temperature variation is displayed in **Figure 8**.

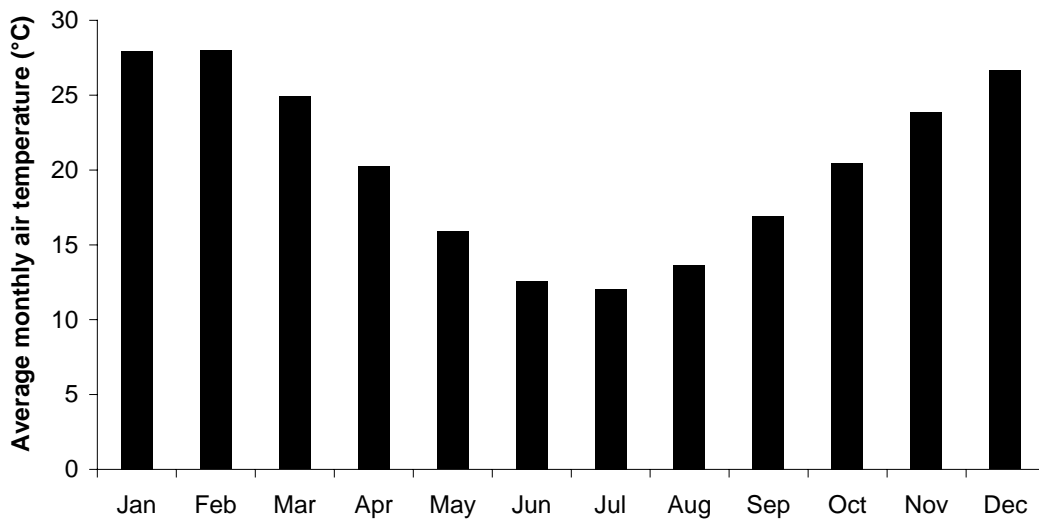


Figure 8: Monthly air temperature variation (°C)

Table 11 below displays the summary statistics of the modelled data, generated from patched-point data.

Table 11: Summary statistics of daily air temperature (°C) modelled for the period 1970 -1997

Statistic	Value	Statistic	Value	Statistic	Value
Mean	20.25	Standard Deviation	4.075	Range	32.0
Standard Error	0.0667	Sample Variance	16.61	Minimum	7.25
Median	20.0	Kurtosis	-1.176	Maximum	39.25
Mode	13.5	Skewness	0.191	Count	10,043

4.2.4 Shortwave Solar Radiation

Figure 9 and Table 12 illustrate the seasonal variation in short wave solar radiation over the period 1970 - 1997.

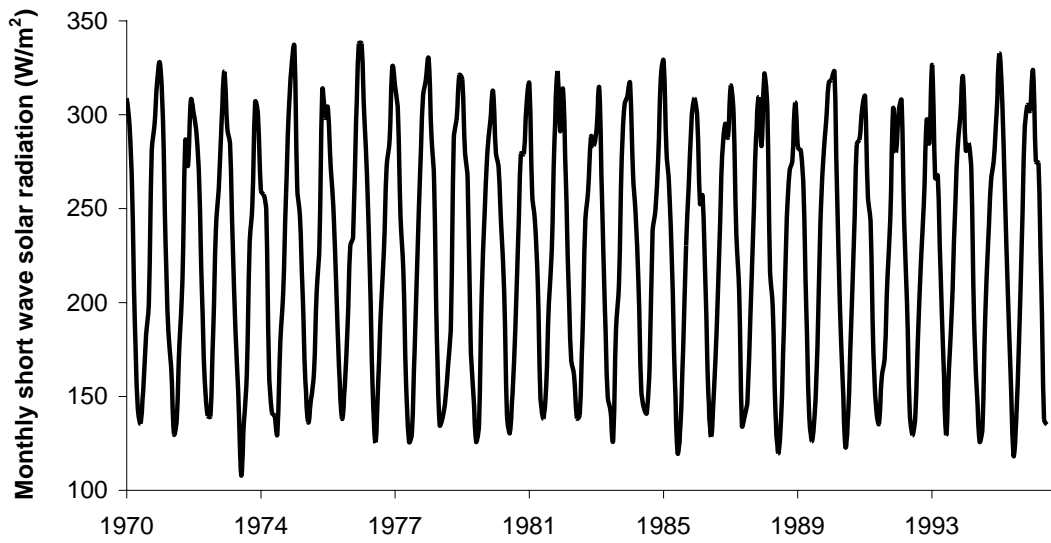


Figure 9: Monthly shortwave solar radiation (W/m^2) for the period 1970 to 1997

Table 12: Shortwave solar radiation summary statistics

Statistic	Value	Statistic	Value	Statistic	Value
Mean	228.9	Standard Deviation	79.13	Range	324.1
Standard Error	0.7896	Sample Variance	6262	Minimum	46.30
Median	231.5	Kurtosis	-1.074	Maximum	370.4
Mode	162.0	Skewness	-0.014	Count	10,043

4.2.5 Water Vapour Pressure

Figure 10 illustrates the seasonal variation in water vapour pressure as modelled for the period 1970 and 1997.

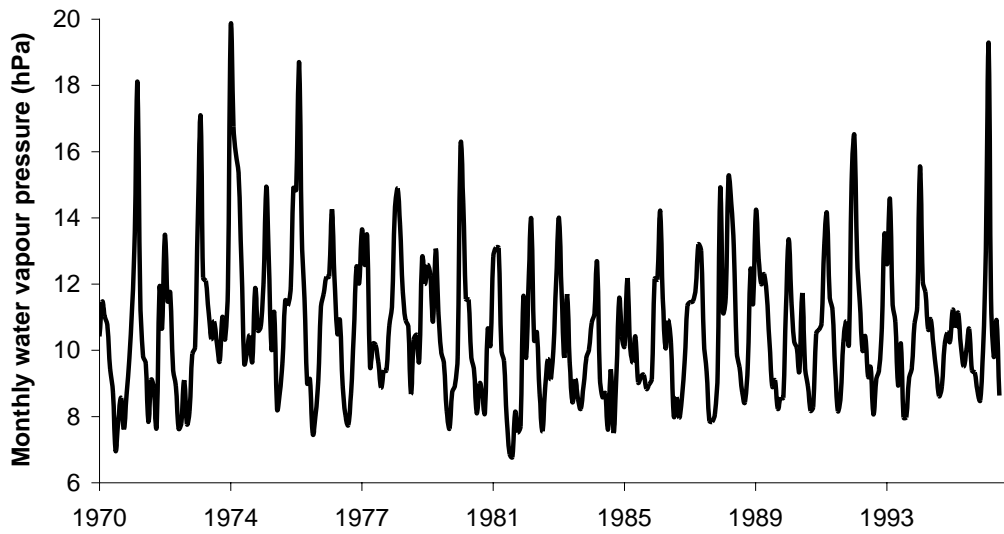


Figure 10: Variation in water vapour pressure (hPa) from 1970 to 1997

4.2.6 Wind Speed

The Olympic Dam weather station has only reliably recorded wind speed over the period 1993 – 1996. The data is recorded hourly, and for the purposes of modelling was averaged over 24 hours and repeated to cover the period 1970 – 1996. Approximately 7 % of the data was absent so the remaining entries were condensed so as not to bias the statistics obtained. A frequency histogram of the data is provided in **Figure 11**.

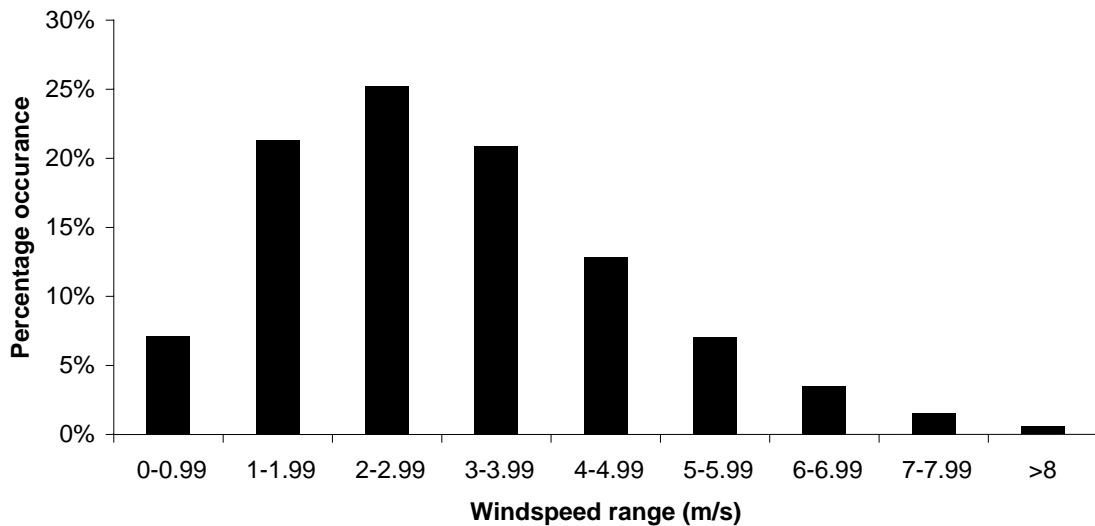


Figure 11: Frequency Histogram

4.3 Climate Change

The predictions made in this report span 3000 years, and therefore it is likely that the observed climatic data collected over the last century (on which the model input data is based) will differ from that occurring in the future. Both natural and anthropogenic causes of climate change are likely to occur.

Over the last decade there has been extensive worldwide research into the potential for anthropogenic climate change. Most climate change projections developed internationally have employed time horizons of approximately one century (e.g. out to 2100). Australian climate projections and estimates of impacts often extend to the late 21st century (i.e. 2070). The maximum 100 year projection timeframe reflects the limit of most greenhouse gas scenarios and climate model simulations (CSIRO, 2007).

A review of climatic conditions over the last 10,000 years (Holocene Epoch) was undertaken in order to address the range of climatic scenarios that could occur over the 3,000 year model period. This approach does not infer that previous climates experienced in the Holocene are necessarily representative of future climates, but provides a basis for understanding the range of variability that has previously occurred.

The water balance is most sensitive to rainfall and evaporation, and therefore the climate change scenarios investigated were constrained to these parameters only.

4.3.1 Rainfall

The Intergovernmental Panel on Climate Change (IPCC) predicts that changes in rainfall averages and in the magnitude and frequency of rainfall extremes will occur due to anthropogenic influences. CSIRO (2007) compiles the outcomes of the Fourth Assessment Report of the Intergovernmental Panel on Climate Change (IPCC), and builds on a large body of climate research that has been undertaken for the Australian region in recent years. This includes research completed within the Australian Climate Change Science Program by CSIRO and the Australian Bureau of Meteorology in partnership with the Australian Greenhouse Office. CSIRO (2007) presents predictions for rainfall change in the Olympic Dam region, and are summarised in Table 13.

Table 13: Rainfall change prediction (%) for 2070 at Olympic Dam

Model spread	Low Emissions	Medium Emissions	High Emissions
10 th percentile	-20	-30	-30
50 th percentile	-7.5	-7.5	-15
90 th percentile	+7.5	+12.5	+12.5

Note: 1. Adapted from CSIRO (2007)
 2. Regional projections are available for low, mid-range and high greenhouse gas emissions scenarios. These scenarios were developed by the Intergovernmental Panel on Climate Change (IPCC), and are based on various assumptions about demographic, economic and technological factors likely to influence future emissions. Emissions scenarios are from the IPCC Special Report on Emission Scenarios. Low emissions is the B1 scenario, medium is A1B and high is A1FI.

The 50th percentile (the mid-point of the spread of model results) provides a “best estimate” result (CSIRO, 2007) and indicates that rainfall is likely to reduce between 7.5% to 15%. The 10th and 90th percentiles provide a range of uncertainty and suggest rainfall could reduce by 30% or increase by 12.5% due to anthropogenic climate change.

Natural climatic variation also needs to be considered. Various researchers have inferred rainfall regimes during the last 10,000 years through the use of palaeo-records, which are proxy records derived from landscape features and biological, chemical and isotopic material stored in sediments, ice sheets, tree rings, cave deposits and corals. The majority of palaeo-information collected to date is from the southern, eastern and northern of Australia (CSIRO, 2007). Arid areas are not well represented in the records, with only Martin (1973) and Singh (1981), who studied the Nullabor Plain and Lake Frome respectively.

Singh (1981) described a pollen record from Lake Frome which lies approximately 280 km east of Olympic Dam, and provides the only indication of previous rainfall regimes in the arid interior of south-eastern Australia (Wright, 1993). The work suggests that moist conditions occurred 9500-8000 years before present (B.P.), drier conditions 8000-7000 years B.P., and peak moisture 7000-4200 years B.P.

Quantitative climatic reconstruction from pollen data has been undertaken by Jones *et al* (1998) and Jones *et al* (2001) for three closed lakes in western Victoria, Lakes Keilambete, Gnotuk and Bullenmerri. The wetting and drying time periods observed in these lake systems are similar to that described by Singh (1981) for Lake Frome, closer to Olympic Dam. The climatic variation is quantitatively expressed as a ratio of precipitation (P) to lake evaporation (EL) (i.e. P/EL ratio). CSIRO (2005) note that the scale of historical P/EL changes would have been regional, affecting much of south-eastern Australia. The work by Jones *et al* (1998, 2001) provides the best currently available quantitative rainfall records during the Holocene for the Olympic Dam region.

The data indicates that most of the Holocene was wetter than modern times (i.e. the instrumented period). Jones *et al* (1998) identifies 11 abrupt changes in P/EL ratio over the past 10,000 years. The total variation over the Holocene ranges from approximately 0.79 (the modern average) to 1.2. Holding evaporation constant, this equates to a maximum 50% rainfall increase above the modern average.

Based on the discussion above, the variation in rainfall could be -30% up to +50%, considering both natural variation and anthropogenic influences. This represents the upper and lower bounds of short-term (100 year) model predictions and long-term (10,000 year) paeleo-climatic investigations. Climate change scenarios are investigated for the water balance over this range.

4.3.2 Evaporation

It is generally accepted that there has been a reduction in pan evaporation over the last 50 years around Australia (Roderick and Farquhar, 2004a), despite an apparent increase in global temperatures. This is because the evaporative demand of the atmosphere is related to changes in net radiation (which is mostly determined by solar radiation), vapour pressure deficit (VPD) of the air, and wind speed (Roderick and Farquhar, 2004b) rather than temperature.

The Intergovernmental Panel on Climate Change (IPCC) predicts that potential evaporation (evaporative demand) is likely to increase as a result of climate change (IPCC, 2007). The CSIRO (2007) compilation of model results is summarised in **Table 14**.

Table 14: Potential evapo-transpiration change prediction (%) for 2070 at Olympic Dam

Model spread	Low Emissions	Medium Emissions	High Emissions
10 percentile	0	0	0
50 percentile	+3	+6	+6
90 percentile	+6	+10	+14

Note: 1. Adapted from <http://www.climatechangeinaustralia.gov.au>
 2. Regional projections are available for low, mid-range and high greenhouse gas emissions scenarios. These scenarios were developed by the Intergovernmental Panel on Climate Change (IPCC), and are based on various assumptions about demographic, economic and technological factors likely to influence future emissions. Emissions scenarios are from the IPCC Special Report on Emission Scenarios. Low emissions is the B1 scenario, medium is A1B and high is A1FI.

The 50th percentile (the mid-point of the spread of model results) provides a “best estimate” result (CSIRO, 2007) and indicates that potential evapo-transpiration is likely to increase between 3% to 6%. The range of uncertainty in the models suggests the variation could be between 0% up to 14% increase due to anthropogenic climate change.

Paeleo-records for evaporation are very limited and focus on temperature, which as discussed above is not necessarily a reliable indicator of evaporation. However the available data suggests that there have been moderate variations in temperature over the past 9,000 years, with some regional variation (CSIRO, 2007). The temperature trends are debated in the literature (CSIRO, 2007). Given the lack of paeleo-climatic evaporation data, evaporation variation due to anthropogenic influences can only be reliably assessed.

The climate change predictions are for increased evaporation, which would act to lower pit lake water levels. On this basis the water balance only considers rainfall variation due to climate change, which has the potential to increase water levels.

It is noted that the pan factor, which is the relationship between measured evaporation and evaporation from an open body of water, presents an additional degree of uncertainty in the evaporation component of the water balance. The range of input parameters considered for pan factor may be considered to also take into account the uncertainty associated with future trends in evaporation rates.

5.0 Water Balance

5.1 Model Components

There are a number of variables that will affect the pit lake water balance. These include: catchment areas, catchment hydrology, evaporation rates and groundwater inflows. This section describes these variables and the basis for selection of parameter values.

5.1.1 External Catchment Runoff

5.1.1.1 Catchment Area

The area of external catchments draining to the pit is likely to be minimised at closure by the construction of a perimeter bund around the pit. It is assumed that the bund would be offset approximately 200 m from the pit rim and cover the full circumference of the pit, making the external catchment approximately 250 ha.

In the event of bund failure, the quantity of water entering the pit would be constrained by the internally draining and typically small external catchments that are characteristic of the region. The external catchment area was estimated by reviewing the existing natural topography and the development plan, including the planned pit extent. Based on analysis of aerial photography and contour data (**Figure 12**), the maximum external catchment area that could drain to the pit would be 2,311 ha.

It is not expected that surface drainage from the RSF and TSF would be directed into the pit because:

- preferred TSF rehabilitation methods utilise covers that minimise runoff (e.g. store-release cover); and
- the RSF concept design results in highest elevations near the pit, lowering with increasing distance from the pit. Therefore it would not be practical to direct the bulk of the surface runoff into the pit.

It is unlikely that any runoff generated from the facilities could be directed to the pit by gravity due to the lack of topographic variation in the region. If, however, at some stage in the future the RSF and TSF design and rehabilitation strategy is modified, then a revised water balance would be required so that the risk of overflow could be reassessed.

The probability distribution adopted in the model for this variable is a discrete distribution with 80% probability that the external catchment area would be constrained by a perimeter bund, resulting in a catchment area of approximately 250 ha. A 20% probability was nominated for failure of the bund resulting in a 2,200 ha external catchment. The selection of probabilities is arbitrary, but reflects the higher likelihood of a small external catchment.

5.1.1.2 Hydrology

There is some uncertainty associated with the composition of the external catchment because of the effects of mining, which contribute to the uncertainty in catchment hydrological response. There is no runoff gauging data in the vicinity of Olympic Dam so a VRC could not be derived explicitly. The nearest stream gauging data is to the south, where the climate and soils differ from the Olympic Dam region. The only arid area stream gauging data is from the Todd River near Alice Springs in the Northern Territory, also with a different climate and soil system, but probably more representative than the other sites. A selection of stream gauging data is provided in **Table 15**.

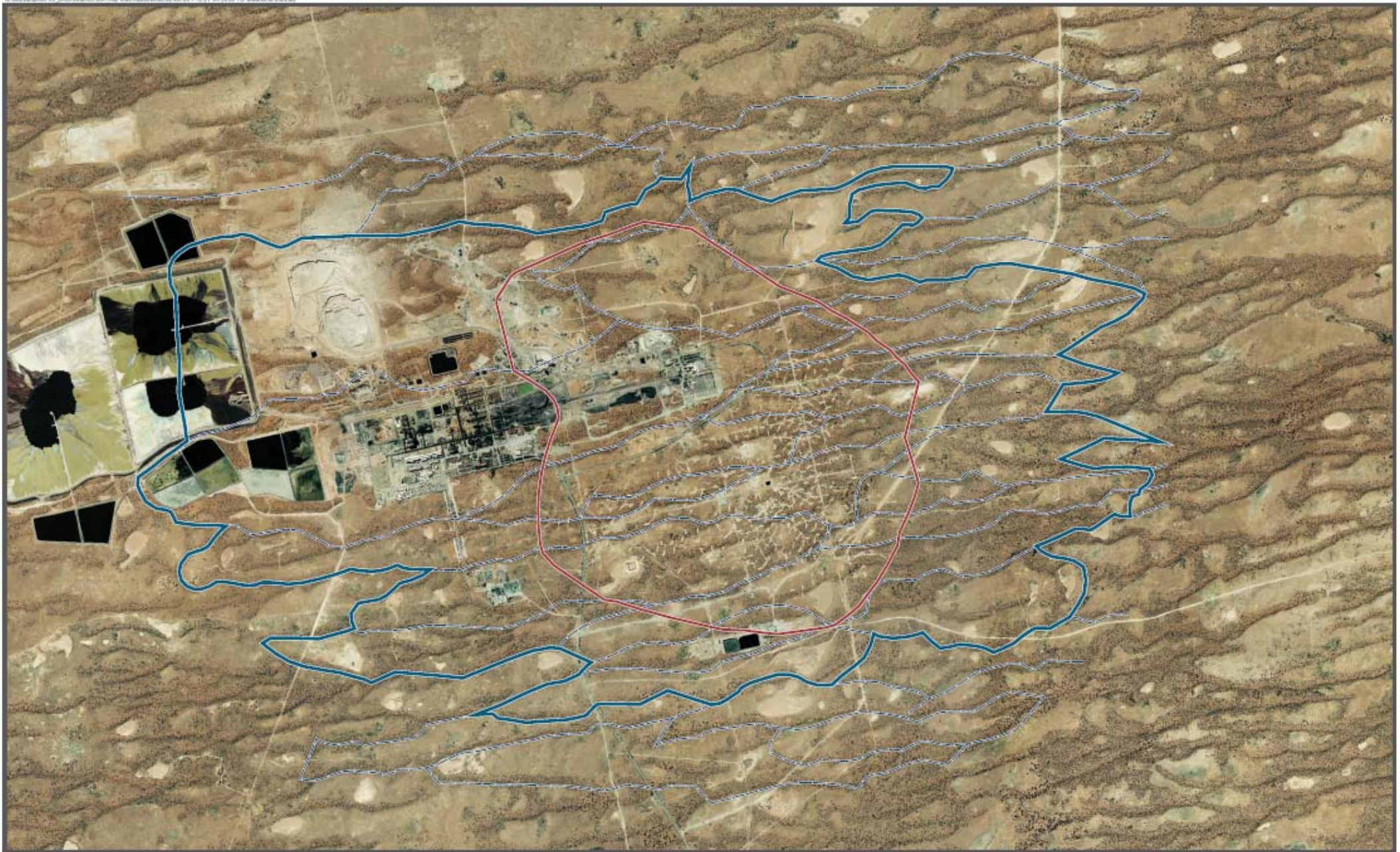


Figure 12 Pit Catchment Plan
BHPBilliton
Final Void Assessment
Olympic Dam, South Australia

Table 15: VRC Based on Stream Gauging Data

Stream Gauging Station	Location	Indicative Rainfall (mm/a)	Catchment Runoff (ML/a)	Catchment Area (km ²)	VRC
Todd River, NT	Near Alice Springs, central Australia	238	3,630	357	0.04
Hill River, SA	Near Hilltown, SA	404	2,239	235	0.02
Tod River, SA	Near Port Lincoln, SA	487	16,369	355	0.09

The table shows that South Australia and the arid regions are characterised by low VRC, generally less than 0.1. Wilkinson *et al* (2005) indicates VRC in Adelaide is higher, ranging from 0.19 to 0.25.

A hydrological model (AWBM) was used to estimate runoff and derive a VRC in order to compare with VRC calculated at other locations (**Table 15**). Boughton *et al* (2007) presents a methodology for applying AWBM on ungauged catchments. The method is based on calibrated models of 213 catchments around Australia, ranging in size from 50 to 2,000 km² and with streamflow records ranging from 10 to 90 years. Olympic Dam lies with Drainage Division V (South Australia Gulf) and the source data utilised seven catchments from this Drainage Division. On the basis of this research, Boughton *et al* (2007) recommend the model parameters presented in **Table 16** for use within Drainage Division V.

Table 16: AWBM Parameters for Drainage Division V for use on Ungauged Catchments (Boughton et al, 2007)

Variable	Value
Ks	0.35
BFI	0.29
Bk	0.958
A1	0.134
A2	0.134
A3	0.433

The variable to which AWBM is most sensitive is the surface storage capacity. Boughton *et al* (2007) suggest the surface storage capacity should be calibrated on ungauged catchments by first estimating the average annual runoff based on regression relationships developed for the Drainage Division. This technique could not be followed for Olympic Dam because the source data were from less arid climates. Instead, published surface storage capacities were trialled for a range of soil-cover systems that may represent the external catchment characteristics at Olympic Dam post-mining. The trial values and associated VRC are presented in **Table 17**.

Table 17: Relationship Between Surface Storage Capacity and VRC

Surface Storage	Soil-cover type	Reference	VRC ⁽²⁾
10 mm	For arid lands, less than 10% cover ⁽¹⁾	Boughton (1984)	0.29
35 mm	Compacted dirt – clayey	Boughton (1993)	0.12
53 mm	Uncompacted dirt – clayey	Boughton (1993)	0.08
157 mm	Compacted dirt - sandy	Boughton (1993)	0.03
172 mm	Uncompacted dirt - sandy	Boughton (1993)	0.03

Notes: Other model parameters were based on Boughton *et al* (2007) and held constant for each model run
 (1) Recommendation is for SFB Model as described by Boughton (1984). Boughton (1993) notes that the surface storage capacity used in the SFB model is sufficiently akin to that used in AWBM that the two can be used interchangeably
 (2) VRC calculated using AWBM, based on 117 years of patched-point daily rainfall and runoff

Table 17 suggests that the VRC would be 0.3 or below. On the basis of the AWBM output, as well as the literature and basin yield assessment, a mean VRC of 0.17 was adopted with a standard deviation of 0.06. This places the lower (2.5 percentile) and upper (97.5 percentile) bound at 0.05 and 0.29 respectively.

The AWBM model was also used to provide daily runoff data for the timestep sensitivity analysis. For the purposes of sensitivity analysis, a surface storage capacity generating the assumed mean VRC of 0.17 was adopted.

5.1.2 Pit Wall Runoff

5.1.2.1 Catchment Area

The surface area of pit wall runoff was estimated based on the total pit footprint (1,119 ha), minus the lake surface area. The lake surface area and pit wall surface area was recalculated each timestep.

5.1.2.2 Hydrology

The amount of runoff from pit wall will depend on the competence of the wall rock and the extent to which a weathered profile develops on benches and in depressions.

A worldwide literature review identified a shortage of published data on pit wall runoff coefficients. All of the studies are based on assumptions rather than measured values and the assumption range widely. For example, AMEC (2005) completed a pit lake study for the Kupol Gold Project in Russia (rainfall 650-700 mm/a), and adopted a VRC of 0.69. Niccoli *et al* (1998) adopted a VRC of 0.15 for an anonymous mine site, which was assigned based on experience at similar mine sites. In the absence of reliable guidance from published literature, two hydrological models were developed to represent the wall rocks and estimate hydrological behaviour.

The first model utilised AWBM, and adopted input parameters recommended by Boughton *et al* (2007) for Drainage Division V, as presented in **Table 16**. The pit wall catchment characteristics were represented by setting the Surface Storage Capacity to 0 mm and nullifying the baseflow component, as recommended by Boughton (1993) for small ungauged catchments where baseflow is negligible. AWBM indicated a VRC of 0.56 based on modelling of 117 years of patched-point daily rainfall data.

The second model utilises an initial and continuing loss model. This model was created by the BHPB Mine Development Team in order to estimate in-pit pumping requirements as part of the Selection Phase Study. The assumptions are based on experience gained from other mine sites in similar climates and include:

- 5 mm initial loss; and
- 0.8 runoff coefficient to account for continuing losses.

The 5 mm initial loss is assumed to apply when there is no rain on the previous day. The model, based on 117 year patched pointed daily rainfall, predicts a VRC of 0.48.

The two hydrological models are in close agreement, and suggest a VRC in the range of 0.50-0.55. For the water balance model, the VRC was represented by a normal distribution with mean 0.55 and standard deviation of 0.1, resulting in a lower (2.5 percentile) and upper (97.5 percentile) bound of 0.35 and 0.75 respectively.

5.1.3 Evaporation

5.1.3.1 Pan factor

The pan factor accounts for the difference between measured “pan evaporation” and evaporation that occurs from an open water body. The pan factor that applies to the pit lake can not be directly measured, calibrated or adopted from similar pits (because there are none in close proximity). However, the existing site evaporation ponds provide some indication. The water balance for this facility is well understood, enabling estimation of evaporative losses.

The evaporation ponds have a combined pan and salt reduction factor of 0.65 (Kinhill, 1997). It is expected that the evaporation rate from the pit lake would be less than the rate from the purpose-built evaporation ponds because of the following effects:

- reduced wind penetration to the water body, reducing mixing of air above the water body, leading to localised increases in humidity; and
- shading from the pit walls.

The evaporation rate may also be influenced by geothermal effects (rocks up to 65°C near base of pit), however this is expected to be less significant than the factors identified above.

The pan factor was represented by a normal distribution with mean 0.50 and standard deviation of 0.1, resulting in a lower (2.5 percentile) and upper (97.5 percentile) bound of 0.3 and 0.7 respectively.

5.1.3.2 Salinity effects

Two generalised formulae are in common use for the estimation of evaporation in non-saline waters: the Harbeck equation (Harbeck *et al*, 1958), and the Meyer equation (Meyer, 1915). While these formulae may be applicable in the early stages of pit lake formation, as the lake ages salinity is likely to increase due to evapo-concentration. Evaporation from saline waters does follow these standard evaporation equations, especially in hypersaline waters (Asmar and Ergenzinger, 1999).

It is well known that as the salinity of a water body increases, the evaporation rate reduces due to the difference in vapour pressure over a saline solution compared to that over freshwater. The change in vapour pressure is a function of the salinity/density and the ionic composition of the saline solution (Oroud, 1999).

Al-Shammiri (2002) provides a review of previous experimentation and correlations of evaporation rates to salinity. Much of the literature is focussed on salinities near that of seawater, with less data available on hypersaline waterbodies, which need to be considered in the Olympic Dam pit lake assessment.

There have been numerous studies of evaporation in the Dead Sea, which have been compiled by Niemi *et al* (1997). Hypersaline conditions ranging from 210 to 278 ppt are considered, which when combined with relationships derived at lower salinities, provide a reasonable relationship over the spectrum of expected salinities.

Ahmadzadeh Kokya *et al* (2007) successfully modified the Harbeck and Meyer equations to account for the effect of salinity. The modification was based on evaporation rate measurements from 0.2 g/l ppm up to 350 g/l. The relationships derived by Ahmadzadeh Kokya *et al* (2007) are generally consistent with observations made in the abovementioned studies, and is therefore considered suitable for application at Olympic Dam. The relationship between salinity and evaporation at selected values is presented in Table 18.

Table 18: Relationship between salinity and evaporation rate

Salinity (g/l)	Evaporative reduction
0.2	1
40	0.963
80	0.906
160	0.814
350	0.547

Source: Adapted from Ahmadzadeh Kokya *et al* (2007)

5.1.4 Groundwater

Groundwater is expected to drain regionally towards the pit. Several aquifers would be intersected by the pit and are therefore of significance to the water balance. These include:

- Andamooka Limestone aquifer:
 - water table typically occurs at about 50 m below ground in the area of the mine;
 - in the vicinity of the mine, the near-surface, unsaturated portion of the Andamooka Limestone has a high porosity and permeability that is associated with karst features; and
 - the karstic nature of the limestone has been shown to reduce rapidly with depth, so that the primary porosity of the Andamooka Limestone is very low at and below the natural water table level (REM, 2007).
- Corraberra Sandstone / Arcoona Quartzite aquifer:
 - an aquifer formed within the Corraberra Sandstone and the lower part of the Arcoona Quartzite. The upper part of the Arcoona Quartzite forms an aquitard above the aquifer and the Tregolana Shale forms an aquitard below the aquifer;
 - the aquifer typically occurs 160 to 200 m below ground level (about -60 m AHD to 100 m AHD); and
 - The Corraberra Sandstone aquifer is extensive, but heterogeneous. Reported values of hydraulic conductivity, transmissivity and storativity are variable.

- Basement aquifer:
 - not a productive aquifer and the rocks have little or no primary porosity and the faults or fractures, where intersected, appear to be mainly tight with limited permeability; and
 - significant for chemistry input rather than water quantity.

A cross-section of the pit showing major geological units and the associated aquifers is provided in **Figure 13**.

Further details on the hydrogeology of the Olympic Dam region are provided in the groundwater chapter of the Draft EIS and supporting technical appendices.

Extensive groundwater monitoring and aquifer testing has been undertaken during EIS hydrogeological studies, depressurisation assessment as part of the Pre-Feasibility Study by BHP Billiton during 2006 / 07, as well as data obtained from the ongoing operation of the mine. The majority of groundwater inflow (95%) would be through the Corraberra Sandstone / Arcoona Quartzite.

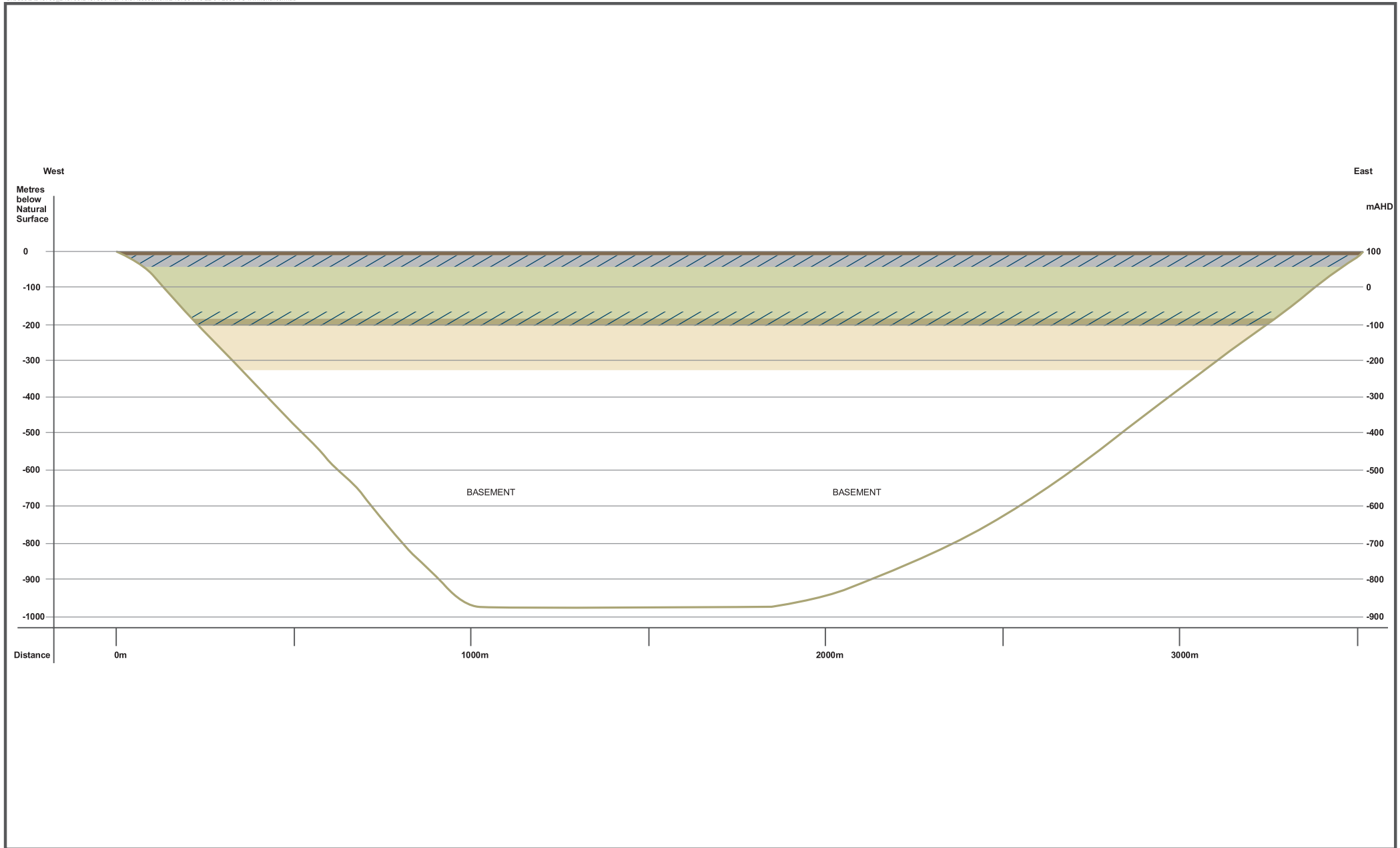
The proposed expansion would result in the creation of a Rock Storage Facility (RSF), as well as an increase in the area of the Tailings Storage Facility (TSF). Predicted seepage flux from these facilities has been described in the EIS (Appendix K) and the "Base Case" hydrological assumptions (refer EIS Appendix K) adopted in the assessment include:

- The seepage flux from the TSF during operation is expected to be approximately 46 l/s, but would decline substantially from closure during the formative period of the pit lake. A seepage rate of 1.2 l/s from the TSF was adopted throughout the model duration; and
- RSF seepage increasing linearly from 0 l/s to 17.8 l/s over the period Year 300 to Year 3000.
- Regional natural groundwater recharge is considered negligible in the model.

On the basis of these assumptions, the hydrogeological model predicts the inflow to the pit would be 43 l/s until Year 300, then would increase to 54 l/s by Year 3000. The model assumes that the pit lake does not fill to the level of the Corraberra Sandstone aquifer (approximately -100 mAHD) and therefore the pit would always act as a groundwater sink. The assumption is verified by the model results (refer **Section 5.1**).

There is uncertainty in some of the parameters feeding into the groundwater model and therefore groundwater inflow predictions were also entered as a probability distribution. A normal distribution was adopted with the mean being the estimates presented above and a standard deviation of 15 at Year 300 (increasing linearly to 19 at Year 3000). This places the lower (2.5 percentile) and upper (97.5 percentile) bound in Year 300 at 14.1 l/s and 72.4 l/s respectively. Similarly the lower and upper bound in Year 3000 is 17.7 l/s and 90.9 l/s respectively.

It is also noted that there is uncertainty relating to the proportion of groundwater entering the pit that is evaporated from the pit wall prior to reaching the lake surface. The extent of evaporative losses will depend on the distribution of flow along the pit face. Where groundwater emerges from major fractures a small stream of water is likely to develop that may be subject to little evaporative loss. The uncertainty associated with evaporative losses is incorporated into the probability distribution described above.



Cover Lithological Unit	Unit Code	Average Thickness
Cainozoic Sands and Clays	ZWS	10m
Andamooka Limestone	ZAL	32m
Arcoona Quartzite	ZWA	146m
Corraberra Sandstone	ZWC	20m
Tregolana Shale	ZWT	125m

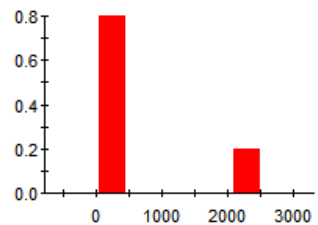
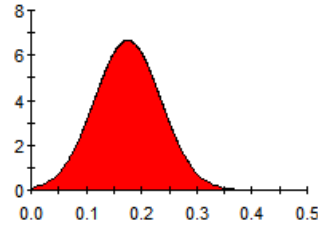
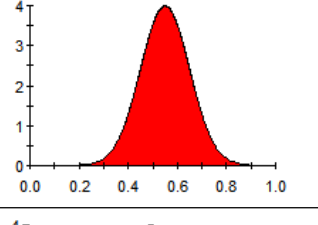
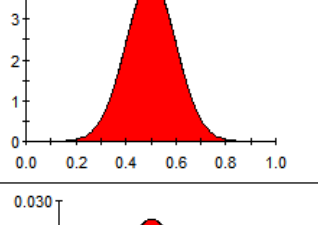
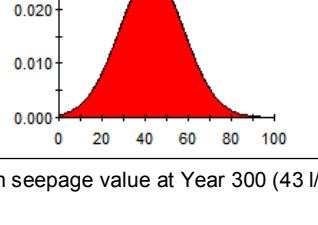
Proposed pit extent
 Major aquifer

Figure 13 Cross-Section Showing Lithological Horizons
BHPBilliton
 Final Void Assessment
 Olympic Dam, South Australia

5.1.5 Summary of Distributions

A summary of the distributions adopted for estimated parameters in the water balance is provided in Table 19.

Table 19: Adopted probability distributions for model input parameters

Independent variable	Adopted Distribution	Percentiles					
		2.5	50	97.5			
External catchment area (ha)	Discrete (80%=250, 20%=2200)				250	250	2311
External catchment VRC	Normal ($\mu=0.17, \sigma=0.06$)				0.05	0.17	0.29
Pit wall VRC	Normal ($\mu=0.55, \sigma=0.1$)				0.35	0.55	0.75
Evaporation pan factor	Normal ($\mu=0.5, \sigma=0.1$)				0.3	0.5	0.7
Seepage (initial) [^] (l/s)	Normal ($\mu=43, \sigma=15$)				14.1	43.0	72.4

Note: [^] distribution increased scaled linearly from seepage value at Year 300 (43 l/s) up to seepage value at year 3,000 (54 l/s)

5.2 Model Results

5.2.1 Pit Lake Water Level

The water balance indicates that a permanent lake would form within the mine void. The predicted water levels are shown in **Figure 14**. A perspective view of the standing water levels and pond extent for the 50th percentile conditions is shown in **Figure 15**.

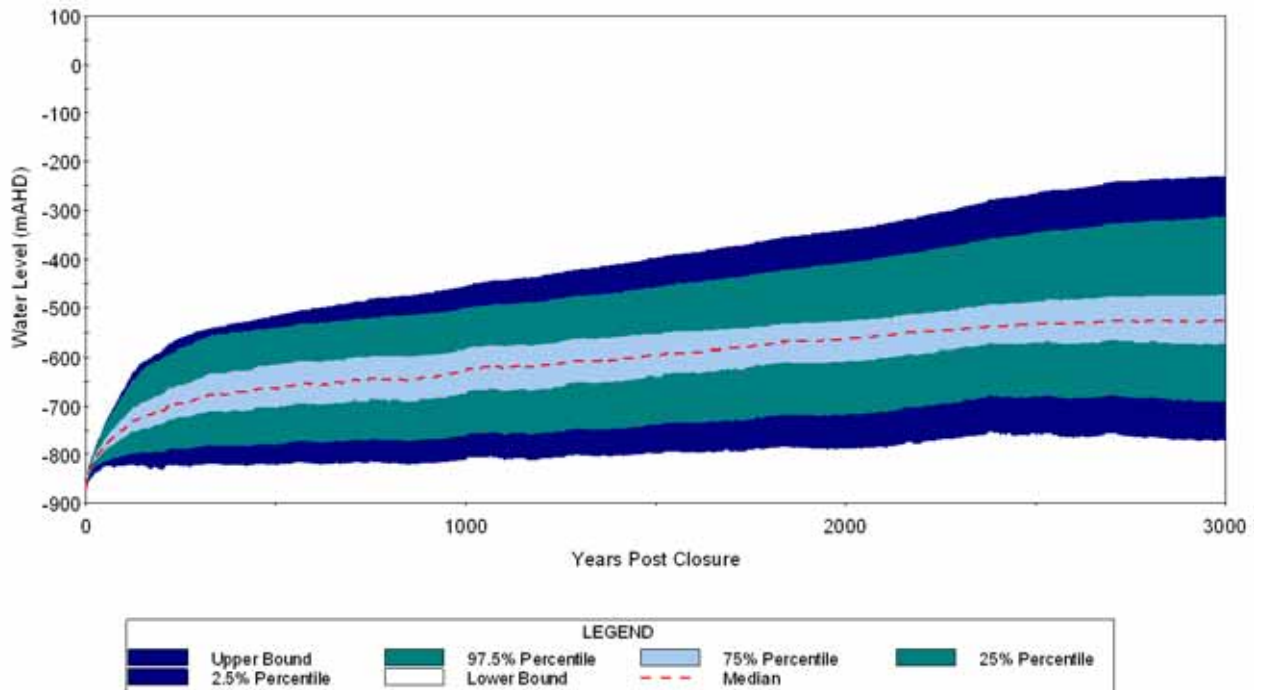


Figure 14: Predicted pit lake water levels

The water level is predicted to rise rapidly over the first ~150 years post closure, followed by a slower rate of rise until a steady state condition is achieved at approximately 3,000 years post closure.

A summary of water level predictions during selected years is provided in **Table 20**.

Table 20: Water Level Predictions (mAHD)

Years post closure	Percentile						
	Lower	2.5	25	50	75	97.5	Upper
50	-825	-814	-791	-781	-767	-739	-736
100	-825	-803	-765	-747	-724	-675	-665
200	-831	-794	-738	-710	-676	-603	-587
500	-822	-779	-704	-665	-617	-542	-517
1000	-810	-761	-673	-628	-585	-502	-455
2000	-788	-718	-608	-564	-527	-408	-340
3000	-771	-690	-574	-527	-473	-313	-228

Visualisation Details
Camera Angle - 45 degrees
Angle Azimuth - 180 degrees
Inclination - 65 degrees
Camera Angle Distance - 10000m

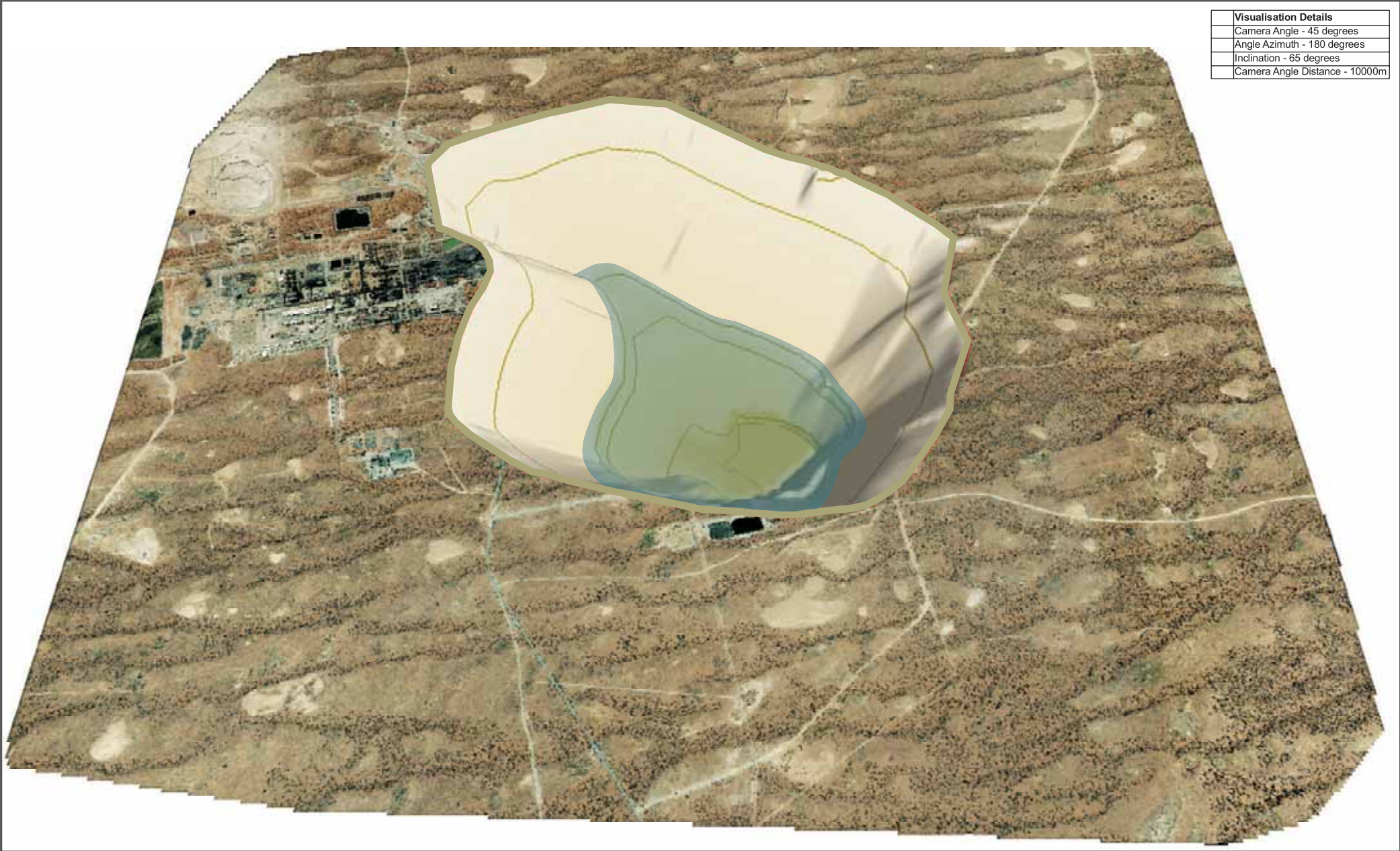


Figure 15 | Final Void Perspective View
BHPBilliton
Final Void Assessment
Olympic Dam, South Australia

The uncertainty of input parameters translates into uncertainty in water level predictions which is evident in the large variation of predictions shown in **Figure 14**. Despite this uncertainty the model demonstrates that an overflow from the pit into the environment would not occur. The upper bound, representing the worst case combination of input parameters, reaches a maximum water level of -230 mAHD after 3000 years, with the lake surface some 330 m below the natural ground level. The depth of water would be 640 m.

The lower bound prediction confirms that a permanent pit lake would form within the mine void and would have a water depth of at least 100 m. The 50th percentile prediction suggests the pit lake would have a water depth of approximately 340 m and would sit some 630 m below natural ground level.

5.2.1.1 Hydrogeological Implications

The water balance indicates that the upper bound water level is -230 mAHD, equating to a water depth of 640 m. The lowest major aquifer, the Corraberra Sandstone aquifer, is located above -100 mAHD.

Over the long term the salinity of the pit lake is likely to be much higher than the aquifer, and in order to compare pressure heads a freshwater equivalent head was calculated. The assessment demonstrated that the pressure head in the Corraberra Sandstone aquifer would be at least 140 m greater than the pit lake.

The modelling therefore indicates that the pit lake would act as a permanent groundwater sink and would drain the regional groundwater system indefinitely. The effect of this on the regional groundwater system and groundwater users is discussed in the EIS.

5.2.1.2 Water Fluxes

The predicted steady-state water inflows are provided in **Table 21**. This demonstrates that groundwater seepage is the major source of water to the pit, followed by pit wall runoff and incident rainfall. Runoff from the external catchment is expected to be a relatively small source.

Table 21: Steady State Inflows (ML/a)

Inflow Source	2.5 percentile	50 percentile	97.5 percentile
Incident rainfall	245 (19%)	470 (16%)	833 (15%)
Pit wall runoff	432 (34%)	697 (24%)	999 (18%)
External catchment runoff	24 (2%)	70 (2%)	791 (15%)
Seepage	572 (45%)	1,700 (58%)	2,863 (52%)

Notes: (1) Fluxes based on average of annual results for period 2950-3000 years post-closure

5.2.2 Sensitivity Analysis

5.2.2.1 Input Variables

Figure 16 presents a Tornado plot which shows the sensitivity of independent variables on the predicted water level. The Tornado plot shows deviation from the median water level predictions when the independent variable being assessed is sampled with a high (97.5 percentile) and low (2.5 percentile) value from the probability distribution. Only one independent variable is varied at a time, with all other values held at their 50th percentile value in order to allow meaningful comparison of sensitivity between variables.

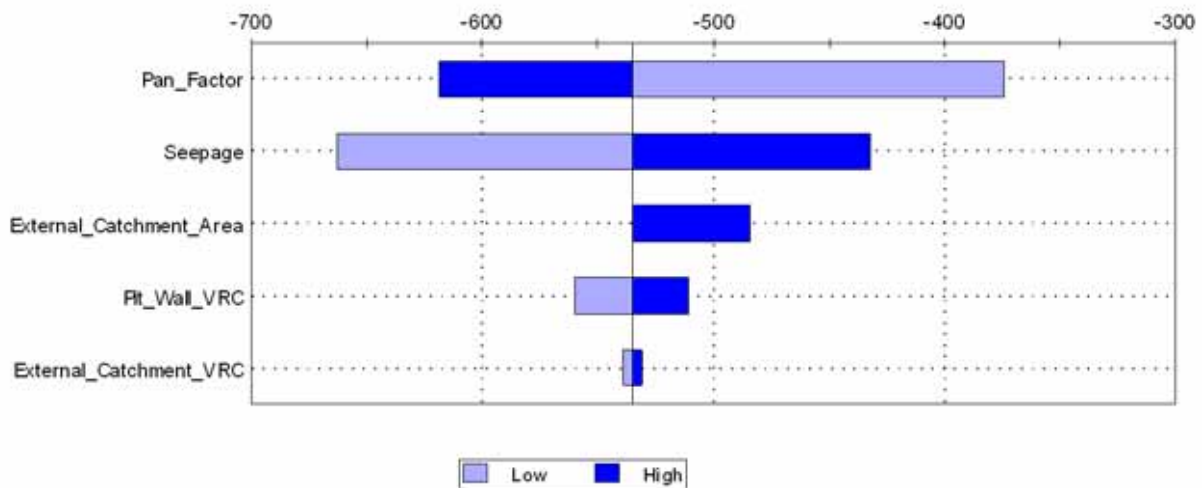


Figure 16: Tornado Chart Showing Parameter Sensitivity

The figure shows that the model is most sensitive to the pan factor, followed by seepage. Catchment hydrology is the least sensitive aspect of the model.

5.2.2.2 Seepage

A trial was undertaken to estimate the groundwater inflow rate that would result in the pit filling to the level at which reversal of flow would occur in the Corraberra Sandstone aquifer. The assessment takes into account density correction due to salinity differences and the results are presented in **Table 22**.

Table 22: Probability of Groundwater Gradient Reversal

Initial Seepage Rate	Probability of Groundwater Gradient Reversal
70 l/s (2,208 MI/a)	0%
80 l/s (2,523 MI/a)	3%
100 l/s (3,154 MI/a)	8%
140 l/s (4,415 MI/a)	34%
180 l/s (5,676 MI/a)	73%

Note: 1. Density correction made by adjusting hypersaline pit lake water and saline aquifer water to equivalent freshwater head
 2. Seepage values trailed are unrealistically high for the hydrogeological conditions at the site. The values are intended to provide an indication of sensitivity only

The table demonstrates that an initial seepage almost twice that predicted would be required for a possible groundwater gradient reversal. It is therefore highly unlikely that any groundwater gradient reversal would occur, even if seepage is much higher than predicted.

5.2.2.3 Timestep

Sensitivity of the model to the selected timestep was assessed by comparison of water levels predicted using daily and annual timesteps. Two model periods were assessed: the formative period (first 117 years) and quasi-steady state conditions. The comparison is shown in **Figure 17** and **Figure 18**.

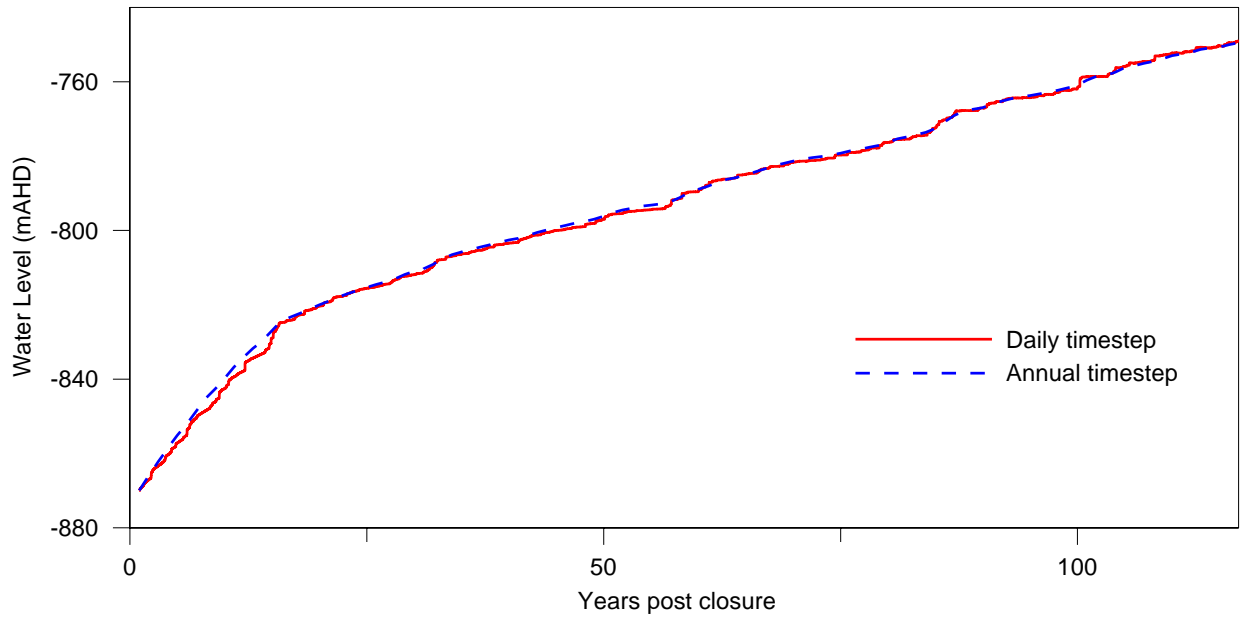


Figure 17: Timestep comparison during initial lake formations

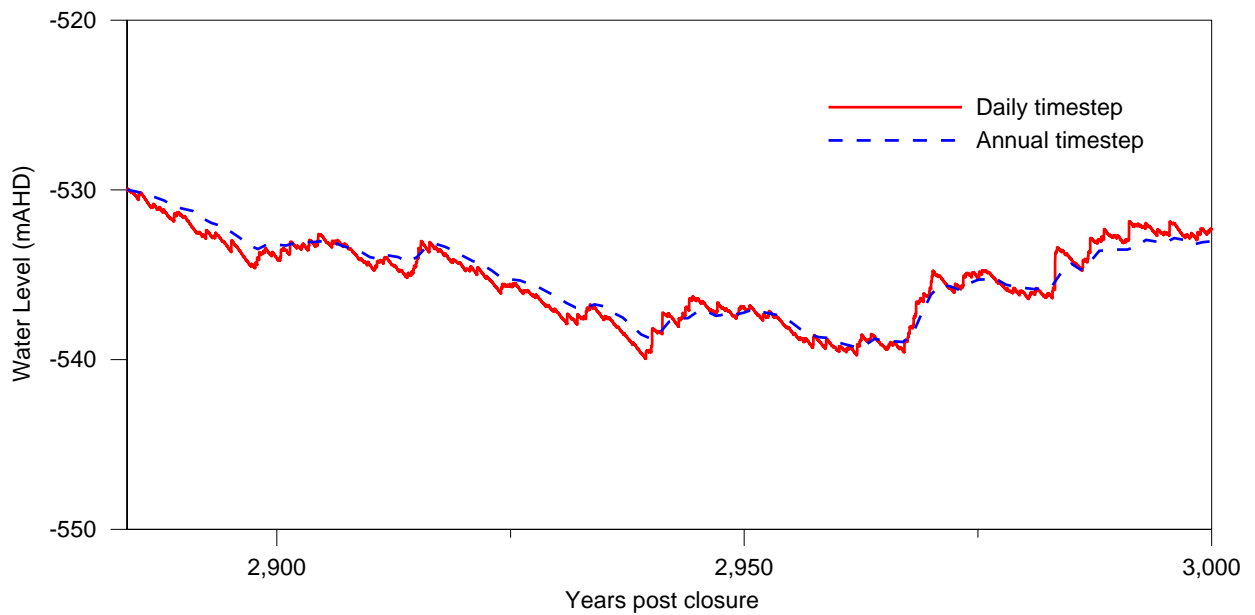


Figure 18: Timestep comparison during quasi-steady state water level condition

Both figures show that the annual timestep tends to smooth the water level variations. However the maximum discrepancy between the annual and daily timestep water levels predictions is 1.5 m, due to the much larger pit storage capacity compared to the peak annual inflow. On this basis the annual timestep adopted in the model is considered adequate for the purposes of this study.

5.2.3 Alternative Scenarios

5.2.3.1 Climate Change

On the basis of discussion provided in **Section 4.3**, the effects of two climate change scenarios on the pit lake levels were assessed. The first scenario considers a 50% increase in mean annual rainfall, on the basis that similar increases were observed in the Holocene epoch (last 10,000 years). The result of this scenario is presented in **Figure 19** with predictions during selected years in **Table 23**.

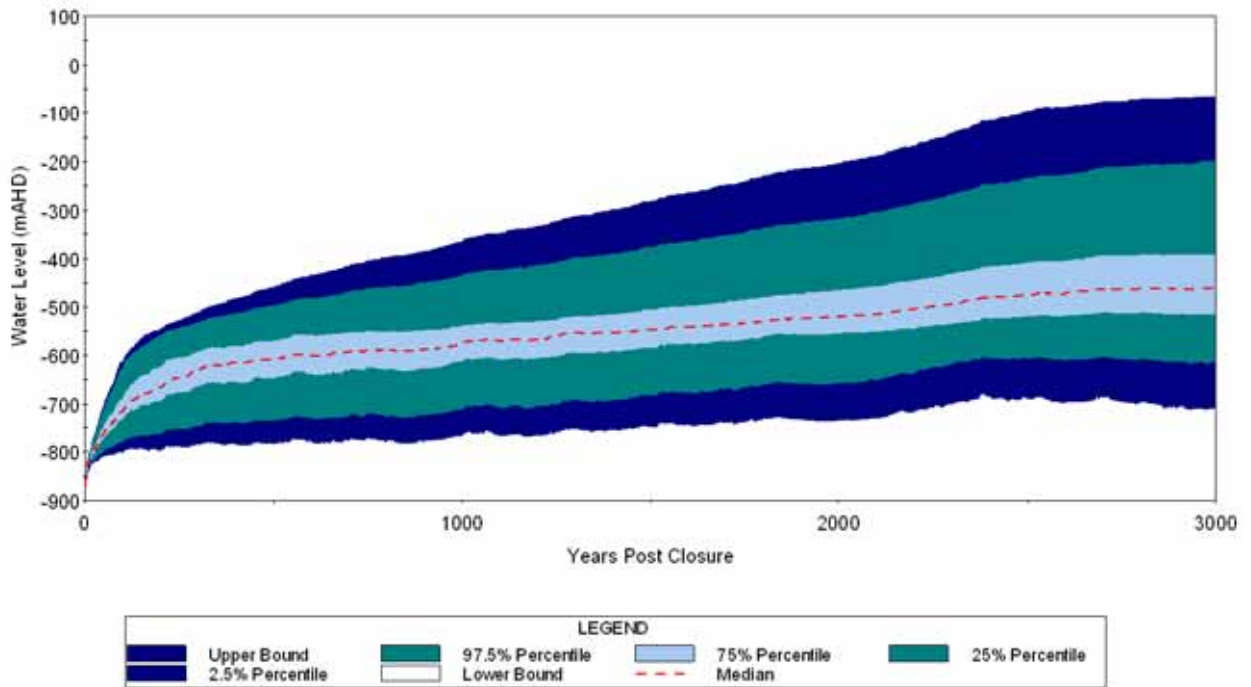


Figure 19: Water Level Predictions with 50% Increase in Mean Annual Rainfall

Table 23: Water Level Predictions – 50% Increase in Mean Annual Rainfall (mAHD)

Years post closure	Percentile						
	Lower	2.5	25	50	75	97.5	Upper
50	-810	-798	-771	-761	-745	-709	-700
100	-801	-779	-732	-715	-688	-624	-611
200	-797	-763	-694	-667	-624	-559	-545
500	-784	-737	-650	-609	-571	-498	-459
1000	-766	-712	-613	-577	-540	-435	-364
2000	-735	-658	-555	-521	-466	-317	-203
3000	-710	-616	-515	-462	-391	-199	-65

This assessment demonstrates that even with a large increase in mean annual rainfall due to climate change the pit lake would not reach the natural ground level. It is noted that there is a very low probability (1.5%) that a groundwater gradient reversal would occur under this scenario.

The second scenario considers a 30% decrease in mean annual rainfall, on the basis of climate change due to anthropogenic greenhouse gas emissions. The result of this scenario is presented in **Figure 20** with predictions during selected years in **Table 24**.

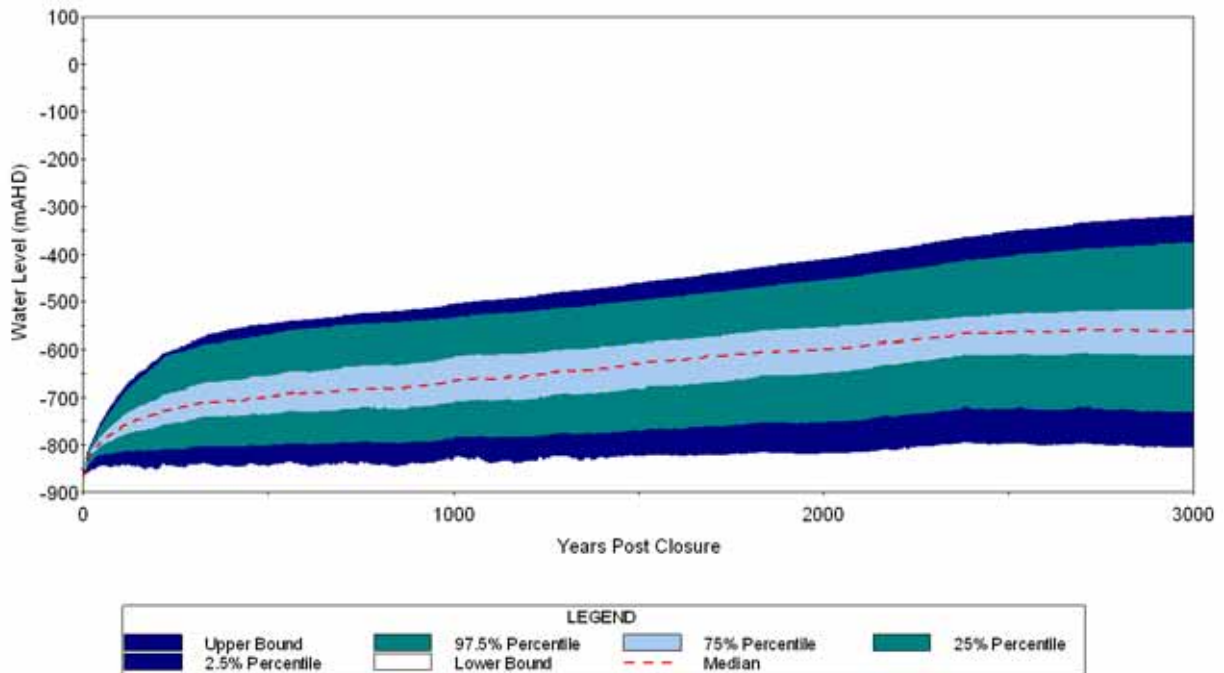


Figure 20: Water Level Predictions with 30% Decrease in Mean Annual Rainfall

Table 24: Water Level Predictions – 30% Decrease in Mean Annual Rainfall (mAHD)

Years post closure	Percentile						
	Lower	2.5	25	50	75	97.5	Upper
50	-845	-822	-803	-793	-781	-758	-749
100	-846	-816	-784	-766	-746	-704	-690
200	-851	-812	-764	-736	-704	-631	-619
500	-846	-802	-736	-701	-657	-570	-548
1000	-831	-787	-711	-667	-616	-533	-506
2000	-818	-752	-649	-599	-554	-455	-411
3000	-806	-730	-611	-563	-516	-376	-317

A decrease in Mean Annual Rainfall would result in a decrease in pit lake water levels. The modelling confirms that a permanent pit lake would still be present, and be at least 60 m deep in the long term.

5.2.3.2 Extreme Rainfall Event

The effect of an extreme rainfall event (i.e. Probable Maximum Precipitation (PMP)) on the water balance was assessed by introducing the event into the model during the lake filling and quasi-steady state stages.

The PMP was calculated in accordance with the Generalised Short-Duration Method developed by Bureau of Meteorology (2003). A three hour storm burst was calculated over the 3430 ha (34.2 km²) catchment (2311 ha external catchment and 1119 ha pit footprint). The calculation is based on a moisture adjustment factor (MAF) of 0.72, an elevation adjustment factor (EAF) of 1.0 and smooth terrain. The corresponding PMP is 420 mm.

Assuming a runoff coefficient of 1.0 the PMP would generate 14.4 ML of runoff, which represents 0.3 % of the total void storage capacity. This suggests that pit lake water level is unlikely to be sensitive to individual extreme rainfall events.

The effect of the PMP on the pit lake water levels was assessed using the daily timestep model. Two scenarios are plotted in **Figure 21**, one with a PMP event and one without. The figure shows that an extreme event would result in a change of water level of maximum 10 m (50th percentile). A water level variation of this amount is within the bounds of long-term water level fluctuations and demonstrates that the pit lake will not be sensitive to specific storm events.

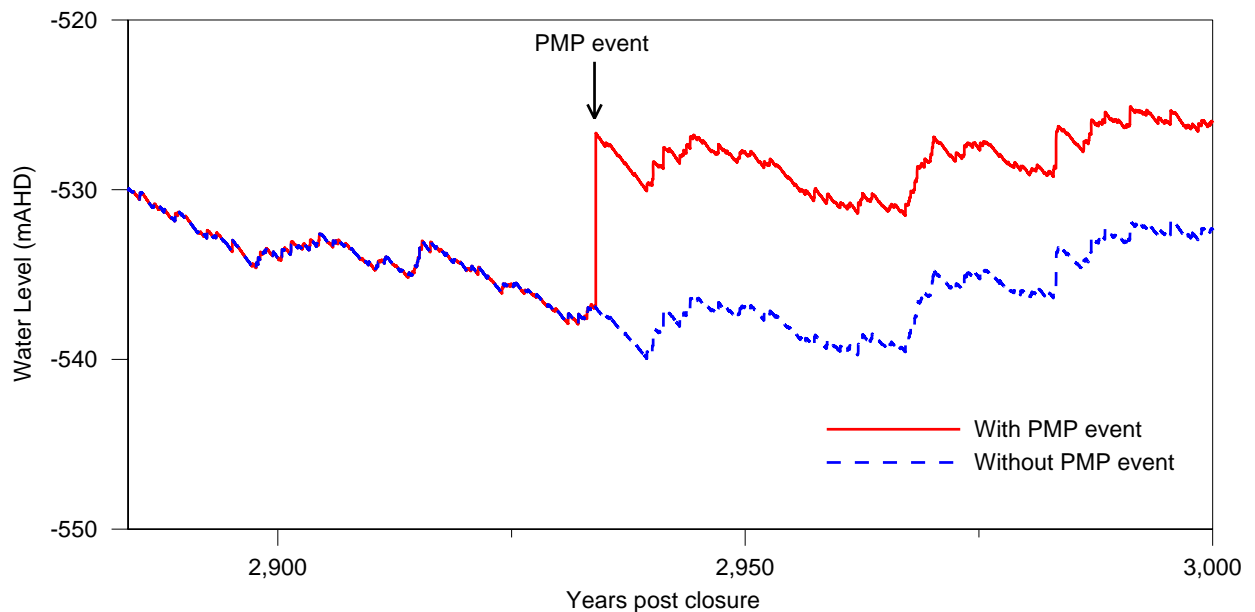


Figure 21: Effect of PMP on 50th percentile pit lake water levels

6.0 Water Chemistry

6.1 Chemistry of Input Waters

6.1.1 Incident Rainfall

Incident rainfall is likely to be a minor contributor of ions into the lake. Rainwater composition is not available for Olympic Dam, and therefore a typical rainwater composition has been adopted for modelling purposes based on a literature review. The assumed incident rainfall chemistry is provided in **Table 25**.

Table 25: Chemistry of incident rainfall (mg/L, unless noted otherwise)

Analyte	Value	Source
Temp (°C)	25	Assumed
pH (pH units)	5.0	Evans <i>et al</i> (2006)
Redox (pe)	+8	Assumed
Chloride	14 ^	Evans <i>et al</i> (2006)
Sulfate	8	Evans <i>et al</i> (2006)
Nitrate	2	Evans <i>et al</i> (2006)
Calcium	3	Evans <i>et al</i> (2006)
Sodium	9	Evans <i>et al</i> (2006)

Notes: ^ concentration adjusted to achieve charge balance

6.1.2 External Catchment Runoff

The chemistry of external catchment runoff was derived based on opportunistic grab sampling during EIS fieldwork programs as described in **Section 2.0**. A compilation of the results is presented in **Table 26** along with the values adopted for this study.

Table 26: Chemistry of the External Catchment Surface Runoff aquifer (mg/l, unless noted otherwise)

Site	SW1	-	SW3	1	2	3	4	5	6	7	Adopted
Description	Tributary of Mason Creek at highway crossing	Tributary of Brackish Swamp	Woocalla Creek - at highway crossing	Creek Bed (near road), 5.5 km out of Andamooka	Creek Bed (Large Pool), 5.5 km out of Andamooka	Large Pool, from Andamooka to Olympic Dam (left)	Pool, from Andamooka to Olympic Dam (left)	Pool, from Andamooka to Olympic Dam (left)	Pool, from Andamooka to Olympic Dam (right)	Large claypan pool, from Andamooka to Olympic Dam (right)	
Date	14/07/06 ^(a)	14/07/06 ^(a)	16/07/06 ^(a)	23/01/07 ^(b)	23/01/07 ^(b)	23/01/07 ^(b)	23/01/07 ^(b)	23/01/07 ^(b)	23/01/07 ^(b)	23/01/07 ^(b)	
Temp (°C)	13.2	nd	13.2	32.4	32.4	33.8	34	30	33	33	20.0
pH (pH units)	8.51	8.95	8.89	8.94	9	8.9	9	8.8	8.86	9.1	8.7
Redox (pe)	nd	nd	nd	nd	nd	nd	nd	nd	nd	nd	+8
EC25 (µS/cm)	287	241	1250	142	105	205	150	240	63	77	
TDS	85	nd	468	73	52	nd	103	126	30	36	
Bicarbonate ¹	29	nd	34	nd	nd	nd	nd	nd	nd	nd	31.5
Carbonate ¹	<1	nd	<1	nd	nd	nd	nd	nd	nd	nd	<1
Chloride	17	nd	14	nd	nd	nd	nd	nd	nd	nd	15.5[^]
Sulfate	2	nd	12	nd	nd	nd	nd	nd	nd	nd	7
Aluminium	nd	nd	nd	nd	nd	nd	nd	nd	nd	nd	0.005*
Arsenic	<0.001	nd	<0.001	nd	nd	nd	nd	nd	nd	nd	0.0005*
Barium	nd	nd	nd	nd	nd	nd	nd	nd	nd	nd	0.0005*
Calcium	1	nd	1	nd	nd	nd	nd	nd	nd	nd	1
Copper	0.004	nd	0.006	nd	nd	nd	nd	nd	nd	nd	0.005
Iron	nd	nd	nd	nd	nd	nd	nd	nd	nd	nd	0.05
Potassium	1	nd	4	nd	nd	nd	nd	nd	nd	nd	2.5
Magnesium	<1	nd	1	nd	nd	nd	nd	nd	nd	nd	1

Site	SW1	-	SW3	1	2	3	4	5	6	7	Adopted
Description	Tributary of Mason Creek at highway crossing	Tributary of Brackish Swamp	Woocalla Creek - at highway crossing	Creek Bed (near road), 5.5 km out of Andamooka	Creek Bed (Large Pool), 5.5 km out of Andamooka	Large Pool, from Andamooka to Olympic Dam (left)	Pool, from Andamooka to Olympic Dam (left)	Pool, from Andamooka to Olympic Dam (left)	Pool, from Andamooka to Olympic Dam (right)	Large claypan pool, from Andamooka to Olympic Dam (right)	
Date	14/07/06 ^(a)	14/07/06 ^(a)	16/07/06 ^(a)	23/01/07 ^(b)	23/01/07 ^(b)	23/01/07 ^(b)	23/01/07 ^(b)	23/01/07 ^(b)	23/01/07 ^(b)	23/01/07 ^(b)	
Manganese	nd	nd	nd	nd	nd	nd	nd	nd	nd	nd	0.0005*
Sodium	20	nd	26	nd	nd	nd	nd	nd	nd	nd	23
Nickel	0.002	nd	0.002	nd	nd	nd	nd	nd	nd	nd	0.002
Lead	0.002	nd	0.001	nd	nd	nd	nd	nd	nd	nd	0.0015
Uranium	nd	nd	nd	nd	nd	nd	nd	nd	nd	nd	0
Zinc	0.018	nd	0.045	nd	nd	nd	nd	nd	nd	nd	0.0315
Flouride	nd	nd	nd	nd	nd	nd	nd	nd	nd	nd	0.05*
Silica	nd	nd	nd	nd	nd	nd	nd	nd	nd	nd	0.025*
Phosphorus	nd	nd	nd	nd	nd	nd	nd	nd	nd	nd	0.005*

Notes: Source: (a) ENSR field trip July 2006
 (b) REM field trip January 2007

* indicates 50% LOR assumed

Adopted value for modelling shown in **bold**

1. Carbonate and bicarbonate as CaCO₃

^ Concentration adjusted to achieve charge balance

6.1.3 Pit Wall Runoff

Pit wall runoff chemistry is estimated based on the proposed pit wall surface area, likely oxidation depth, weathering kinetics and flushing assumptions. The surface area exposure of various rock types exposed in the pit wall is provided in **Table 27**.

Table 27: Surface Area of Rock Types Exposed in the Pit Wall

Lithological Unit	Average Thickness (m)	RL (mAHD)	Wall surface area (m ²)	Proportion
Cainozoic Sands and clays (ZWS)	10	105 to 95	292,000	1.9 %
Andamooka Limestone (ZAL)	32	95 to 63	582,000	3.9 %
Arcoona Quartzite – Transition (ZWA)	5	63 to 58	291,000	1.9 %
Arcoona Quartzite – Red (ZWAR)	111	58 to -53	2,523,000	16.8 %
Arcoona Quartzite – White (ZWAW)	30	-53 to -83	796,000	5.3 %
Corraberra Sandstone (ZWC)	20	-83 to -103	262,000	1.7 %
Tregolana Shale (ZWT)	125	-103 to -228	2,669,000	17.8 %
Pebble Conglomerate (ZWP)	9	-228 to -237	212,000	1.4 %
Basement	800	-237 to -1035	7,410,000	49.3 %, comprising*: HEMH (148187) 0.8% GRNL (148207) 0.8% HEM (148194) 0.8% HEMQ 12.0% HEMH 0.8% GRNH 5.5% GRNB 21.6% GRNL 0.8% KASH 1.3% KASH Lam 1.3% VHEM 2.2% KHEMQ-VASH 1.3% CONGLO 1.4%
TOTAL			15,037,000	100.0%

Notes: * basement lithologies weighted by mass

The rate of solute generation (estimated by kinetic testing) is multiplied by the mass of rock exposed to weathering in the pit wall (using surface area in **Table 27** and assumed oxidation depth). It is assumed that any weathering products generated are flushed from the pit wall during runoff events. A summary of the calculation is provided in **Table 28**.

Table 28: Chemistry of the Pit Wall Runoff

Analyte	Production rate (g/t/y)	Solute production (g/y)	Wall runoff (ML/y)	Runoff concentration (mg/L)
Temp (°C)	nd	nd	nd	25.0
pH (pH units)	nd	nd	nd	8.3
Redox (pe)	nd	nd	nd	+4
EC25 (µS/cm)	nd	nd	nd	nd
TDS	nd	nd	nd	nd
(Bi)carbonate	nd	nd	nd	Fixed by CO₂(g) partial pressure[^]
Sulfate	nd [#]	nd [#]	697	0.5 *
Aluminium	2.719	558,121	697	0.801
Arsenic	0.088	18,054	697	0.026
Barium	1.191	244,406	697	0.350
Calcium	14.733	3,024,005	697	4.339
Copper	0.129	26,471	697	0.038
Iron	2.460	504,977	697	0.724
Potassium ¹	12.267	2,517,719	697	3.613
Magnesium	8.656	1,776,547	697	2.548
Manganese	0.225	46,130	697	0.066
Sodium	nd [^]	nd [^]	697	0.5*
Nickel	0.006	1,288	697	0.002
Lead	0.010	2,153	697	0.003
Uranium	0.022	4.564	697	0.006
Zinc	0.068	13,985	697	0.020
Fluoride	3.786	777,165	697	1.114
Silica	6.820	1,399,872	697	2.009
Phosphorus	0.086	17,745	697	0.025

Notes: Based on oxidation depth of 5mm, density 2.73 t/m³

Adopted value for modelling shown in **bold**

* indicates 50% LOR assumed

indicates value produced from kinetic testing is not representative of long-term trends because no significant source minerals were detected. Nominal value 50% LOR adopted

1. Potassium used for charge balance

[^] concentration adjusted to achieve charge balance

6.1.4 Andamooka Limestone Aquifer

A summary of groundwater monitoring of the Andamooka Limestone aquifer over the period 1997-2007 is provided in **Table 29**. Values adopted for modelling are shown in bold.

Table 29: Chemistry of the Andamooka Limestone Aquifer (mg/L, unless noted otherwise)

Analyte	n	Min	20%ile	50%ile	80%ile	Max	Source	G5	G6
Temp (°C)	10	19.4	19.9	21.8	23.1	26.5	REM (2006)	nc	nc
pH (pH units)	47	6.32	6.71	7.02	7.34	8.00	ODO (2007)	nc	nc
Redox (mV)	10	-69	-58	-40	27	82	REM (2006)	nc	nc
EC25 (µS/cm)	29	12400	23660	30200	36500	45100	ODO (2007)	nc	nc
TDS	50	2400	16080	22107	29960	34400	ODO (2007)	nc	nc
Bicarbonate ¹	29	110	150	188	291	484	ODO (2007)	2740	nc
Carbonate ¹	16	1	1	1	1	3	ODO (2007)	nc	nc
Chloride	35	3460	8770	11300 [^]	14540	17010	ODO (2007)	[^]	[^]
Sulfate	50	1	2608	4015	5000	8820	ODO (2007)	nc	2155
Aluminium	29	0.01	0.02	0.05	0.23	3.10	ODO (2007)	nc	nc
Arsenic	29	<0.001	0.001	0.003	0.010	0.023	ODO (2007)	nc	nc
Barium	29	0.004	0.015	0.029	0.050	0.131	ODO (2007)	nc	nc
Calcium	50	1	652	900	1020	1230	ODO (2007)	nc	nc
Cobalt	29	0.001	0.003	0.004	0.009	0.018	ODO (2007)	nc	nc
Chromium	29	0.001	0.001	0.003	0.010	0.020	ODO (2007)	nc	nc
Copper	50	0.001	0.005	0.013	0.026	0.100	ODO (2007)	nc	nc
Iron	46	0.001	0.100	0.667	3.20	24.9	ODO (2007)	nc	nc
Potassium	29	24	33.0	44.1	56.2	73.9	ODO (2007)	nc	nc
Magnesium	29	139	394	614	840	1110	ODO (2007)	545	nc
Manganese	50	0.003	0.196	0.762	2.12	4.11	ODO (2007)	nc	nc
Sodium	29	2280	4256	5790	7164	9080	ODO (2007)	nc	nc
Nickel	29	0.001	0.010	0.015	0.027	0.056	ODO (2007)	nc	nc
Lead	29	<0.001	0.001	0.003	0.005	0.031	ODO (2007)	nc	nc
Uranium	47	0.004	0.019	0.026	0.055	0.080	ODO (2007)	nc	nc
Zinc	29	0.011	0.021	0.033	0.074	0.164	ODO (2007)	nc	nc
Fluoride	0	na	na	1.4	na	na	Assumed	nc	nc
Silica	0	na	na	1.2	na	na	Assumed	nc	nc

Notes: adopted value for modelling shown in **bold**
nc – no change from observed values
1. Carbonate and bicarbonate as CaCO₃
[^] Concentration adjusted to achieve charge balance

6.1.5 Corraberra Sandstone Aquifer

A summary of groundwater monitoring of the Corraberra Sandstone aquifer over the period 1994-2003 is provided in **Table 30**. Values adopted for modelling are shown in bold.

Table 30: Chemistry of the Corraberra Sandstone/Arcoona Quartzite Aquifer (mg/L, unless noted otherwise)

Analyte	n	Min	20%ile	50%ile	80%ile	Max	Source	G5	G6
Temp (°C)	3	19.9	nd	24.4	nd	25.7	REM (2006)	nc	nc
pH (pH units)	17	6.69	6.83	6.99	7.46	8.00	ODO (2007)	nc	nc
Redox (mV)	3	-112	nd	-100	nd	-109	REM (2006)	nc	nc
EC25 (µS/cm)	11	27400	31700	35100	44800	49300	ODO (2007)	nc	nc
TDS	17	17000	24030	24800	25660	32500	ODO (2007)	nc	nc
Bicarbonate ¹	11	151	201	260	289	311	ODO (2007)	1700	nc
Carbonate ¹	8	1	1	1	2.2	3	ODO (2007)	nc	nc
Chloride	12	8950	9440	10532 [^]	11031	13100	ODO (2007)	[^]	[^]
Sulfate	17	1	3750	4320	4850	5520	ODO (2007)	nc	1335
Aluminium	11	0.010	0.010	0.032	0.172	0.284	ODO (2007)	nc	nc
Arsenic	11	0.001	0.005	0.009	0.010	0.017	ODO (2007)	nc	nc
Barium	11	0.009	0.016	0.018	0.020	0.024	ODO (2007)	nc	nc
Calcium	17	1	464	558	591	866	ODO (2007)	nc	nc
Cobalt	11	0.001	0.001	0.005	0.008	0.012	ODO (2007)	nc	nc
Chromium	11	0.001	0.001	0.001	0.003	0.005	ODO (2007)	nc	nc
Copper	17	0.002	0.013	0.018	0.028	0.218	ODO (2007)	nc	nc
Iron	12	3.10	4.34	5.13	13.9	17.4	ODO (2007)	nc	nc
Potassium	11	40	47	56	63	67.3	ODO (2007)	nc	nc
Magnesium	10	524	571	673	762	964	ODO (2007)	338	nc
Manganese	17	0.089	0.255	0.467	0.812	0.906	ODO (2007)	nc	nc
Sodium	11	6390	6800	6870	9540	10400	ODO (2007)	nc	nc
Nickel	11	0.001	0.002	0.013	0.023	0.027	ODO (2007)	nc	nc
Lead	10	0.001	0.001	0.001	0.003	0.005	ODO (2007)	nc	nc
Uranium	15	0.001	0.001	0.001	0.006	0.026	ODO (2007)	nc	nc
Zinc	11	0.007	0.013	0.060	0.140	0.532	ODO (2007)	nc	nc
Fluoride		0.10		1.45		2.50	AGC (1982)	nc	nc

Analyte	n	Min	20%ile	50%ile	80%ile	Max	Source	G5	G6
Silica		0.70		4.08		9.50	Giblin (1980)	nc	nc
Phosphorus	0			0.005*			Assumed	nc	nc

Notes: adopted value for modelling shown in **bold**
nc – no change from observed values
1. Carbonate and bicarbonate as CaCO₃
* indicates 50% LOR assumed
^ concentration adjusted to achieve charge balance

6.1.6 Basement Aquifer

Water samples that have been collected from the Basement indicate high and variable salinity from 20,000-95,000 mg/L. Data collected by AGC (1982) and representing the most complete dataset available is provided in **Table 31**. Values adopted for modelling are shown in bold. In addition to the AGC data, samples have been collected from the underground workings by BHP Billiton environmental staff in November 2006 and are also provided in **Table 31**.

Table 31: Chemistry of the Basement Aquifer (mg/L, unless noted otherwise)

Analyte	n ^(d)	Min	20%ile	50%ile	80%ile	Max	UG1 ^(a)	UG2 ^(b)	Source(UNO)	G5	G6
Temp (°C)	0	na	na	28	na	na	na	na	Assumed	nc	nc
pH (pH units)	7	6.8	7.0	7.7	7.9		6.8	7.3	Kinhill (1982)	nc	nc
Redox (mV)	0	na	na	-150	na	na	-3	74	Assumed	nc	nc
EC25 (µS/cm)	0	na	na	na	na	na	112000	98400	Underground(a,b)	nc	nc
TDS	7	22100	34805	38500	57545.4	95100	na	na	Kinhill (1982)	nc	nc
Bicarbonate ¹	7	32	60	186	372.4	380	138	141	Kinhill (1982)	2770	nc
Carbonate ¹	0	na	na	na	na	na	<1	<1	Underground(a,b)	nc	nc
Chloride	7	8250	16680	18840[^]	31800	55770	46200	35000	Kinhill (1982)	^	^
Sulfate	7	3620	4140	4500	4930	5150	8730	8630	Kinhill (1982)	nc	2180
Aluminium	0	na	na	0.05	na	na	<0.10	<0.01	Assumed*	nc	nc
Arsenic	0	na	na	0.005	na	na	<0.010	<0.001	Assumed*	nc	nc
Barium	0	na	na	na	na	na	0.048	0.005	Underground(a,b)	nc	nc
Calcium	7	560	644	910	1040	1090	1170	1120	Kinhill (1982)	nc	nc
Cobalt	0	na	na	na	na	na	<0.010	<0.001	Underground(a,b)	nc	nc
Chromium	0	na	na	na	na	na	na	na		nc	nc
Copper	3	0.100	na	0.280	na	0.350	0.049	0.006	Kinhill (1982)	nc	nc
Iron	3	5.3	na	55	na	60	4.0	0.02	Kinhill (1982)	nc	nc
Potassium	7	37	62	79	185.8	430	360	339	Kinhill (1982)	nc	nc
Magnesium	7	570	861	990	1060	1090	1870	1460	Kinhill (1982)	550	nc
Manganese	3	1.40	na	2.85	na	5.00	2.13	0.15	Kinhill (1982)	nc	nc
Sodium	7	5750	10330	11800	18868	32580	27800	23800	Kinhill (1982)	nc	nc

Analyte	n ^(d)	Min	20%ile	50%ile	80%ile	Max	UG1 ^(a)	UG2 ^(b)	Source(UNO)	G5	G6
Nickel	2	0.005	na	0.005	na	0.005	na	na	Kinhill (1982)	nc	nc
Lead	3	0.10	na	0.22	na	1.95	<0.010	<0.001	Kinhill (1982)	nc	nc
Uranium	3	0.003	na	0.012	na	0.014	<0.010	<0.001	Kinhill (1982)	nc	nc
Zinc	3	2.15	na	7.35	na	56	<0.050	0.007	Kinhill (1982)	nc	nc
Fluoride	3	1.1	na	1.5	na	3.0	2.5	3.4	Kinhill (1982)	nc	nc
Silica	2	9.56	na	11.31	na	13.06	9.05	10.70	Kinhill (1982)	nc	nc
Phosphorus	0	na	na	0.005	na	na	na	na	Assumed*	nc	nc

Notes: (a) Underground sample hole near to RB25, provided by ODO December 2006
 (b) Underground sample 200 m back down the drive before you get to RB25, provided by ODO December 2006
 (c) Number of samples excluding water samples collected from underground
 * indicates 50% LOR assumed
 Adopted value for modelling shown in **bold**
 nc – no change from observed values
 1. Carbonate and Bicarbonate expressed as HCO₃
 ^ Concentration adjusted to achieve charge balance

6.2 Saturation State of Mineral Phases for Input Waters

Minerals are chemical precipitates generated when constituent ions jointly exceed the "solubility product" for that mineral. Waters where this occurs are described as "saturated" with respect to that mineral.

Characterisation of waters by the minerals with which each is saturated provides a system for classifying waters in terms of potential mineral formation. This classification can be quantified by calculation of a 'saturation index' (SI):

Minerals that have SI values that equal or exceed zero are saturated and if environmental conditions are suitable and kinetics favourable, the supersaturated mineral phases may begin to precipitate.

Table 32 presents a summary of the saturation state of major mineral phases for input waters to the pit lake. The table indicates whether a mineral phase is either supersaturated (✓) or under-saturated (✗).

Table 32: Saturation state of mineral phases for input waters

Mineral phase	External catchment runoff	Pit wall runoff	Andamooka limestone aquifer	Corraberra sandstone aquifer	Basement aquifer
Barite	✗	✗	✓	✓	✓
Apatite phases	✗	✓	✓	✓	✓
Ferrihydrite	✓	✓	✓	✓	✓
Aluminium oxyhydroxides	✓	✓	✓	✓	✓
Calcite	✗	✗	✗	✗	✓
Smectite-like phases	✗	✓	✓	✓	✓
Gypsum	✗	✗	✓	✗	✗
Magnesite	✗	✗	✗	✗	✓
Fluorite	✗	✗	✗	✗	✗
Malachite	✗	✗	✗	✗	✗
Amorphous silica	✗	✗	✗	✗	✗
Manganese oxides	✓	✓	✗	✗	✗
Sodium autinite	✗	✗	✗	✗	✗
Halite	✗	✗	✗	✗	✗

Notes: ✓ supersaturated
✗ under-saturated

Charge balance achieved using chloride; however, carbonate used for pit wall runoff (since no chloride source)

Table 32 indicates that input waters are supersaturated with respect to some mineral phases. It is expected that redox sensitive and low solubility minerals such as iron and aluminium oxyhydroxides may precipitate near the water source (e.g. on the walls of the pit near the seepage discharge). Over a long period these secondary salts are likely to be redissolved during large storm events and transported into the pit lake. For the purposes of modelling pit lake evolution these processes are not considered important since their effect over the long term is likely to be small.

6.3 Transient Model Evolution

6.3.1 Mineral Precipitation

A transient model of the pit lake evolution was developed in PHREEQC as described in **Section 2**. A summary of the major minerals predicted to form within the lake, and the anticipated time at which they may form, is provided in **Table 33**. **Table 33** presents results for the 'Base Case' scenario (Case G1).

Table 33: Predicted Mineral Precipitation for 'Base Case' scenario (Case G1)

Mineral	Influences	Timing (post closure)
Barite	Barium, Sulfate, Arsenic ^(a) , Lead ^(a)	Throughout
Apatite phases	Aluminium, Fluorine, Calcium, Carbonate, Phosphorus, Lead ^(a)	Throughout
Ferrihydrite	Iron, Lead ^(b) , Zinc ^(b) , Copper ^(b) , Calcium ^(b) , Nickel ^(b) , Manganese ^(b) , Barium ^(b) , Uranium ^(b) , Magnesium ^(b) , Sulfate ^(b) , Fluorine ^(b) , Phosphorus ^(b) , Arsenic ^(b)	Throughout
Aluminium oxyhydroxides	Aluminium	Until 190 years
Calcite	Calcium, Carbonate, Manganese ^(a) , Zinc ^(a) , Nickel ^(a) , Magnesium ^(a)	Until 260 years
Smectite-like phases	Aluminium, Magnesium, Iron, Silicon	20 years onwards
Gypsum	Calcium, Sulfate, Barium ^(a)	180 years onwards
Magnesite	Magnesium, Carbonate	260 years onwards
Fluorite	Calcium, Fluorine, Lead ^(a)	200 years onwards
Malachite	Copper, Carbonate	1,500-2,780
Amorphous silica	Silicon	680 years onwards
Manganese oxides	Manganese	Until 1,080 years
Sodium autinite	Uranium, Phosphorus	3,100 years onwards
Halite	Sodium, Chloride, Lead ^(a)	>3,000 years onwards

Notes: (a) co-precipitation

(b) adsorption

Assumes oxic conditions, $10^{-3.5}$ CO₂(g) partial pressure

There is some uncertainty behind the underlying assumptions of the water balance and input water chemistry. The effect of this uncertainty on mineral precipitation was assessed through sensitivity analyses and the results are presented in **Table 34**.

Table 34: Sensitivity to Mineral Precipitation – Expressed as Timing (post closure)

Mineral	Scenario							
	G1	G2a	G2b	G3a	G3b	G4	G5	G6
Barite	0 onwards	0 onwards	0 onwards	40 onwards	0 onwards	0 onwards	0 onwards	0 onwards
Apatite phases	0 onwards	0 onwards	0 onwards	0 onwards	0 onwards	0 onwards	0 onwards	0 onwards
Ferrihydrite	0 onwards	0 onwards	0 onwards	0 onwards	0 onwards	0 onwards	0 onwards	0 onwards
Aluminium oxyhydroxides	until 190	until 790	until 230	until 60	until 280	until 280	until 140	until 140
Calcite	until 260	until 450	until 390	until 250	until 250	120 – 250	until 2930	until 660
Smectite-like phases	20 onwards	50 onwards	90 onwards	60 onwards	0 onwards	70 onwards	0 onwards	0 onwards
Gypsum	180 onwards	350 onwards	250 onwards	160 onwards	170 onwards	160 onwards	490 onwards	530 onwards
Magnesite	260 onwards	450 onwards	380 onwards	250 onwards	250 onwards	250 onwards	0 onwards	600 onwards
Fluorite	200 onwards	260 onwards	350 onwards	520 onwards	150 onwards	190 onwards	330 onwards	220 onwards
Malachite	1500 – 2780	1080 onwards	nil	nil	840 onwards	nil	930 onwards	nil
Amorphous silica	680 onwards	2540 onwards	1160 onwards	430 onwards	810 onwards	660 onwards	600 onwards	580 onwards
Manganese oxides	until 1080	until 2580	0 onwards	until 890	until 1080	nil	0 onwards	until 250
Sodium autinite	>3000	>3000	nil	>3000	3000 onwards	2830 onwards	>3000	nil
Halite	>3000	>3000	nil	>3000	>3000	>3000	>3000	>3000

Notes: (a) co-precipitation
(b) adsorption

The range of scenarios investigated suggests apatite phases, ferrihydrite and aluminium oxy-hydroxides are likely to precipitate through the evolution of the pit lake. These phases are likely to adsorb a range of anions and cations onto their surface and cause a reduction in concentration in the water column. Other phases that are likely to have an important role in pit lake chemistry include calcite initially, followed by gypsum and eventually halite. The gypsum competes with calcite for calcium ions, resulting in the dissolution of calcite in the range of 250 to 660 years post closure except for scenario G5 where both gypsum and calcite overlap for an appreciable period. The combination of both gypsum and calcite is observed in natural lakes from the area which suggests this aspect of scenario G5 may be reliable.

All scenarios predict that magnesite would form, usually taking the place of calcite. The formation of magnesite in natural systems is rare, which suggests this phase may not occur. The formation of magnesite in the early evolution of the lake, as predicted in scenario G5, is considered very unlikely.

The precipitation of sodium autinite is a notable control on the concentration of uranium in the long term (>3,000 years).

Halite is expected to exert significant control of pit lake behaviour. Salinity and metal concentrations are expected to reach a quasi-steady state condition when halite precipitation is initiated beyond 3,000 years.

Based on comparison to natural analogues and review of predicted precipitation sequences, components of each of the sensitivity scenarios appear realistic. Given the inherent limitations of geochemical modelling the precipitation sequences should be used only as a guide, with the timing of formation being indicative only.

It is also useful to compare the precipitation phases and sequences with those observed from other mine sites. Summer Camp in Nevada USA is in a comparable geological setting within a brecciated deposit containing granodiorite, limestone and some pyrite. Minerals present at Summer Camp pit and whose solubilities may control metal concentrations in the pit lake include: barite, bukovskyite, calcite, copiapite, ferrihydrite, gypsum, jarosite, pickeringite, langite, manganite, melanterite, scorodite, siderite. Leaching of these minerals by rainwater was the main mechanism that controlled the water quality of the pit during the lake filling. After that initial stage, the leaching effect lessened and the groundwater inflow diminished the relative importance of wall rock leachate (Bowell and Parshley, 2005).

Eary (1999) reviewed approximately 50 mine lakes with acidic and neutral waters. A summary of the geochemical controls he identified from this research is presented in **Table 35**.

Table 35: Summary of probable geochemical controls for specific solutes in pit lakes (Eary, 1999)

Solute	Neutral lake water
Al	Gibbsite
Alkalinity	Calcite (pH < 8.5)
As	Adsorption on ferrihydrite (decreases in efficiency with increases in sulfate concentrations)
Ba	Barite/Witherite
Cd	Adsorption on ferrihydrite
Ca	Gypsum
Cu	Brochantite (requires the presence of dissolved silica)
F	Fluorite
Fe	Not identified

Solute	Neutral lake water
Pb	Anglesite (requires relatively high sulfate concentrations, close to gypsum saturation); Chloropyromorphite (dependant on the presence of phosphate)
Mn	MnHPO ₄ (dependant on the presence of phosphate)
Sulfate	Gypsum
Zn	ZnSiO ₃ (requires the presence of dissolved silica)

The studies support the predicted mineral phases predicted to form within the Olympic Dam pit lake. The timing of formation is highly dependent on the proportion and composition of input waters, and the findings of the model cannot be compared to other sites.

6.3.2 Water Chemistry

Table 36 presents water quality predictions from the geochemical model during the major stages of pit lake evolution.

Table 36: Predicted Pit Lake Water Quality Based on ‘Base Case’ Scenario (Case G1) (mg/L, unless noted otherwise)

Parameter	100 years	500 years	1,000 years	3,000 years
pH (pH units)	7.8	7.7	7.5	7.3
pe	7.5	7.7	7.8	8.1
Salinity	25,900	71,100	123,000	247,000
Carbonate as HCO ₃	36.6	31.300	24.800	16.3
Chloride	11,800	34,100	60,200	122,000
Sulfate	4,880	11,400	18,400	35,300
Aluminium	<0.001	<0.001	<0.001	<0.001
Arsenic	0.031	0.081	0.137	0.255
Barium	0.015	0.009	0.006	0.003
Calcium	612	742	604	363
Copper	0.051	0.136	0.236	0.463
Iron	0.001	0.001	0.001	0.001
Potassium	66.3	191	336	679
Magnesium	766	2,120	3,750	7,600
Manganese	0.543	1.290	3.010	6.32
Sodium	7,800	22,600	39,900	80,900
Nickel	0.017	0.047	0.083	0.166
Lead	0.006	0.019	0.034	0.061
Uranium	0.008	0.020	0.032	0.056
Zinc	0.170	0.484	0.851	1.70
Fluorine	8.84	16.5	22.6	36.0
Silicon as SiO ₂	3.87	7.50	8.34	4.54
Phosphorus	<0.001	<0.001	<0.001	<0.001

Notes: Values rounded to 3 significant figures
 Assumes oxic conditions, $10^{-3.5}$ CO₂(g) partial pressure
 Charge balance achieved using chloride; however, carbonate used for pit wall runoff (since no chloride source)

The sensitivity analyses results indicate a range of possible water qualities, and are summarised in **Table 37**. Detailed results from each scenario are also provided in **Attachment 1**.

Table 37: Ranges of Pit Lake Water Quality for all Sensitivity Scenarios Investigated (mg/L, unless noted otherwise)

Parameter	100 years	500 years	1,000 years	3,000 years
pH (pH units)	7.0 – 8.1	6.9 – 7.9	6.7 – 7.9	6.5 – 7.9
pe	7.2 – 8.3	7.4 – 8.4	7.4 – 8.6	7.4 – 8.9
Salinity	17,000 – 26,100	46,700 – 72,200	75,100 – 123,000	97,400 – 247,000
Carbonate as HCO ₃	34.5 – 190	27.6 – 183	23.1 – 146	14.4 – 96.8
Chloride	7,720 – 14,200	21,900 – 41,000	36,100 – 72,500	47,300 – 147,000
Sulfate	1,560 – 4,890	4,500 – 14,000	4,950 – 20,100	5,220 – 35,300
Aluminium	<0.001	<0.001	<0.001	<0.001
Arsenic	0.009 – 0.039	0.025 – 0.102	0.046 – 0.172	0.089 – 0.316
Barium	0.013 – 0.034	0.008 – 0.015	0.006 – 0.009	0.003 – 0.007
Calcium	198 – 656	562 – 1,740	483 – 2,070	301 – 2,190
Copper	0.021 – 0.062	0.062 – 0.164	0.110 – 0.266	0.140 – 0.482
Iron	0.001 – 0.002	0.001 – 0.002	0.001 – 0.002	0.001 – 0.002
Potassium	45.3 – 67.4	127 – 193	202 – 341	264 – 687
Magnesium	334 – 766	903 – 2,200	744 – 3,770	467 – 7,620
Manganese	0.177 – 0.625	0.488 – 1.79	0.486 – 3.15	0.570 – 6.46
Sodium	5,120 – 7,810	14,500 – 22,600	23,900 – 39,900	31,300 – 80,900
Nickel	0.012 – 0.017	0.033 – 0.047	0.051 – 0.083	0.066 – 0.166
Lead	0.004 – 0.007	0.012 – 0.022	0.019 – 0.038	0.024 – 0.068
Uranium	0.003 – 0.009	0.007 – 0.024	0.013 – 0.039	0.022 – 0.067
Zinc	0.121 – 0.176	0.335 – 0.501	0.532 – 0.879	0.689 – 1.75
Fluorine	5.66 – 10.0	11.4 – 16.5	13.3 – 22.6	12.1 – 36.1
Silicon as SiO ₂	3.8 – 5.47	3.32 – 10.8	3.64 – 9.24	4.02 – 9.32
Phosphorus	<0.001	<0.001	<0.001	<0.001

Notes: Values rounded to 3 significant figures
Assumes oxic conditions, $10^{-3.5}$ CO₂(g) partial pressure

The results suggest pH is likely to be circum neutral and salinity would increase over time due to evapo-concentration effects.

6.3.3 Crust Development

Soluble salts (largely crystalline ionic species) and other materials (possibly non-ionic / amorphous species) are predicted to reach saturation and begin to precipitate. It is noted that some solids may require relatively high degrees of supersaturation to precipitate and may remain in solution in metastable states. If degrees of supersaturation are high, then sudden events (e.g. inputs of cold water and consequent mixing of fresh and saline waters with dilution) may induce nucleation and growth as long as the resulting solution still remains supersaturated.

The modelling suggests that a surface crust may develop. The crust is predicted to be largely of gypsum ($\text{CaSO}_4 \cdot 2\text{H}_2\text{O}$). Over time the gypsum crust is likely to be accompanied by halite (NaCl). Other minerals such as epsomite ($\text{MgSO}_4 \cdot 7\text{H}_2\text{O}$), sylvite (KCl) and polyhalite may also form, possibly by reaction with previously formed gypsum.

Crust development would require very high salinities which are likely to first appear in isolated, surface, marginal zones. These would be most pronounced during summer when evaporative concentration is highest and thermal stratification is strongest.

7.0 Limnology

7.1 Limnological Processes

The distribution and stability of waters within the pit lake depends on three important physical characteristics of the water: salinity, temperature and circulation.

Thermal stratification occurs on a seasonal basis in water-bodies due to the warming of the surface waters (concurrent with the onset of summer) and the development of a warmer, less-dense surface layer overlying a cooler, denser layer (**Figure 22**). The resultant stratification is due to the logarithmic absorption of incident energy (insolation) in the water column. The Beer-Lambert Law described this absorption. The depth of the resultant thermocline (where there is a relatively rapid decrease in temperature) is dependant on the limit of energy penetration (extinction depth) which in turn depends on the optical density of the water-body as influenced by turbidity, algal density and true colour.

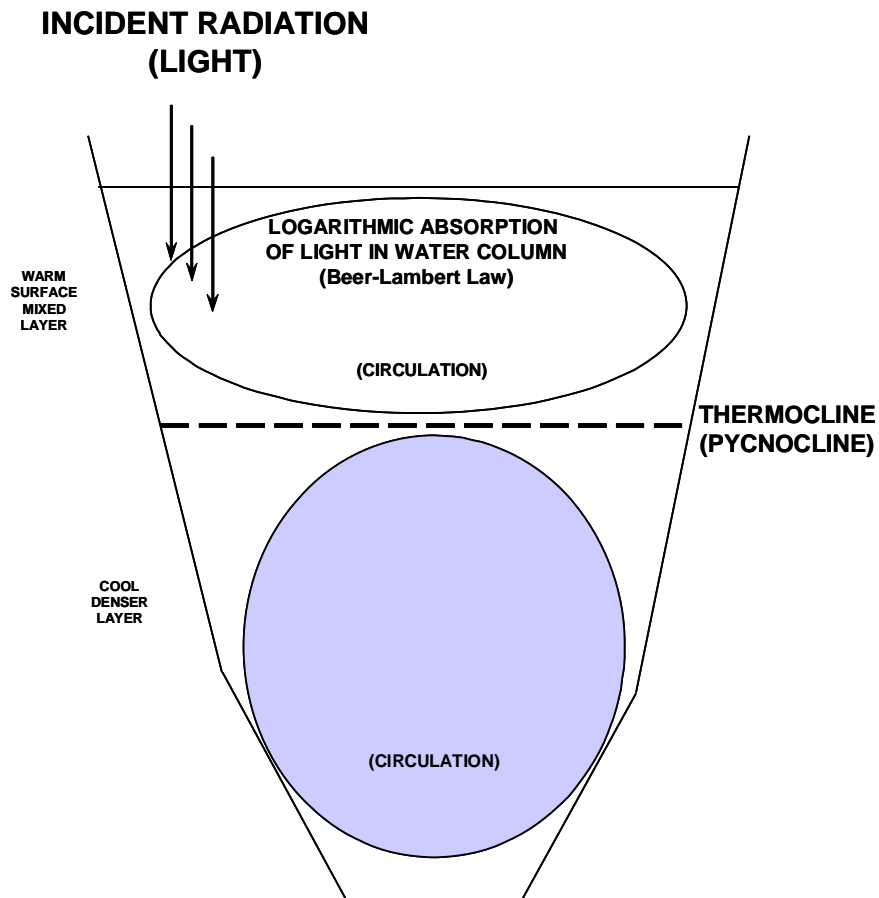
The stability (strength) of stratification may vary diurnally due to the short-term warming and cooling at the surface of a lake, although the high latent heat of water means that it tends to change temperature relatively slowly in response to short-term environmental fluctuations. Since the predicted pit lake is expected to be deep (50th percentile ~340 m water depth), its capacity to store heat over time is relatively large. As a result, water temperature at depth is not expected to fluctuate significantly through a given year. Given the depth of the lake geothermal heat is also expected to warm and moderate water temperatures throughout the year.

Mixing of a water body may occur through several means as illustrated in **Figure 23**. The relative role of each of these mixing forces varies depending on bathymetry and the regional dominance of each of these environmental forcing variables.

The predicted lake has a much smaller surface area to depth ratio than natural lakes. Thus the susceptibility of the deeper regions to wind driven mixing is comparatively low since there is less surface exposure to the forcing energy of the given wind. Further, the lake would be depressed some 630 m below natural ground level (50th percentile) further reducing the exposure to wind.

Seasonal (winter) mixing in such water bodies is dominated by the loss of energy from the surface layer. This is caused by seasonal cooling with the onset of winter such that the surface layer approaches the same temperature as the deeper layer and hence the same density. Under such circumstances these layers would usually merge to become a single homogenous unit.

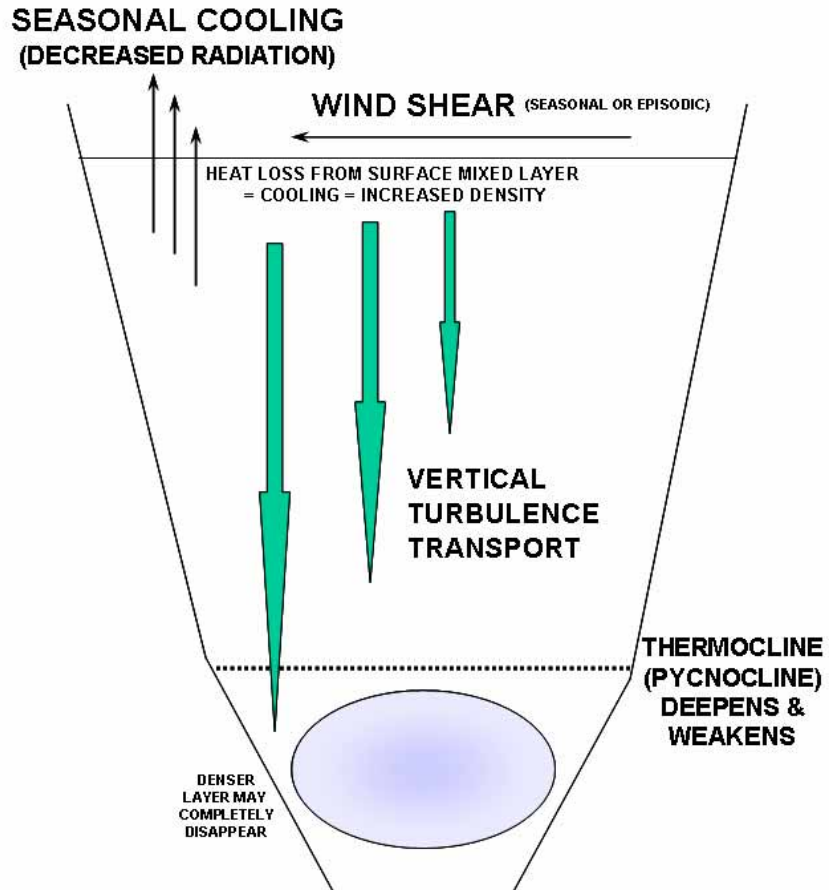
Additionally, unusual seasonal cooling (and to a lesser degree, wind energy) may cause partial or complete mixing at any time during the seasonal cycle. Wind-driven mixing results from turbulent transport through the water column due to the effect of shear created at the water surface. In shallow lakes this is often the dominant mixing mechanism and results in a source of energy sufficient to prevent persistent stratification even during warm summer months. As described above; however, this is unlikely to occur at Olympic Dam.



IMPORTANT POINTS

- NON-LINEARITY OF WATER TEMPERATURE & DENSITY RELATIONSHIP
- OPTICAL CLARITY AFFECTS LIGHT/ENERGY ATTENUATION IN SURFACE LAYER
- WATER QUALITY BELOW PYCNOCLINE WILL BE DIFFERENT TO SURFACE MIXED LAYER - eg. ANOXIA, LOW pH, HIGH E.C.₂₅ etc.

Figure 22: Major Factors in Stratification (redrawn after Boland and Lawton, 1996)



IMPORTANT POINTS

- COMPLETE VERTICAL UNIFORMITY MAY NOT OCCUR EVERY COOL SEASON
- EROSION OF PYCNOCLINE CAN CAUSE WATER QUALITY CHANGES AT THE SURFACE

Figure 23: Major Factors in Mixing (redrawn after Boland and Lawton, 1996)

7.2 Factors Influencing Mixing

7.2.1 Meteorological Drivers

Thermal stratification occurs as a result of seasonal heating and cooling cycles. The closest reliable long term weather station is Andamooka, approximately 30 km north-east of Olympic Dam. Analysis of this data indicates the following:

- The January maximum temperatures exceed 35°C on average for 18.5 days per year and 40 °C for 7.9 days per year. Such warm summer temperatures driven by high rates in insolation are expected to cause strong thermal stratification in the surface layers of the pit lake. It should be noted that the high temperature at the surface of the lake may induce the early formation of crusting based on gypsum or carbonate minerals, these phases generally exhibiting inverse solubility with temperature increase in saline waters (> 40,000 mg/L) above approximately 35°C.
- Regional rainfall is unpredictable during any one year and varies markedly between years, often with extended periods between storm events. Thus the main effects of rainfall on the pit lake would be evident during episodic storm events.
- Mean daily minimum temperatures of 5.9°C occur in July, with -1.6°C being the coldest temperature on record. Minimum temperatures can be very important in the long term water temperature of the lake, since cooling of surface layers increases density and promotes mixing and associated temperature reduction throughout the water column.

7.2.2 Salinity

Geochemical modelling has allowed the prediction of salinity variation in the pit lake over time. The change in salinity as a result of evapo-concentration, precipitation of salts and dilution from runoff events is considered in the model. **Figure 24** presents the salinity time series for each sensitivity scenario investigated.

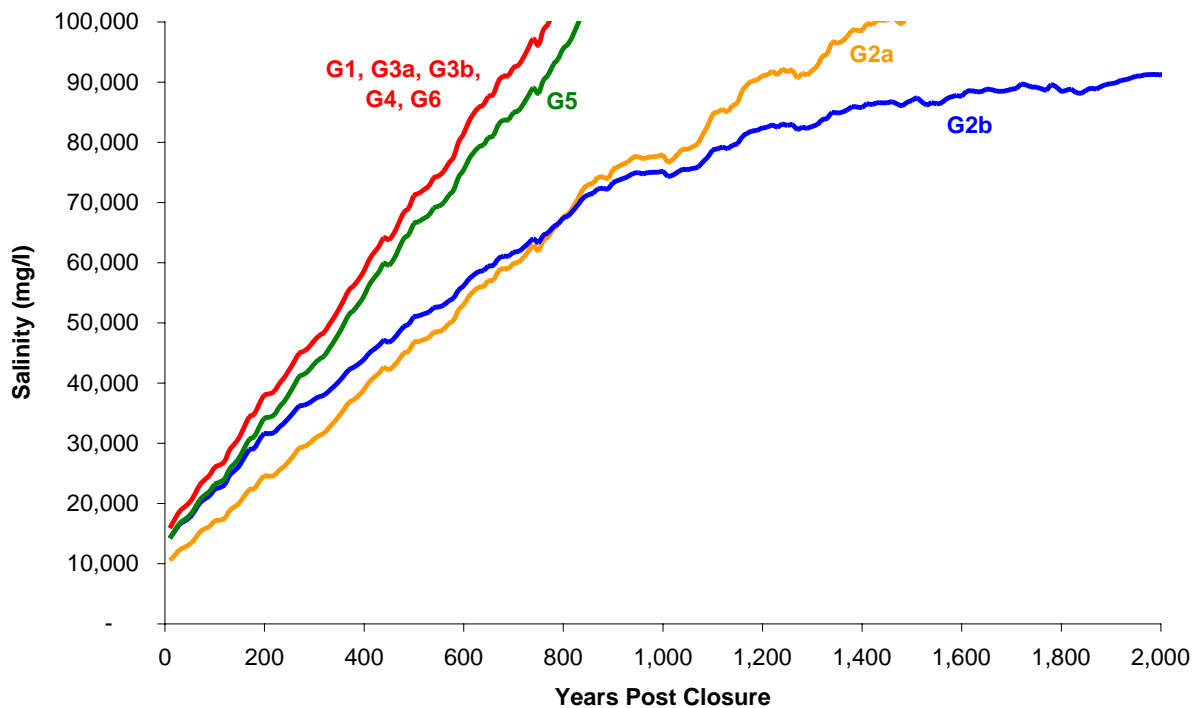


Figure 24: Salinity of Inflow Surface Water

In **Figure 24** the irregular nature of the salinity as a function of time for Case G2a represents the effect of evapo-concentration and dilution in a small lake.

7.3 Model Scenarios

The limnological model considers the effect of temperature and salinity on stratification. There are several limitations to the model including:

- Salinity ceiling - DYRESM uses a series of 'look up tables' based on United Nations Educational Scientific and Cultural Organisation (UNESCO) values for the salinity / density relationship in water. This table has however, an upper limit of salinity concentration of 42 practical salinity units (psu) or approximately 42,000 mg/L total dissolved solids (TDS). Scenarios of up to 42 psu were investigated in this study.
- Temperature ceiling - DYRESM has an upper water temperature input / output limit of 40 °C. In a deep waterbody surface temperatures in excess of 40 °C are rarely observed and this is not considered to be a major limitation in the near-surface layers. The effect of geothermal heat on temperature variation and mixing is described below.
- Geothermal effects - The temperatures in the bed of the pit lake would be influenced by geothermal properties with the walls at maximum depth estimated to be 60-65°C. This would influence the bed layers but the heat flux density resulting from this is not able to be entered using DYRESM due to the temperature ceiling as described above. The influence of this deeper heat on water column seasonal hydraulics is difficult to estimate but it would, to an unknown extent, affect the vertical turbulence transport through the deeper parts of the lake. Nonetheless, the surface behaviour of the lake would not be greatly influenced and would resemble the outputs shown in the following Section.
- Two and three dimensional effects - The graphical outputs from the modelling describe the water column structure of the pit lake as a one-dimensional Lagrangian figure. In real terms there may be periods where short-term discrete lateral or spatial variations occur at the surface and / or through the water column. Such effects are generated by the density flux in the lake through time at particular locations and are important in reservoirs and lakes with large surface areas. However, in the context of the Olympic Dam pit lake, such variations are inherently unstable. Thus, the one-dimensional descriptions provided adequately describe the gross seasonal and inter-seasonal behaviour of the water column in the Olympic Dam pit lake.

The model is therefore useful as a guide only, and prediction of limnological behaviour requires consideration of the above factors not included in the model.

Four salinity scenarios were modelled: 10, 20, 30, 40 psu, which is approximately equivalent to salinities of 10,000 mg/l, 20,000 mg/l, 30,000 mg/l and 40,000 mg/l respectively. These salinities would be realised over different time periods depending on the water balance and input water composition (i.e. geochemical scenarios). **Table 38** provides the relationship between time and salinity for each geochemical scenario, which can be extracted from **Figure 24**.

Table 38: Establishment time for salinity scenarios

Scenario	10,000 mg/l (Case L1a)	20,000 mg/l (Case L1b)	30,000 mg/l (Case L1c)	40,000 mg/l (Case L1d)
Case G1, G3a, G3b, G4, G6	0 years	50 years	150 years	240 years
Case G2a	0 years	150 years	300 years	410 years
Case G2b	0 years	70 years	190 years	350 years

7.4 Model Results

Model results for all scenarios investigated (refer **Section 2.4.1**) are presented in **Figure 25** through **Figure 31**.

7.4.1 Case L1a (salinity 10,000 mg/L)

Figure 25 shows that surface thermal variability is based on seasonal variations in insolation with surface warming occurring in the summer months of each year and surface cooling (and vertical mixing) occurring in winter months due to seasonal decreases in incoming solar radiation. This is expected and this general trend has been recorded in a number of pit lakes subject to similar seasonal meteorological patterns. The most pronounced feature is the steady warming of the deeper region of the lake over the simulation period. This occurs even though winter cooling in a conventional freshwater reservoir would lead to the development of much cooler conditions in the deepest sections of such a lake and a deep parent thermocline (Imberger and Patterson, 1990) would develop at approximately 5°C.

The general trend for the density of the deep portion of the water column over the full simulation period, shows that while maintaining vertical discontinuity the density increases slightly due to evapo-concentration (**Figure 19**).

7.4.2 Case L1b (salinity 20,000 mg/L)

At 20,000 mg/L there is more structure in the salinity distribution within the lake, with seasonal salinity fluctuations penetrating deeper into the lake (5 m as distinct from 10 m at deepest) as can be seen in **Figure 26**.

Between years 4 and 7 there is a discrete, relatively lower salinity period at the surface of the lake. This presumably reflects the net result of inputs of fresher waters into the system in the early years of its life. This lower salinity period is also reflected in temperature and density variation plots.

Given the higher thermal capacities and densities of the higher salinity waters, these parameters generally follow those of salinity.

7.4.3 Case L1c (salinity 30,000 mg/L)

Figure 27 shows that at 30,000 mg/L the salinity structure in the lake relative to Case L1b appears to have become more diffuse. This may represent the greater thermal capacity at higher salinity and the ability to resist seasonal changes. That is, the distinctions between winter and summer become less distinct. Where distinction is possible, salinity variations may now penetrate to 20-25 m into the lake. This compares with 5 m in the case of 20,000 mg/L salinity.

As with Case L1b, there is the appearance of a discrete, relatively lower salinity period in the surface zones of the lake between years 3.5 to 12.5. Similar explanations to those advanced in Case L1b are likely. Trends in temperature and density are largely consistent with those of salinity.

7.4.4 Case L1d (salinity 40,000 mg/L)

At 40,000 mg/L, a seasonal variability in salinity is distinct in the surface zones of the lake as can be seen in **Figure 28**. As with Case L1c, this variability may extend to 30-40 m depth into the lake. Also, a relatively low salinity period appears in the surface zones of the lake extending between years 3.5 – 12.5.

There is a well developed seasonal cycle in temperature variation with a small discrete thermal maximum, above 40 °C at approximately 10 m depth at approximately year 5. The thermal maximum at this salinity may have profound effects upon the possible precipitation of carbonate mineral phases. The small thermal maximum dissipates and appears to increase in depths towards 20 m at year 12.

As would be expected, the density variations are consistent with those exhibited by salinity and temperature.

7.4.5 Cases L2a,b,c

Cases L2a, L2b and L2c are variations on Case L1c to assess the sensitivity of the model to the extinction coefficient (K_d), being a critical parameter related to the optical clarity of the water. Case L2a represents a less turbid water than assessed in Case L1, while Case L2b is slightly more turbid and Case L2c is considerably more turbid.

As with Case L1c, seasonal fluctuation in salinity and temperature are evident. The major difference is the penetration of the thermal and salinity gradients into the lake. In Case L2a the temperature gradient penetrates some 30-40 m deep into the lake (**Figure 29**), whereas penetration in Case L2c is only to a depth of 5-10 m.

The salinity gradient is more pronounced in Case 2c than 2a, with strong evapoconcentration occurring in the surface layers under the more turbid scenario, creating a strong salinity gradient to a depth of 50 m.

The overall effect of the temperature and salinity profiles is a deeper density gradient in the less turbid scenario (approximately 35 m) compared with the more turbid scenario (approximately 5-10 m). The density gradient becomes more pronounced in summer periods in both scenarios.

The sensitivity analysis predicts that mixed conditions are likely to occur on a seasonal basis throughout the water column, regardless of the extinction coefficient assumed.

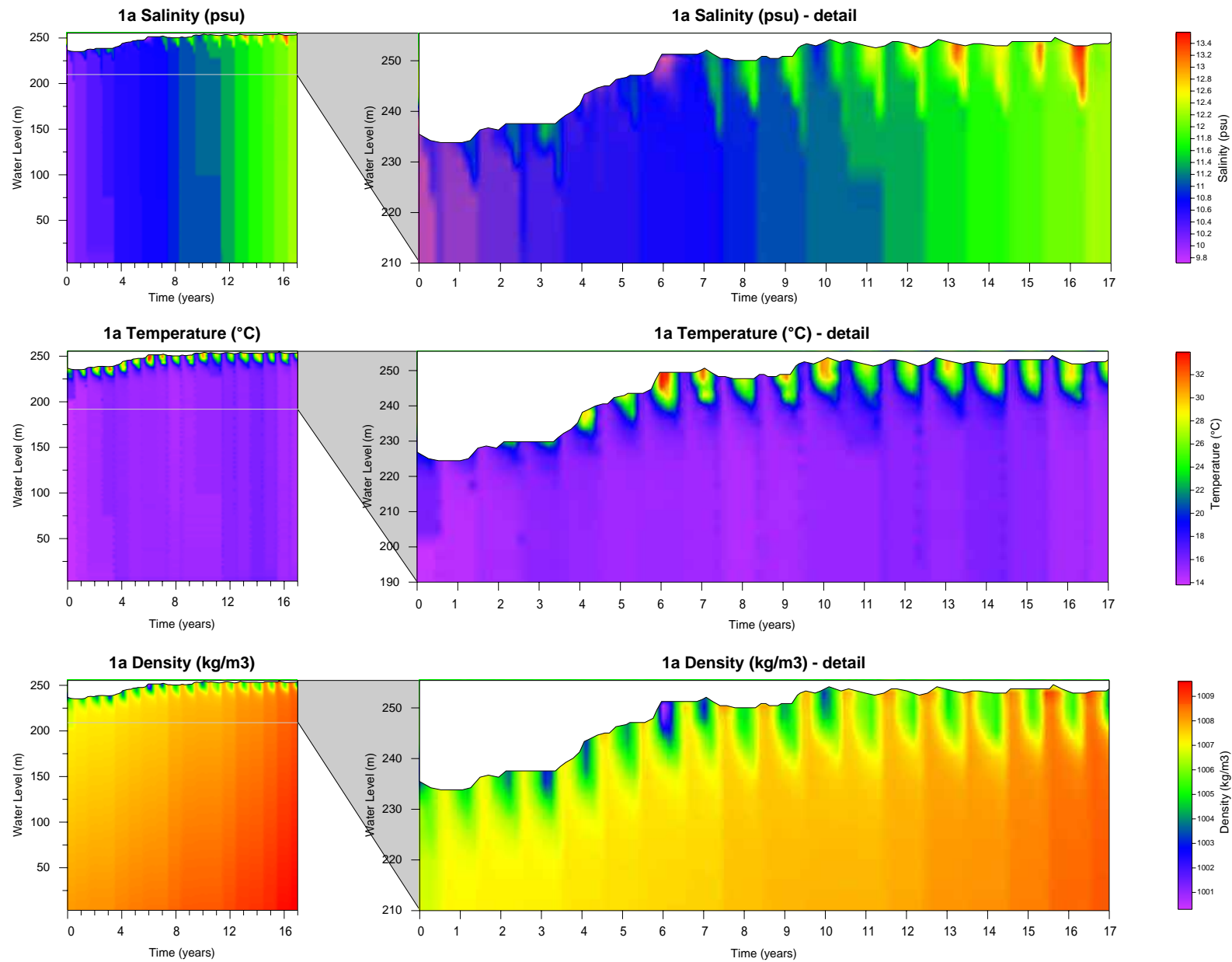


Figure 25: Case L1a (salinity 10,000 mg/L)

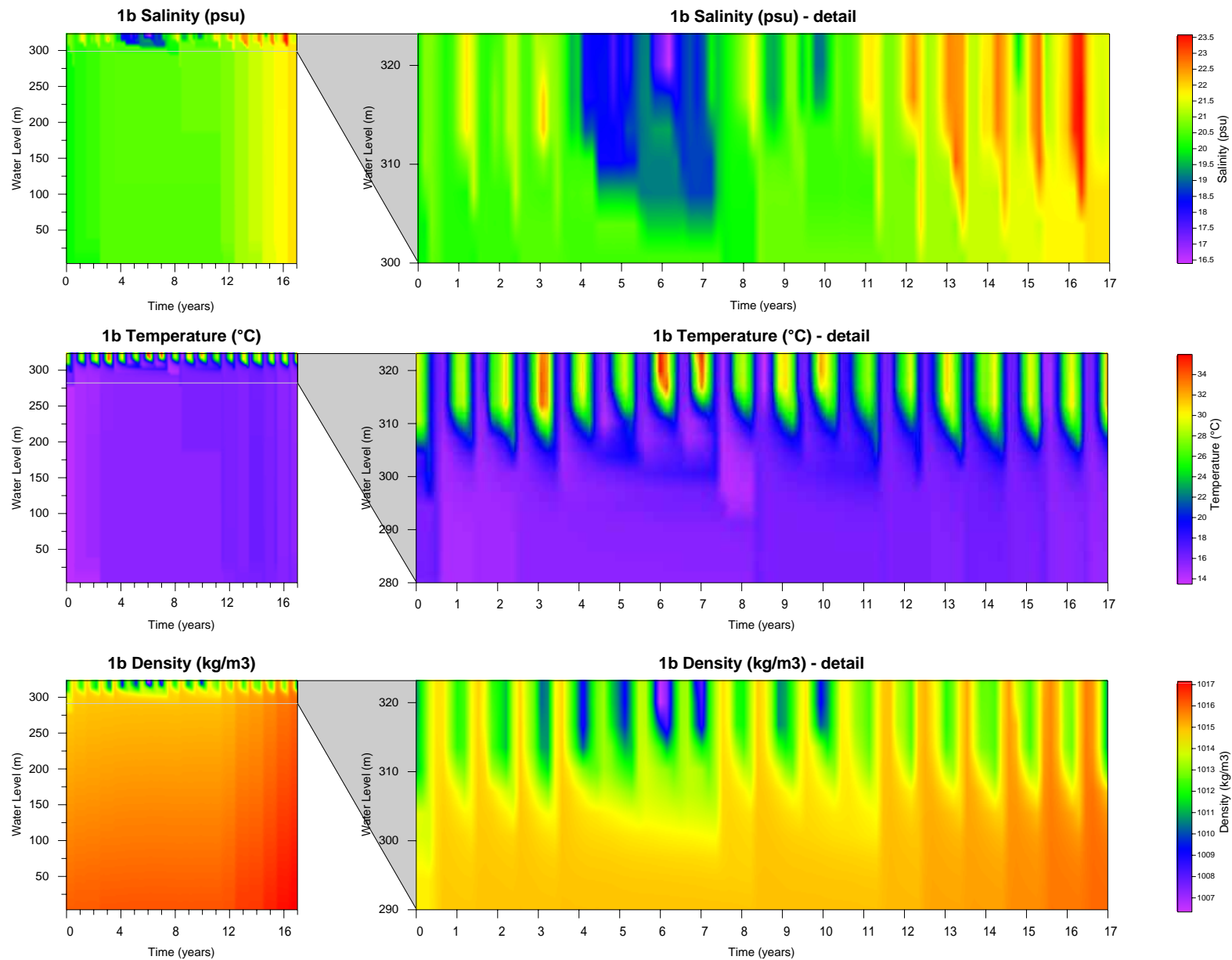


Figure 26: Case L1b (salinity 20,000 mg/L)

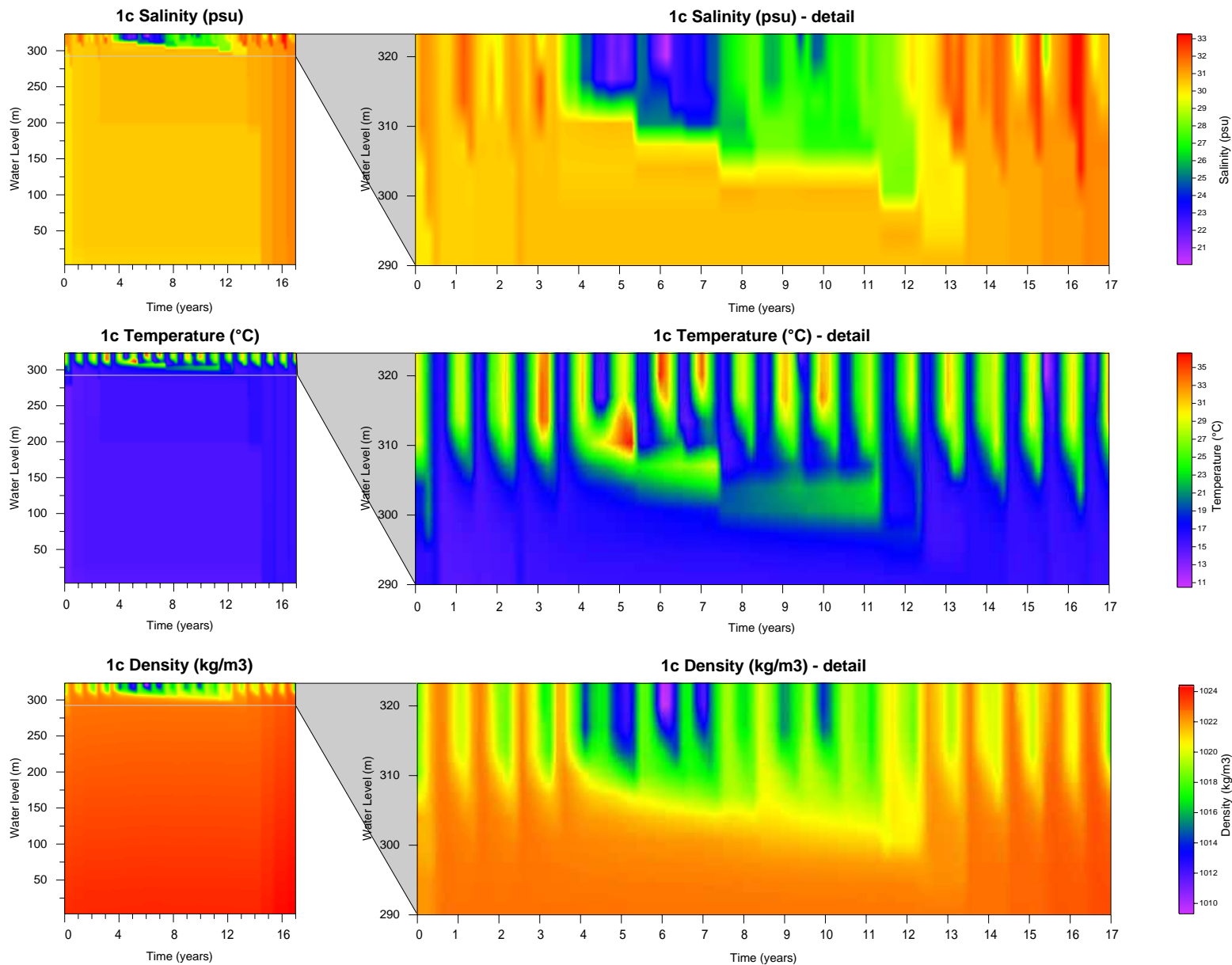


Figure 27: Case L1c (salinity 30,000 mg/L)

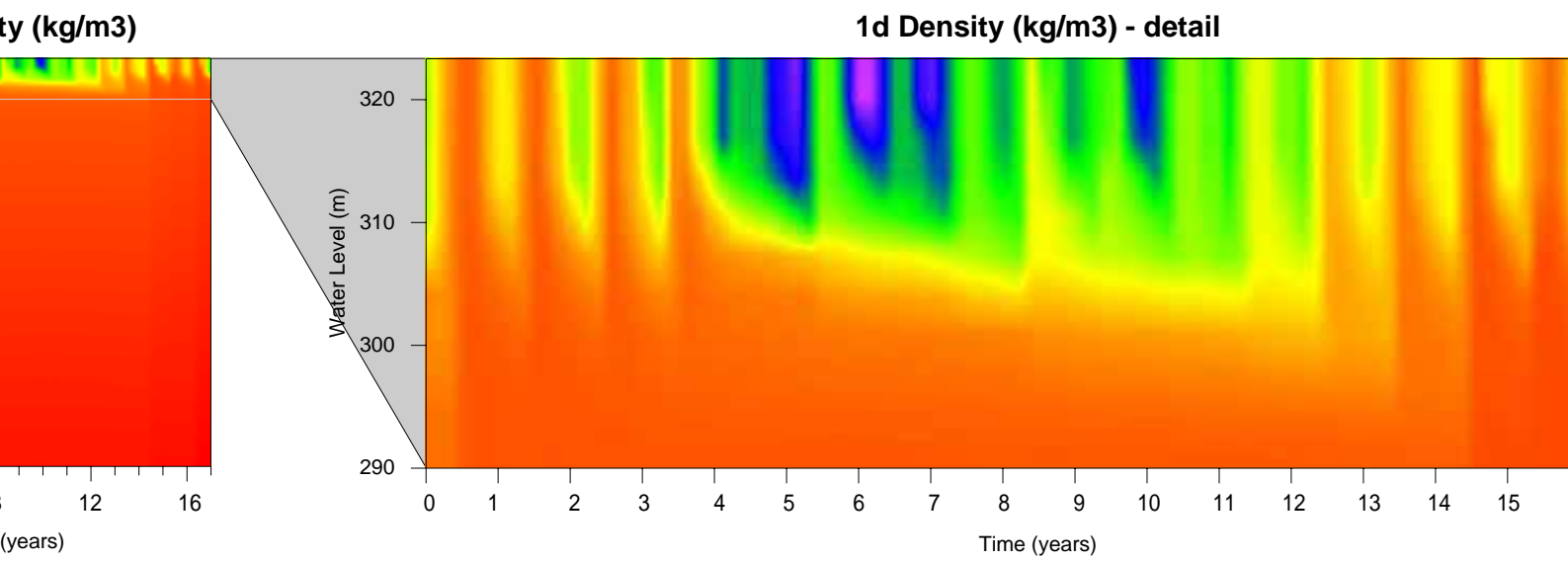
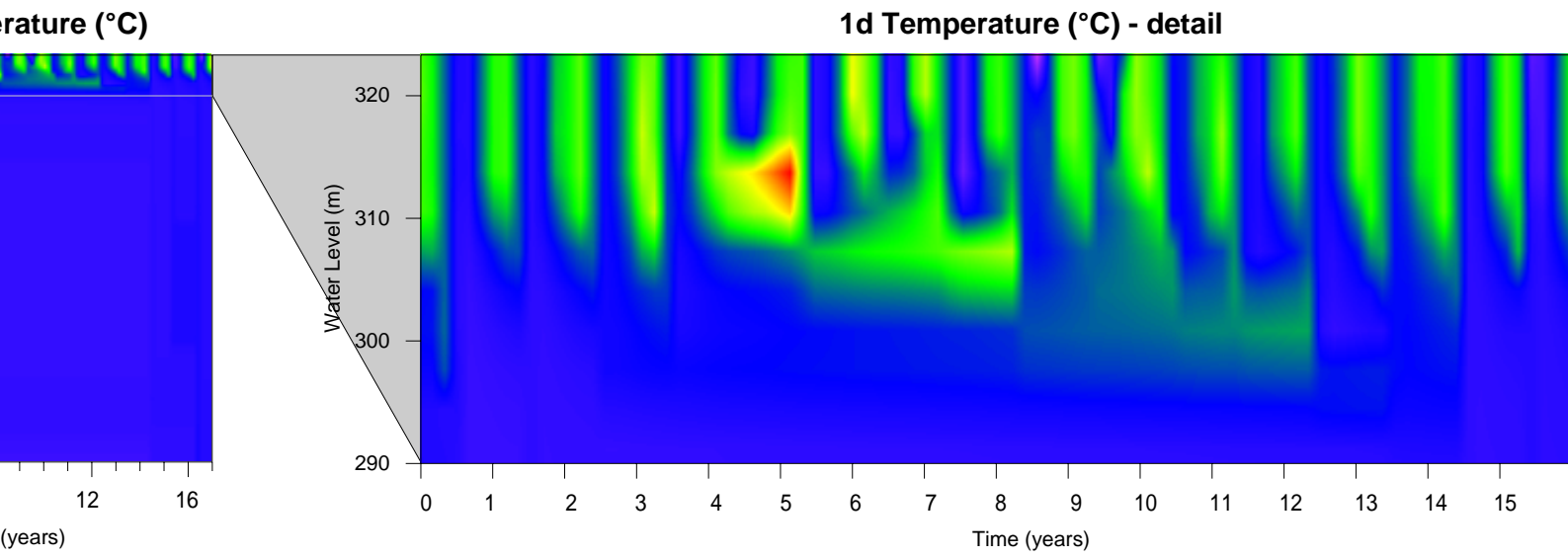
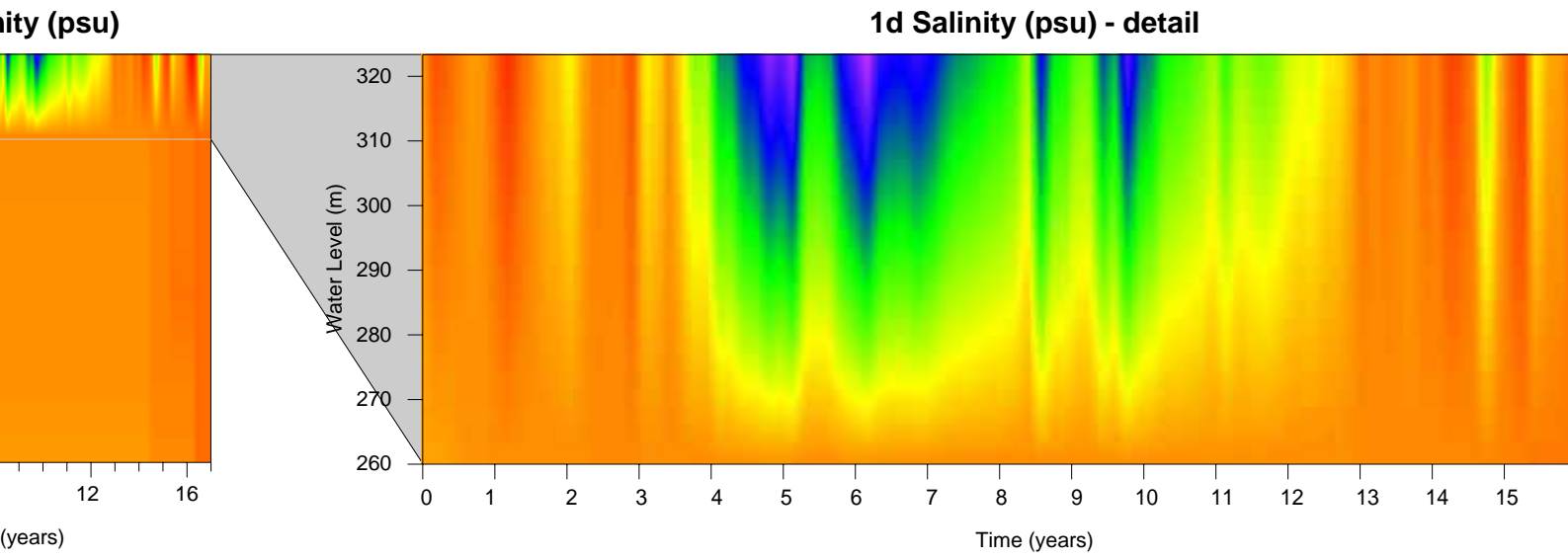


Figure 28: Case L1d (salinity 40,000 mg/L)

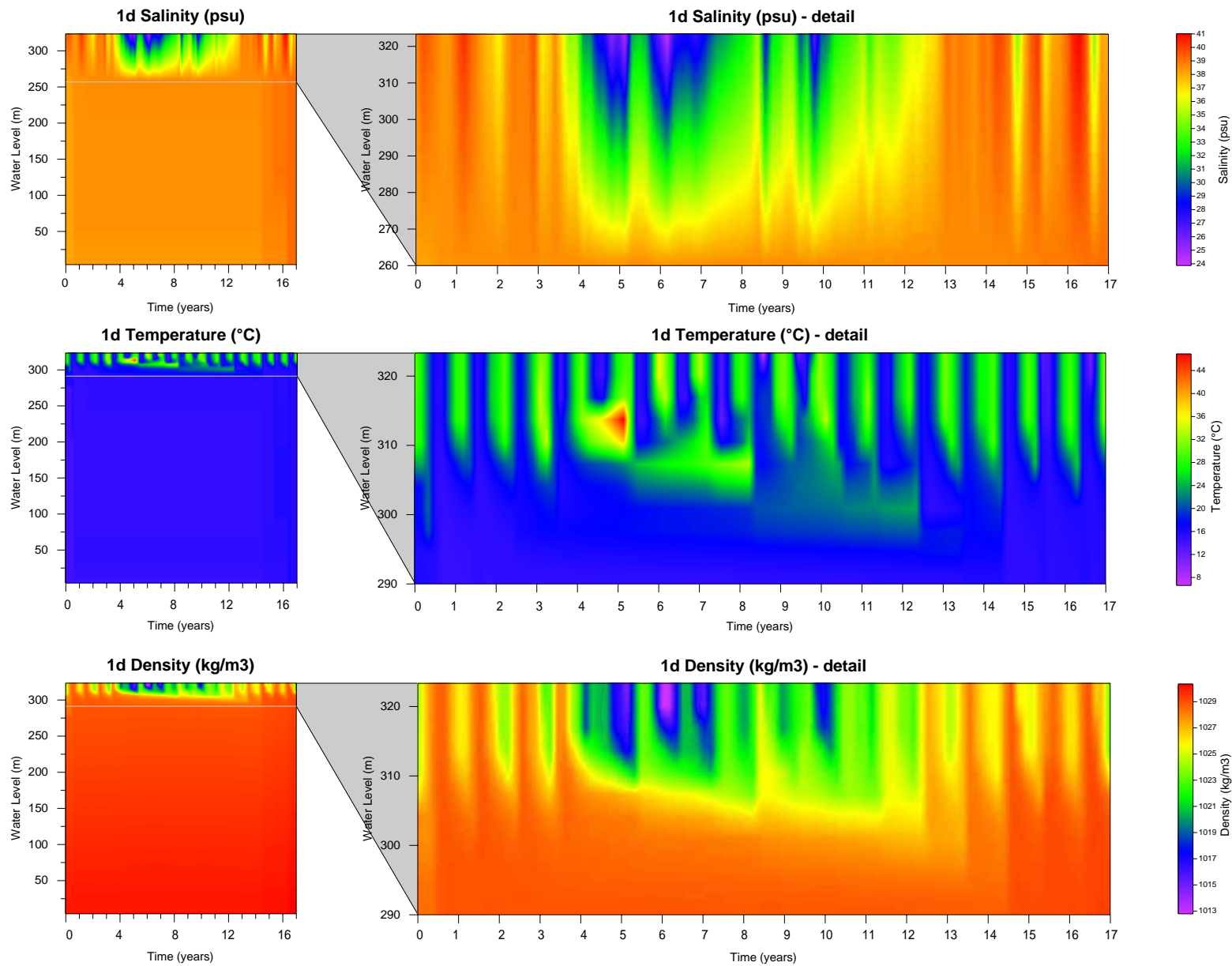


Figure 28: Case L1d (salinity 40,000 mg/L)

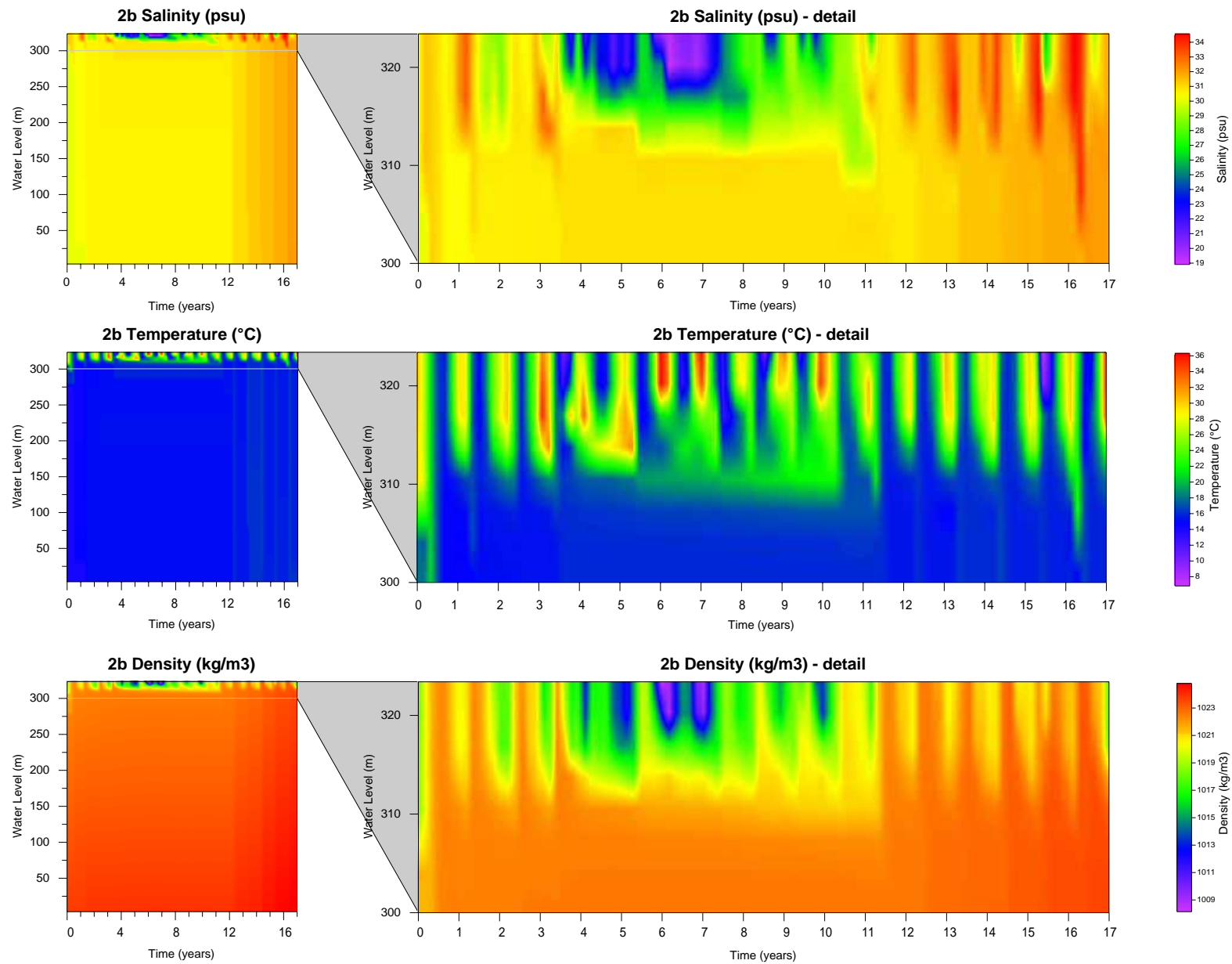


Figure 30: Case L2b (salinity 30,000 mg/L, K_d 0.5)

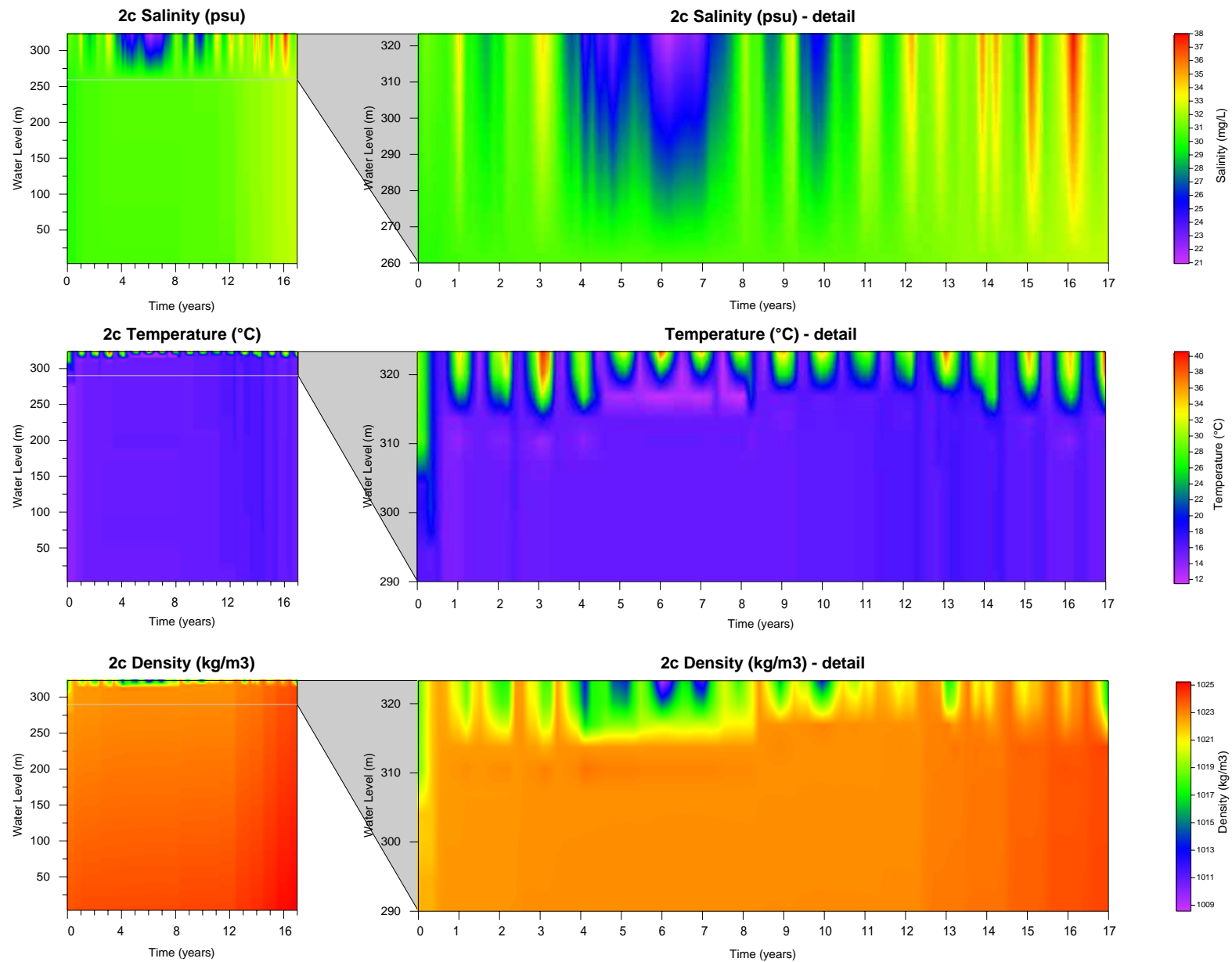


Figure 31: Case L2c (salinity 30,000 mg/L, K_d 2.0)

7.5 Predicted Stratification and Mixing Cycles

The lake is likely to experience strong thermal stratification in the early stages of development during summer months, for perhaps 3-4 months. The thermocline may extend from 10 – 40 m depth, depending on the turbidity of the water and climatic conditions. A salinity gradient is also likely to form. Following large episodic storm events, freshwater may overlie saline water for several seasons. During dry periods, evapo-concentration at the surface would result in more saline water overlying less saline water.

The extent to which geothermal heat affects lake mixing is difficult to quantitatively predict. It is expected that convective streams would form within the lake, driven by temperatures of perhaps 60-65 °C in the bed of the lake. Circulation of water by convective processes is likely to occur year-round and would enhance mixing.

Mixed conditions are predicted to occur in winter months when temperature gradients (and to a lesser extent salinity gradients) diminish, and may also occur in summer months depending on the extent of geothermal mixing.

Over several hundred years the salinity of the lake is predicted to approach that of seawater, and over thousands of years would become a concentrated brine. While heating and cooling would continue at the surface the increasing salinity-driven density renders temperature driven density changes virtually irrelevant and the water column as a whole is expected to approach near homogeneity, with respect to salinity, at the end of the simulation period.

While it is predicted that in the long term salinity is likely to be virtually uniform throughout the water column, water chemistry is likely to vary with depth, primarily due to a reduction in redox potential with depth.

8.0 Discussion

8.1 Proposed Lake Uses

The water balance confirms that a pit lake would form within the final void. It is unlikely that the pit lake water would have beneficial uses because it is expected to become saline to hypersaline, and would be depressed at least 330 m, and probably 630 m, below the natural ground surface.

8.2 Lake Development Stages

The quality of water and mixing processes within the lake would change over time as a result of solute input, evapo-concentration, biological activity, hydrothermal inputs and climatic conditions. On the basis of the water balance, water quality and limnological modelling, the major stages of pit lake evolution are predicted to be as follows:

- Lake formation (0-100 years post closure).
 - water levels would rise rapidly;
 - metal concentrations would be relatively low, but increase over time since the pit would act as a sink for groundwater and surface water inflows;
 - ferrihydrite is predicted to readily precipitate and form a coating over the bed of the pit lake, and would also influence (reduce) the concentration of a range of metals through adsorption;
 - barium and arsenic concentrations would be maintained very low due to precipitation of barite; and
 - the lake may periodically stratify during summer, causing anoxic zones to form at depth, however the surface water inflows and increasing water levels may cause periodic mixing.
- Stratified lake (100-250 years post closure).
 - water level increases would begin to slow;
 - localised calcite crusting may form at the edges of the lake due to evapo-concentration. Co-precipitation of metals (e.g. manganese, zinc and nickel) may occur; and
 - stratification is likely to be pronounced during summer, with mixed conditions during winter.
- Periodic surface crust (250-3,000 years post closure).
 - salinity is expected to approach that of sea water by about 250 years post closure;
 - the salinity would become the dominant factor affecting water density and stratification during summer is expected to decline. Near mixed conditions would occur throughout the year (i.e. water parameters would be the same throughout the entire water column);
 - gypsum surface crusting is expected to form, possibly displacing or coexisting with calcite;
 - it is expected that the crust would be relatively insoluble, but may be periodically redissolved during large storm events; and

- uranium concentrations may begin to decline in the latter part of this stage due to precipitation of sodium autinite.
- Extensive salt crusting (> 3,000 years post closure).
 - an extensive halite salt crust is predicted to form at the surface; and
 - the salt crust is likely to be permanent, but could possibly dissolve during large storm events.

8.3 Ongoing Review of Model Predictions

A range of assumptions were required in order to develop the predictions for this assessment. This is because some of the model variables cannot be measured until the open cut mine is operational. Details of assumptions and the basis for selection of variables are described within **Sections 5.0, 6.0 and 7.0**.

It is recommended that a data collection program is instigated during the operational phase of the mine. Measured data would monitor against model predictions, which would in turn allow for further planning and implementation of mitigative measures.

The major areas in which the data collection program would focus include:

- external catchment surface water quality data. This would include data on seasonal and inter-annual variability;
- pit wall hydrology, determined through depressurisation and pit dewatering yields;
- seepage rates. This should include revised estimates of seepage from the TSF and RSF, and be coupled with the regional groundwater flow model to revise long term inflow predictions;
- RSF and TSF seepage chemistry, the impact of this on the Andamooka Limestone aquifer, and any changes to the inflow chemistry from this aquifer;
- pit wall oxidation rates and drainage chemistry; and
- climate data, particularly revised climate change projections.

In addition it is also necessary to review the effect of any changes in the closure plan (e.g. removal of perimeter bund wall, final void geometry) on the predictions. Consideration of these effects would be made when modifying the closure plan.

9.0 Conclusion

Based on the current mine closure scenario it is predicted that a permanent lake would form within the open cut mine void. The primary source of water to the open pit is expected to be groundwater seepage, followed by pit wall runoff and incident rainfall. Runoff from external catchments intersected by the pit is expected to be a relatively small source.

The water balance indicates that overflows from the pit are not expected to occur at any time, including consideration of climate change, extreme rainfall events and enhanced groundwater inflow. No specific management measures are considered necessary to manage the risk of overflow.

The pit lake is expected to equilibrate at a quasi steady state elevation of between -310 mAHD (97.5 percentile) and -690 mAHD (2.5 percentile). The 50th percentile water level is -530 mAHD, which equates to a water depth of approximately 340 m and would sit some 630 m below natural ground level.

The major stages of pit lake evolution have been identified to be:

- Lake formation (0-100 years post closure).
- Stratified lake (100-250 years post closure).
- Periodic surface crust (250-3000 years post closure).
- Extensive salt crusting (>3000 years post closure).

Limnological assessment and modelling suggests that as the salinity increases (and hence also the density), near mixed conditions would occur throughout the year. Heating and cooling would continue to occur at the surface, however the density changes associated with this would be small and mixed conditions are expected to prevail.

Limnological and geochemical modelling suggests that a calcite and/or gypsum crust may develop on the water surface. Over time the crust may be accompanied by other phases including halite. It is expected that the crust would become increasingly persistent over time.

Over the life of the project, an updated evaluation of the open pit water balance and water quality after the end of mining, through pit lake filling and into mine closure should be used to plan for the long-term pit lake behaviour. Additionally, the updated pit lake evaluations can be used as a predictive tool for closure alternative design feasibility.

10.0 Bibliography

AGC (1982), Hydrogeology and impact of mining on the groundwater regime, Olympic Dam Project Environmental Studies, Australian Groundwater Consultants, July 1982.

Ahmadzadeh Kokya, B. and Ahmadzadeh Kokya, T. (2007), Proposing a formula for evaporation measurement from salt water resources, Hydrological Processes, Urmia, Iran,

Asmar BN, Ergenzinger P. 1999. Estimation of evaporation from the Dead Sea. Hydrological Processes 13: 2743–2750.

Bass-Becking, L.G.M., Kaplan, L.R. and Moore, D (1960): Limits of the Natural Environment in Terms of pH and Oxidation-Reduction Potentials; Journal of Geology, Volume 68, pages 243-283.

Boland K.T. and M. Lawton, M. (1996) Seasonal Water Quality Variations in the Rum Jungle Voids, in; Proceedings of the Post-mining Landform Stability and Design Workshop, Brisbane Queensland, (eds. L.C. Bell and R.W. McLean) Australian Centre for Minesite Rehabilitation Research, Brisbane Queensland.

Boland, K and Padovan, A.V. (2002). Seasonal stratification and mixing in a recently flooded mining void in tropical Australia. Lakes & Reservoirs Research and Management, 7: 125-131, Blackwell Scientific.

Boland, K. (2000). The limnology of water-filled open-cut mining voids. Abstracts of 39th Annual Congress of the Australian Society for Limnology, Darwin, 7-10 July 2000.

Boland, K.T. (1993) A Comparison of Two Lakes in Northwest Queensland, Ph.D. thesis, James Cook University of North Queensland, 252 pp.

Boland, K.T. and Griffiths, D.J. (1995). Seasonal Changes in the Dissolved Oxygen Status of Two Tropical Reservoirs. Lakes and Reservoirs: Research and Management. 1: 213-219.

Boland, K.T. and Griffiths, D.J. (1996). Water Column Stability as a Major Determinant of Shifts in Phytoplankton Composition - Evidence from Two Tropical Lakes in Northern Australia. In; Perspectives in Tropical Limnology, F. Schiemer & K.T. Boland (eds), SBP Academic Publishing, Amsterdam.

Boland, K.T. and Imberger, J., (1994). An Analysis of Dynamic Stability in Two Inland Lakes of Northern Australia. Mitt. int. Ver. Limnol. 24: pp 337-344.

Boland, K.T., Lawton, M.D., Jefree, R.A. and Twining, J.R. (1993). Heavy Metal Output from The Rehabilitated Rum Jungle Minesite (Australia) and Downstream Effects. In: Abstracts, First SETAC World Congress, Ecotoxicology and Environmental Chemistry - A Global Perspective. April 1993, Lisbon, Portugal.

Bowell R. J. and Parchley J. V., 2005. Control of pit-lake water chemistry by secondary minerals, Summer Camp pit, Getchell mine, Nevada. Chemical Geology 215, 373-385.

Bureau of Meteorology (2003), The Estimation of Probable Maximum Precipitation in Australia: Generalised Short-Duration Method, Hydrometeorological Advisory Service, Canberra, June 2003

CSIRO (2005). Building a future on knowledge from the past: what palaeo-science can reveal about climate change and its potential impacts in Australia, A research brief for the Australian Greenhouse Office prepared by CSIRO in association with scientific collaborators, June 2005, Canberra

CSIRO (2007), Climate Change in Australia – Technical Report, <http://www.climatechangeinaustralia.gov.au>, Canberra

Dzombak, D.A., and Morel, F.M.M., 1990, Surface complexation modeling--Hydrous ferric oxide: New York, John Wiley & Sons, 393 p

Eary, L.E. (1999), Geochemical and equilibrium trends in mine pit lakes, Applied Geochemistry 14, pp.963-987

- ENSR (2008), Draft Olympic Dam Mine Rock Characterisation and RSF Hydrogeochemical Assessment, 7 April 08
- Evans C. A., Coombes P. J. and Dunstan, R. H., 2006. Wind, rain and bacteria: The effect of weather on the microbial composition of roof-harvested rainwater. *Water Research* 40, 37-44.
- Evans C. A., Coombes P. J. and Dunstan, R. H., 2006. Wind, rain and bacteria: The effect of weather on the microbial composition of roof-harvested rainwater. *Water Research* 40, 37-44.
- Giblin, A. (1980), Hydrogeochemical Study of Ground Waters in the vicinity of Olympic Dam, CSIRO Division of Mineralogy, Sept 1980.
- GRM (2005), Draft Report on Olympic Dam Hydrogeology; prepared for SRK as part of the WMC PFS, February 2005.
- Harbeck GE, Kohler MA, Koberg GE, et al. 1958. Water-loss investigations. Lake Mead studies. United States, Geological Survey, Professional Papers 298.
- Harrison, S.P. and Dodson, J. (1993). Climates of Australia and New Guinea Since 18,000 yr B.P. In: Wright, H.E., Kutzbach, J.E. (Eds.) *Global Climates Since the Last Glacial Maximum*. Chapter 11, 265-293. University of Minnesota Press. St Paul.
- Herpich, D (2002), Discussion Paper: TSF – Decommissioning and Rehabilitation Research. Unpublished Report 15 November 2002.
- Imberger, J. and Patterson, J.C. (1990). Physical Limnology, in; *Advances in Applied Mechanics*, Volume 27. Academic Press. pp.303-475.
- IPCC (2007), *Climate Change 2007: Synthesis Report, Fourth Assessment Report, Intergovernmental Panel on Climate Change*
- Jones, R.N., Bowler, J.M. and MacMahon, T.A. (1998) A high resolution Holocene record of P/E ratio from closed lakes in Western Victoria. *Palaeoclimates*, 3, 51 er 0 years. e f ral. rm -long intervals. –82.
- Jones, R.N., McMahon, T.A. and Bowler, J.M. (2001) Modelling historical lake levels and recent climate change at three closed lakes, Western Victoria, Australia (c.1840-1990), *Journal of Hydrology*, 246, 158-179.
- Kinhill, 1997a, Olympic Dam Expansion Project. Environmental Impact Statement. Prepared for WMC (Olympic Dam Corporation).
- Kraatz, M. and Applegate, R.J. (1992) eds. 'Rum Jungle Rehabilitation Project Monitoring Report 1986-88'. Conservation Commission of the Northern Territory: Darwin.
- Lawton, M.D. (1996). The Rum Jungle Copper/Uranium Mine (Northern Australia): Open Cut Water Quality Prior to and 10 Years after Rehabilitation. In; *Proceedings of the National Engineering Conference, Darwin NT, 21-24 May, 1996*. pp 355-360.
- Lewis,Jr. W.M. (1973) The Thermal Regime of Lake Lanao (Philippines) and its Theoretical Implications for Tropical Lakes. *Limnol. and Oceanogr.*, 18(2).
- Lewis,Jr. W.M. (1983) Temperature, Heat, and Mixing in Lake Valencia, Venezuela. *Limnol. and Oceanogr.*, 28(2), 273-286.
- M. Al-Shammiri, Evaporation rate as a function of water salinity, *Desalination*, 150 (2002) 189–203.
- Manahan, S.E., 2005, *Environmental Geochemistry*, 8th Edition, CRC Press
- Meyer AF. 1915. Computing run-off from rainfall and other physical data. *Transactions of the American Society of Civil Engineers* 79: 1056–1224.
- Niemi, T.M., Ben-Avraham, Z., Gat, J.R. (1997), *The Dead Sea: The Lake and Its Setting*, Oxford University Press, US

- Nordstrom, D.K., and Alpers, C.N., 1999, Geochemistry of acid mine waters, in Plumlee, G.S., and Logsdon, M.J., eds., *The environmental geochemistry of mineral deposits: processes, methods and health issues: Reviews in Economic Geology*, v. 6A, p. 133-160.
- ODO (2007), Groundwater monitoring data supplied by site, Olympic Dam Operations, BHP Billiton
- Oroud, I.M. (1999), Temperature and evaporation dynamics of saline solutions, Department of Physical Geography, Mu'tah University, Kerak, Jordan, *Journal of Hydrology* 226 (1999) 1–10
- Parkhurst, D.L., 1995, User's guide to PHREEQC--A computer program for speciation, reaction-path, advective-transport, and inverse geochemical calculations: U.S. Geological Survey Water-Resources Investigations Report 95-4227
- REM (2007), Olympic Dam Expansion: Hydrogeological investigations, unpublished.
- Roderick M.L. & Farquhar G.D. (2004a) Changes in Australian pan evaporation from 1970.
- Roderick M.L. & Farquhar G.D. (2004b) The pan evaporation paradox – an overview of the scope of the problem, *Proceedings: Pan evaporation: an example of the detection and attribution of trends in climate variables*, Australian Academy of Science, Canberra, November 22-23, 2004. to 2002. *International Journal of Climatology*, 24, 1077-1090.
- Singh, G. (1981), Late Quaternary pollen records and seasonal paeloclimates of Lake Frome, South Australia, *Hydrobiologia* 82, 419-452
- SRK (2007), Olympic Dam Tailings Storage Facility Geochemical Model, BHP 021, Rev 2, August 2007
- Suppiah R, Preston B, Whetton P, McInnes K, Jones R, Macadam I, Bathols J, Kirono D (2006) 'Climate change under enhanced greenhouse conditions in South Australia', an updated report on: Assessment of climate change, impacts and risk management strategies relevant to South Australia, CSIRO, Melbourne.
- Talling, J.F. (1957). Some Observations on the Stratification of Lake Victoria, *Limnol. and Oceanogr.* 2: pp.213-221.
- Talling, J.F. (1963). Origin of Stratification in an African Rift Lake. *Limnol. and Oceanogr.* 8:1. pp 68-78.
- Talling, J.F. and Lemoalle J. (1998). *Ecological Dynamics of Tropical Inland Waters*, Cambridge University Press, Cambridge UK.
- Townsend S.A. and Boland, K.T. (1987). Reservoir Stratification and Mixing in the Monsoonal Region of the Northern Territory. In; *Technical Papers*, Australian Water and Wastewater Association, 12th Federal Convention, Adelaide, 1987. pp.424-431.
- Townsend S.A., Boland, K.T. and Luong-Van, J., (1994). The Thermal Regime of a Medium Sized Water Body (Darwin River Reservoir) in the Australian Wet/Dry Tropics. *Arch. Hydrobiol.*
- Wilkinson, J., Hutson, J., Bestland, E. and H. Fallowfield. (2005). "Audit of contemporary and historical quality and quantity data of stormwater discharging into the marine environment, and field work programme". ACWS Technical Report No.3 prepared for the Adelaide Coastal Waters Study Steering Committee, July 2005. Department of Environmental Health, Flinders University of South Australia.

Attachment 1

Water Quality Sensitivity Analyses

Table A1: Water Quality Based on Case G2a (mg/L, unless noted otherwise)

Parameter	100 years	500 years	1,000 years	3,000 years
pH (pH units)	7.9	7.8	7.7	7.4
pe	7.4	7.5	7.7	8.0
Salinity	17,000	46,700	77,800	177,000
Carbonate as HCO ₃	39.5	36.2	30.1	20.4
Chloride	7,720	21,900	37,400	87,000
Sulfate	3,200	8,060	12,300	25,600
Aluminium	<0.001	<0.001	<0.001	<0.001
Arsenic	0.033	0.084	0.138	0.286
Barium	0.017	0.012	0.009	0.004
Calcium	404	801	725	484
Copper	0.052	0.135	0.222	0.334
Iron	0.001	0.001	0.001	0.001
Potassium	45.3	127	216	498
Magnesium	504	1,360	2,330	5,400
Manganese	0.361	0.768	1.460	4.760
Sodium	5,120	14,500	24,800	57,600
Nickel	0.012	0.033	0.056	0.126
Lead	0.005	0.015	0.026	0.056
Uranium	0.008	0.020	0.033	0.065
Zinc	0.121	0.335	0.569	1.29
Fluorine	7.70	13.5	17.3	28.6
Silicon as SiO ₂	4.07	3.32	3.64	6.43
Phosphorus	<0.001	<0.001	<0.001	<0.001

Notes: Values rounded to 3 significant figures
 Assumes oxic conditions, 10^{-3.5} CO₂(g) partial pressure
 Value in brackets indicates deviation from Base Case scenario value

Table A2: Water Quality Based on Case G2b (mg/L, unless noted otherwise)

Parameter	100 years	500 years	1,000 years	2,000 years [^]
pH (pH units)	7.9	7.8	7.7	7.6
pe	7.5	7.6	7.7	7.8
Salinity	22,300	51,000	75,100	97,400
Carbonate as HCO ₃	38.2	35.9	31.3	28.1
Chloride	10,100	24,000	36,100	47,300
Sulfate	4,190	8,640	11,900	14,900
Aluminium	<0.001	<0.001	<0.001	<0.001
Arsenic	0.023	0.050	0.072	0.089
Barium	0.015	0.011	0.009	0.007
Calcium	527	787	727	667
Copper	0.041	0.091	0.134	0.170
Iron	0.001	0.001	0.001	0.001
Potassium	57.2	135	202	264
Magnesium	657	1,500	2,250	2,940
Manganese	0.460	0.826	1.34	1.97
Sodium	6,700	15,900	23,900	31,300
Nickel	0.015	0.034	0.051	0.066
Lead	0.005	0.013	0.019	0.024
Uranium	0.006	0.012	0.018	0.022
Zinc	0.153	0.356	0.532	0.689
Fluorine	7.09	13.9	16.8	19.4
Silicon as SiO ₂	4.06	5.97	9.24	9.32
Phosphorus	<0.001	<0.001	<0.001	<0.001

Notes: Values rounded to 3 significant figures

Assumes oxic conditions, $10^{-3.5}$ CO₂(g) partial pressure

Value in brackets indicates deviation from Base Case scenario value

[^] 3,000 year results not reported due to high ionic strength and model unreliability. Comparison to Base Case not possible

Table A3: Water Quality Based on Case G3a (mg/L, unless noted otherwise)

Parameter	100 years	500 years	1,000 years	3,000 years
pH (pH units)	7.8	7.7	7.5	7.3
pe	7.5	7.7	7.8	8.1
Salinity	25,900	71,100	123,000	247,000
Carbonate as HCO ₃	36.5	31.2	24.8	16.3
Chloride	11,800	34,100	60,200	122,000
Sulfate	4,880.	11,400	18,400	35,300
Aluminium	<0.001	<0.001	<0.001	<0.001
Arsenic	0.009	0.025	0.046	0.097
Barium	0.015	0.009	0.006	0.003
Calcium	616	741	603	363
Copper	0.021	0.062	0.110	0.236
Iron	0.001	0.001	0.001	0.001
Potassium	63.4	183	324	657
Magnesium	764	2,130	3,760	7,620
Manganese	0.547	1.29	2.92	5.92
Sodium	7,800	22,600	39,900	80,900
Nickel	0.015	0.043	0.076	0.154
Lead	0.004	0.012	0.022	0.042
Uranium	0.003	0.007	0.013	0.022
Zinc	0.153	0.442	0.781	1.58
Fluorine	5.66	16.4	22.6	36.1
Silicon as SiO ₂	4.37	10.8	8.34	4.54
Phosphorus	<0.001	<0.001	<0.001	<0.001

Notes: Values rounded to 3 significant figures
 Assumes oxic conditions, $10^{-3.5}$ CO₂(g) partial pressure
 Value in brackets indicates deviation from Base Case scenario value

Table A4: Water Quality Based on Case G3b (mg/L, unless noted otherwise)

Parameter	100 years	500 years	1,000 years	3,000 years
pH (pH units)	7.8	7.7	7.5	7.3
pe	7.5	7.7	7.8	8.1
Salinity	25,900	71,100	123,000	247,000
Carbonate as HCO ₃	36.7	31.3	24.8	16.4
Chloride	11,800	34,100	60,200	122,000
Sulfate	4,880	11,400	18,400	35,300
Aluminium	<0.001	<0.001	<0.001	<0.001
Arsenic	0.039	0.102	0.172	0.316
Barium	0.015	0.009	0.006	0.003
Calcium	610	742	604	363
Copper	0.062	0.164	0.266	0.482
Iron	0.001	0.001	0.001	0.001
Potassium	67.4	193	341	687
Magnesium	766	2,120	3,750	7,590
Manganese	0.542	1.290	3.010	6.460
Sodium	7,800	22,600	39,900	80,900
Nickel	0.017	0.047	0.083	0.166
Lead	0.007	0.022	0.038	0.068
Uranium	0.009	0.024	0.039	0.067
Zinc	0.176	0.501	0.879	1.750
Fluorine	10.0	16.5	22.5	36.0
Silicon as SiO ₂	3.86	5.63	8.34	4.54
Phosphorus	<0.001	<0.001	<0.001	<0.001

Notes: Values rounded to 3 significant figures
 Assumes oxic conditions, $10^{-3.5}$ CO₂(g) partial pressure
 Value in brackets indicates deviation from Base Case scenario value

Table A5: Water Quality Based on Case G4 (mg/L, unless noted otherwise)

Parameter	100 years	500 years	1,000 years	3,000 years
pH (pH units)	7.0	6.9	6.7	6.5
pe	8.3	8.4	8.6	8.9
Salinity	26,100	71,300	123,000	247,000
Carbonate as HCO ₃	190	183	146	96.8
Chloride	11,800	34,100	60,200	122,000
Sulfate	4,880	11,400	18,400	35,300
Aluminium	<0.001	<0.001	<0.001	<0.001
Arsenic	0.028	0.077	0.134	0.253
Barium	0.015	0.009	0.006	0.003
Calcium	656	745	605	363
Copper	0.050	0.133	0.237	0.468
Iron	0.002	0.002	0.002	0.002
Potassium	66.4	191	336	679
Magnesium	766	2,150	3,770	7,620
Manganese	0.625	1.79	3.15	6.32
Sodium	7,800	22,600	39,900	80,900
Nickel	0.017	0.047	0.083	0.166
Lead	0.006	0.019	0.032	0.059
Uranium	0.008	0.020	0.033	0.027
Zinc	0.169	0.483	0.850	1.700
Fluorine	8.84	16.5	22.6	36.1
Silicon as SiO ₂	5.47	7.50	8.28	4.53
Phosphorus	<0.001	<0.001	<0.001	<0.001

Notes: Values rounded to 3 significant figures
 Assumes oxic conditions, $10^{-3.5}$ CO₂(g) partial pressure
 Value in brackets indicates deviation from Base Case scenario value

Table A6: Water Quality Based on Case G5 (mg/L, unless noted otherwise)

Parameter	100 years	500 years	1,000 years	3,000 years
pH (pH units)	8.1	7.9	7.9	7.9
pe	7.2	7.4	7.4	7.4
Salinity	23,100	66,500	112,000	219,000
Carbonate as HCO ₃	61.3	47.7	53.8	62.4
Chloride	9,770	28,200	49,900	101,000
Sulfate	4,890	14,000	20,100	35,100
Aluminium	0.001	<0.001	<0.001	<0.001
Arsenic	0.024	0.063	0.107	0.202
Barium	0.013	0.008	0.006	0.003
Calcium	198	562	483	301
Copper	0.042	0.111	0.186	0.140
Iron	0.001	0.001	0.001	0.001
Potassium	65.5	188	332	671
Magnesium	334	903	744	467
Manganese	0.177	0.488	0.486	0.570
Sodium	7,810	22,600	39,900	80,800
Nickel	0.016	0.045	0.079	0.160
Lead	0.005	0.015	0.027	0.052
Uranium	0.006	0.016	0.027	0.050
Zinc	0.165	0.471	0.829	1.67
Fluorine	7.83	14.0	13.4	12.1
Silicon as SiO ₂	3.80	9.14	9.09	5.35
Phosphorus	<0.001	<0.001	<0.001	<0.001

Notes: Values rounded to 3 significant figures
 Assumes oxic conditions, $10^{-3.5}$ CO₂(g) partial pressure
 Value in brackets indicates deviation from Base Case scenario value

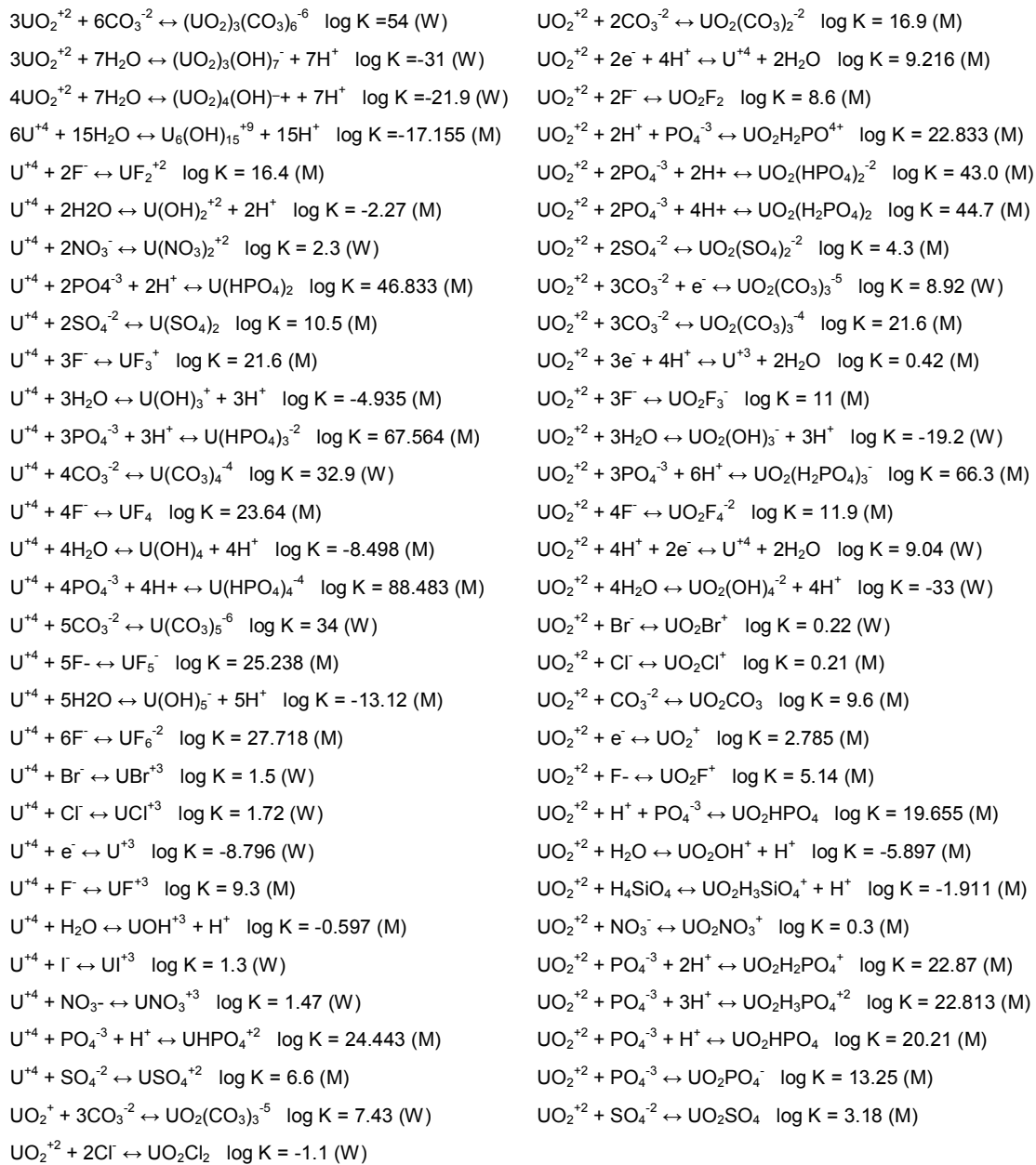
Table A7: Water Quality Based on Case G6 (mg/L, unless noted otherwise)

Parameter	100 years	500 years	1,000 years	3,000 years
pH (pH units)	7.8	7.6	7.4	7.1
pe	7.5	7.8	7.9	8.3
Salinity	25,000	72,200	123,000	243,000
Carbonate as HCO ₃	34.5	27.6	23.1	14.4
Chloride	14,200	41,000	72,500	147,000
Sulfate	1,560	4,500	4,950	5,220
Aluminium	<0.001	<0.001	<0.001	<0.001
Arsenic	0.024	0.064	0.109	0.207
Barium	0.034	0.015	0.009	0.003
Calcium	611	1,740	2,070	2,190
Copper	0.042	0.111	0.197	0.393
Iron	0.001	0.001	0.001	0.001
Potassium	65.2	188	331	669
Magnesium	763	2,200	3,740	7,570
Manganese	0.595	1.740	3.060	6.160
Sodium	7,770	22,500	39,700	80,600
Nickel	0.016	0.045	0.079	0.159
Lead	0.006	0.018	0.031	0.055
Uranium	0.006	0.015	0.025	0.042
Zinc	0.164	0.470	0.827	1.66
Fluorine	7.81	11.4	13.3	18.3
Silicon as SiO ₂	3.85	9.09	7.88	4.02
Phosphorus	<0.001	<0.001	<0.001	<0.001

Notes: Values rounded to 3 significant figures
 Assumes oxic conditions, $10^{-3.5}$ CO₂(g) partial pressure
 Value in brackets indicates deviation from Base Case scenario value

Attachment 2

Uranium species included in the geochemical model



Worldwide Locations

Australia	+61-2-8484-8999
Azerbaijan	+994 12 4975881
Belgium	+32-3-540-95-86
Bolivia	+591-3-354-8564
Brazil	+55-21-3526-8160
China	+86-20-8130-3737
England	+44 1928-726006
France	+33(0)1 48 42 59 53
Germany	+49-631-341-13-62
Ireland	+353 1631 9356
Italy	+39-02-3180 77 1
Japan	+813-3541 5926
Malaysia	+603-7725-0380
Netherlands	+31 10 2120 744
Philippines	+632 910 6226
Scotland	+44 (0) 1224-624624
Singapore	+65 6295 5752
Thailand	+662 642 6161
Turkey	+90-312-428-3667
United States	+1 978-589-3200
Venezuela	+58-212-762-63 39

Australian Locations

Adelaide
Brisbane
Canberra
Darwin
Mackay
Melbourne
Newcastle
Sydney
Singleton

www.ensr.com.au